HOXA5/GALECTIN-1 REGULATION OF BRAIN TUMOUR STEM CELLS

GHAZAL RAFSANJANI-SADEGHI

Thesis submitted to the University of Ottawa
in partial Fulfillment of the requirements for the
Master of Science

Department of Cellular and Molecular Medicine
Faculty of Medicine
University of Ottawa

Table of Contents

Abstract

Glioblastoma (GB) is the most aggressive primary brain tumour in adults, with a median survival of 15 months following maximal surgical resection, ionizing radiation (IR), and temozolomide (TMZ) chemotherapy. Tumour recurrence is largely driven by brain tumour stem cells (BTSCs), a specialized population of cells in GB tumours that exhibit persistent self-renewal, proliferation, and therapeutic resistance, driving tumour recurrence following treatment. Thus, a deeper understanding of the molecular mechanisms regulating BTSCs is essential for the development of novel therapeutic strategies aimed at improving long-term patient survival.

The galectin-1/homeobox A5 (HOXA5) signalling has been implicated in sustaining BTSC stemness and tumourigenic transcriptional programs, yet the precise mechanisms by which galectin-1 regulates HOXA5's function remain unclear. Galectin-1 primarily functions as a non-covalent homodimer, and structural docking models predict that homodimeric galectin-1 interacts with the N-terminal region of HOXA5 to promote DNA binding, whereas monomeric galectin-1 may impede DNA binding by directly interacting with the homeodomain.

To assess the docking model which predicts that galectin-1 dimerization is necessary for HOXA5's regulatory functions, we generated plasmids encoding either wild-type (WT) homodimeric galectin-1 or a dimerization-deficient mutant (Mut) and expressed them in patient-derived BTSCs via electroporation. Analysis conducted in three genetically distinct BTSC lines revealed that WT galectin-1 enhanced BTSC self-renewal and sphere-forming capacity, whereas the Mut galectin-1 consistently attenuated stemness and growth. Complementary chromatin immunoprecipitation-quantitative PCR (ChIP-qPCR) experiments in human embryonic kidney 293T (HEK293T) cells co-expressing HOXA5 and either galectin-1 WT or Mut revealed that the Mut was associated with reduced HOXA5 enrichment at the promoters of key target genes

compared to WT. These findings support a model in which galectin-1 dimerization promotes HOXA5 chromatin binding and transcriptional regulation of genes critical for BTSC maintenance. Thus, targeting galectin-1's oligomeric state may be a potential novel therapeutic strategy for disrupting BTSC-driven GB recurrence.

Acknowledgments

I would like to thank Dr. Jahani-Asl for welcoming me into her laboratory and granting me the opportunity to contribute to glioblastoma research. Her technical and financial support through her CIHR grants has been invaluable throughout my training. I also extend my sincere thanks to Dr. Dianbo Qu for generously sharing his expertise, and to my lab colleagues and friends for their encouragement during my academic journey. I am equally thankful to the members of my thesis advisory committee, Dr. Christine Pratt and Dr. Michael Rudnicki, whose constructive feedback has been instrumental in shaping my work.

Contributions

All experiments described in this thesis were carried out under the guidance and supervision of Dr. Jahani-Asl. The generation of protein docking models, along with the assessment of protein expression, oligomerization status and *in-vitro* binding assay for the galectin-1 WT and mutant constructs, were conducted by Dr. Dianbo Qu. The characterization of HA-tagged HOXA5 WT and mutant over-expressing BTSCs was conducted by Dr. Behnaz Nateghi and Chelsea Leduc.

List of Figures

List of Tables

List of Abbreviations

2-HG – 2-Hydroxyglutarate

ABC transporter – ATP-binding cassette transporter

AML – Acute myeloid leukemia

Arp2/3 – Actin-related protein 2/3 complex

BAD – Bcl-2-associated death promoter

BAX – Bcl-2-associated X protein

BBB – Blood–brain barrier

BSA – Bovine serum albumin

BTSCs – Brain tumour stem cells

CBP – CREB-binding protein

CCL2 – Chemokine (C-C motif) ligand 2

CD133 – Prominin-1

CDK – Cyclin-dependent kinase

CDKIs – Cyclin-dependent kinase inhibitors

CDKN1A – Cyclin-dependent kinase inhibitor 1A (p21, Cip1)

CDKN2A – Cyclin-dependent kinase inhibitor 2A (p16, ARF)

ChIP-qPCR – Chromatin immunoprecipitation followed by quantitative PCR

ChIP-seq – Chromatin immunoprecipitation followed by sequencing

CNS – Central nervous system

Co-IP – Co-immunoprecipitation

CRD – Carbohydrate recognition domain

CSC – Cancer stem cell

DMSO – Dimethyl sulfoxide

E2F1 – E2F transcription factor 1

ECM – Extracellular matrix

EGFR – Epidermal growth factor receptor

EGFRvIII – Epidermal growth factor receptor variant III

ELDA – Extreme limiting dilution assay

EMT – Epithelial-to-mesenchymal transition

GB – Glioblastoma

GFP – Green fluorescent protein

GST – Glutathione S-transferase

HA – Hemagglutinin epitope tag

HADDOCK 4.0 – High Ambiguity Driven protein–protein DOCKing version 4.0

HEK293T – Human embryonic kidney 293T cell line

HIFs – Hypoxia-inducible factors

HOXA5 – Homeobox protein A5

IDH – Isocitrate dehydrogenase

IL – Interleukin

IR – Ionizing radiation

MDM2 – Mouse double minute 2 homolog

MGMT – O6-methylguanine-DNA methyltransferase

MH1 – Mad homology domain 1

MMR – Mismatch repair

MMP – Matrix metalloproteinase

MXI1 – MAX interactor 1

Myc – Myelocytomatosis oncogene

NF1 – Neurofibromin 1

NF-kB – Nuclear factor kappa-light-chain-enhancer of activated B cells

NK cells – Natural killer cells

NSCLC – Non-small cell lung cancer

NSCs – Neural stem cells

OSMR – Oncostatin M receptor

OXPHOS – Oxidative phosphorylation

PBX – Pre-B-cell leukemia homeobox

PDGFRA – Platelet-derived growth factor receptor alpha

PI3K/AKT – Phosphoinositide 3-kinase / Protein kinase B pathway

PMTs – Post-translational modifications

PTEN – Phosphatase and tensin homolog

PTN – Pleiotrophin

PTPRZ1 – Protein tyrosine phosphatase receptor type Z1

PXN – Paxillin

RAD51 – DNA repair protein RAD51 homolog

RAS/MAPK – Rat sarcoma virus / Mitogen-activated protein kinase pathway

RNA-seq – RNA sequencing

ROS – Reactive oxygen species

SCIP –Oct-6/POU3F1 transcription factor

Smad – SMAD family proteins

SOX2 – SRY-box transcription factor 2

STAT – Signal transducer and activator of transcription

SVZ – Subventricular zone

TALE – Three amino acid loop extension (homeodomain protein family)

TAMs – Tumour-associated macrophages

TMZ – Temozolomide

TME – Tumour microenvironment

TP53 – Tumour protein p53

Tregs – Regulatory T cells

VEGF – Vascular endothelial growth factor

1. Introduction

1.1. Glioblastoma

1.1.1. Epidemiology

Glioblastoma (GB) is a fast-growing primary malignant tumour that arises in the central nervous system (CNS) (Hanif et al., 2017). GB accounts for 46.8% of all malignant CNS tumours, with a global incidence between 3 to 5 per 100,000 persons (Grochans et al., 2022). The incidence of this disease increases with age, typically presenting in individuals over 40 years of age, peaking at 75-84 years (Grochans et al., 2022). Pediatric GB is rarer, occurring in individuals aged 0-18 years at an incidence of 0.85 per 100,000 children, and accounts for 3-15% of pediatric primary brain tumours (Hanif et al., 2017). GB exhibits higher incidence in the male population, as epidemiological data shows a male-to-female ratio of 1.3-1.6:1 (Grochans et al., 2022). Furthermore, GB incidence varies by ethnicity and is more commonly observed in Caucasians compared to Black or Asian populations (Hanif et al., 2017). GB diagnosis appears higher in developed countries compared to developing nations with lower socioeconomic status and more limited access to health care and diagnostic tools (Grochans et al., 2022). GB patients exhibit poor survival despite multimodal treatments, with a median life expectancy of 15 months following diagnosis (Hanif et al., 2017; Sabouri et al., 2024). These trends point towards an urgent need for improved understanding of disease pathogenesis and the development of more effective treatment strategies aimed at improving patient outcomes (Hanif et al., 2017; Sabouri et al., 2024).

1.1.2. Standard Treatments and Limitations

The current standard treatment for GB includes maximal surgical tumour resection, followed by concurrent ionizing radiation (IR) and temozolomide (TMZ) chemotherapy (Stupp et al., 2005). Treatment remains a significant clinical challenge due to tumour invasiveness, recurrence and resistance to conventional therapies (Stupp et al., 2005). Surgical resection aims to reduce the tumour mass and its effects on surrounding brain structures, which can relieve some neurological symptoms and improve the effects of subsequent IR and TMZ; however, surgical resection is often limited by the location of the tumour in important brain areas, such as those responsible for locomotion and speech (Sanai et al., 2011). Complete tumour removal is further hindered by invasive cancer cells that migrate beyond the tumour margin to surrounding brain tissues (Sanai et al., 2011). IR targets remaining tumour cells, and in combination with chemotherapy, can improve median survival by 3 months (Stupp et al., 2005). IR induces single- and double-stranded breaks in DNA molecules of GB cells and generates reactive oxygen species (ROS) which interfere with normal cellular processes, leading to cell damage, cell cycle arrest and death (Stupp et al., 2005). Side effects of IR can include radiation necrosis of healthy brain tissue leading to cognitive issues and other neurological deficits, which is carefully balanced against therapeutic gains (Weller et al., 2013). TMZ is an oral alkylating agent which induces DNA damage and enhances sensitivity of GB cells to IR (Stupp et al., 2005). TMZ works by adding alkyl groups to the O6 position of guanine, which mismatches with thymine during DNA replication (Stupp et al., 2005). The GB cell's mismatch repair (MMR) system subsequently aims to repair the mispairing but fails to remove the alkyl group, and instead can only excise the thymine from the newly synthesized DNA strand (Stupp et al., 2005). After several repair attempts, replication becomes stalled, DNA strand breaks accumulate and the cell enters cell

cycle arrest and apoptosis (Stupp et al., 2005). TMZ is most effective for GB cells which have O6-methylguanine-DNA methyltransferase (MGMT) promoter methylation, which leads to epigenetic silencing of the MGMT gene (Hegi et al., 2005). MGMT encodes a DNA repair enzyme which can remove the alkyl groups introduced by TMZ, thereby counteracting its cytotoxic effects (Hegi et al., 2005). 35-45 % of GB patients exhibit MGMT promoter methylation, and show increased overall survival compared to their counterparts with unmethylated MGMT promoters (Hegi et al., 2005; Dunn et al., 2009).

Despite these conventional therapies which modestly improve overall survival, treatment limitations remain significant due to intratumoural and interpatient heterogeneity, which results in variable therapeutic responses and promotes the emergence of resistance mechanisms (Bao et al., 2006; Carruthers et al., 2018). The genetic and phenotypic heterogeneity of GB tumours confers a major survival advantage, as the cancer cells can adapt and respond to changes in their environment to evade therapy (Bao et al., 2006). Radioresistance mechanisms include preferential activation of DNA damage checkpoint response and enhanced DNA repair signalling in glioma stem-like cells following IR (Bao et al., 2006; Carruthers et al., 2018). TMZ chemotherapy improves the median survival of GB patients by just 3 months, due to intrinsic and adaptive TMZ-resistant cancer cell subpopulations that proliferate and differentiate to repopulate tumours (Stupp et al., 2005; Begicevic & Falasca, 2017). GB cells develop resistance to TMZ through various pathways, including increased DNA repair, inhibition of apoptosis pathways, and enhanced drug efflux via ATP-binding cassette (ABC) transporters (Begicevic & Falasca, 2017). Tumour recurrence is typically seen within 6-9 months post-treatment in 90 % of GB

patients, and these recurrent tumours exhibit heightened resistance to IR and TMZ, highlighting the urgent need for novel therapeutics (Stupp et al., 2005; Bao et al., 2006).

Additionally, conventional treatment regimens can result in neurotoxicity, which may compromise patient quality of life (Makale et al., 2017). Experimental approaches such as targeted molecular therapies and immunotherapies have shown limited clinical success due to the genetic heterogeneity of GB and the immunosuppressive nature of the tumour microenvironment (Zhou et al., 2025). Additionally, the blood-brain barrier (BBB) poses a major obstacle to proper drug delivery, as it limits the penetration of many potentially effective therapeutics into the tumour microenvironment (TME), thereby reducing their efficacy (Deeken & Loscher, 2007). Consequently, while standard therapies have modestly improved median survival, poor long-term patient survival necessitates a greater understanding of GB pathogenesis, such that new drug targets can be identified and more effective therapeutic strategies can be developed (Stupp et al., 2005; Bao et al., 2006).

1.1.3. Interpatient and Intratumoural Heterogeneity

GB exhibits interpatient heterogeneity, with tumours differing between patients in their genetic, epigenetic and phenotypic profiles (**Figure 1**) (Verhaak et al., 2010; Brennan et al., 2013). The genetic and phenotypic diversity of GB cells influences disease progression, treatment response and patient survival. GB is classified into the following distinct molecular subtypes: classical, proneural and mesenchymal (Verhaak et al., 2010; Brennan et al., 2013). Each subtype is characterized by unique patterns of gene expression, mutations and signalling pathway over- or under-activation (Verhaak et al., 2010; Brennan et al., 2013).

The classical subtype of GB is characterized by amplification of the epidermal growth factor receptor (EGFR) gene, deletion of cyclin-dependent kinase inhibitor 2A (CDKN2A), and a lack of tumour protein 53 (TP53) mutations (Verhaak et al., 2010; Brennan et al., 2013). EGFR amplification is also associated with the presence of the truncated mutant form EGFR variant III (EGFRvIII), which is constitutively active, leading to unregulated cell survival and proliferation (Verhaak et al., 2010; Brennan et al., 2013). Loss of CDKN2A causes deregulation of the cell cycle and inhibition of key tumour suppressors, such as p16INK4a and p14ARF (Verhaak et al., 2010; Brennan et al., 2013). Consequently, in the absence of these key tumour suppressors, the cell's ability to halt cell cycle progression and induce apoptosis is disrupted (Verhaak et al., 2010; Brennan et al., 2013). Despite maintaining wild-type TP53, its tumour suppressor function may be impacted by amplified mouse double minute 2 (MDM2) which targets p53 for proteasomal degradation (Verhaak et al., 2010). Additionally, the loss of p14ARF leads to MDM2 overactivity, as p14ARF normally inhibits MDM2 under physiologic conditions (Verhaak et al., 2010; Brennan et al., 2013). Classical GB tumours tend to have upregulated Notch and sonic hedgehog (SHH) signalling pathways, resulting in highly proliferative, undifferentiated cells with aggressive growth and resistance to apoptosis (Verhaak et al., 2010).

The proneural subtype occurs more frequently in younger patients, under 40 years of age, and is associated with a better prognosis (Verhaak et al., 2010; Lin et al., 2014). Proneural GB contains mutations in platelet-derived growth factor receptor alpha (PDGFRA), isocitrate dehydrogenase 1 (IDH1), and TP53 genes (Verhaak et al., 2010; Brennan et al., 2013). Amplification and activating mutations in PDGFRA promote downstream signalling pathway

activation, including Phosphoinositide 3-kinase/Protein kinase B (PI3K/AKT) and rat sarcoma viral oncogene homolog/Mitogen-Activated Protein Kinase (RAS/MAPK), which drive tumour survival, proliferation, and invasion (Verhaak et al., 2010; Brennan et al., 2013). Mutations in TP53 result in the loss of its tumour suppressor function and unchecked cell survival and proliferation even in the presence of DNA damage induced by conventional therapeutics (Verhaak et al., 2010; Brennan et al., 2013). Another feature of proneural GB is metabolic and epigenetic reprogramming due to mutations in the IDH1 gene (Verhaak et al., 2010; Brennan et al., 2013; Dang et al., 2009). Instead of producing its normal metabolite, mutant IDH1 generates 2-hydroxyglutarate (2-HG), which interferes with DNA and histone demethylating enzymes (Dang et al., 2009). This epigenetic reprogramming contributes to a pattern of CpG island hypermethylation at gene promoters, particularly at key tumour suppressor genes and differentiation-related genes, inhibiting differentiation and promoting a stem cell-like phenotype (Dang et al., 2009). Furthermore, the transcriptional profile of proneural GB mimics that of early brain development, due to activation of genes related to neural stem cells and oligodendrocyte precursor cells (Verhaak et al., 2010; Kriegstein & Alvarez-Buylla, 2009). This proneural transcriptional profile explains this subtype's neural progenitor-like phenotype and may point to its origin from a neural stem-like or progenitor-like cells (Brennan et al., 2013; Tirosh et al., 2016).

Mesenchymal GB is characterized by its highly invasive, angiogenic and inflammatory phenotype, as well as overexpression of mesenchymal markers, such as CHI3L1, CD44, and STAT3 (Phillips et al., 2006; Verhaak et al., 2010; Zhang et al., 2021). It is considered one of the most aggressive and treatment-resistant subtypes, exhibiting frequent inactivation or loss of

neurofibromatosis 1 (NF1), resulting in unchecked RAS pathway activation, which leads to tumour growth and invasion to surrounding tissue (Brennan et al., 2013; Verhaak et al., 2010). Mutations in key tumour suppressors, TP53 and phosphatase and tensin homolog (PTEN), hinder cell cycle regulation, resulting in highly proliferative cells with increased activation of anti-apoptotic pathways (Brennan et al., 2013; Verhaak et al., 2010). Mesenchymal GB also frequently displays upregulation of pro-inflammatory genes and those associated with tumour-associated macrophages (TAMs), such as interleukin 6 (IL6), IL8, chemokine (C-C motif) ligand 2 (CCL2), which promote tumour growth, invasion and angiogenesis (Hara et al., 2021; Hambardzumyan et al., 2016). This subtype has increased activation of nuclear factor-kappa B (NF-kB) signalling which drives inflammation by upregulating key cytokines, chemokines and adhesion molecules which promote the recruitment of immune cells, including TAMs (Bhat et al., 2013). These TAMs display M2-polarization which is associated with an immunosuppressive and pro-tumourigenic response (Hambardzumyan et al., 2016; Quail & Joyce, 2017). Infiltrating TAMs secrete growth factors which promote angiogenesis, matrix remodelling proteases that facilitate cell invasion, and anti-inflammatory cytokines which allow the tumour to evade immune surveillance (Quail & Joyce, 2017). Additionally, NF-kB signalling enhances the tumour's resistance to apoptosis, allowing the cells to resist therapeutic stress (Bhat et al., 2013). Notably, exposure to conventional therapeutics is associated with recurrent tumours which display the mesenchymal signature, even if the original tumour was classified as proneural or classical (Phillips et al., 2006). This is believed to be a result of selective pressure, which eliminates more treatment-sensitive cancer cells, leaving behind mesenchymal-like clones which repopulate the tumour (Bao et al., 2006; Wang et al., 2017). This underscores the role of the

mesenchymal-like gene signature and its associated NF-kB signalling in driving therapeutic resistance and tumour recurrence (Bhat et al., 2013; Wang et al., 2017).

Interpatient heterogeneity involves genetic mutations, epigenetic reprogramming, metabolic reprogramming, and changes in the tumour microenvironment (TME), including variations in immune cell type and abundance (Patel et al., 2014; Lathia et al., 2015). All these factors contribute to the tumour's distinct phenotype, behaviour, and varying response to therapy, thus therapeutics that are effective for one subtype may be ineffective for another (Phillips et al., 2006; Verhaak et al., 2010). Furthermore, single-cell RNA sequencing data of GB tumours have revealed that within an individual tumour, transcriptional features of multiple subtypes may be found (Patel et al., 2014; Neftel et al., 2019). Intratumoural heterogeneity, whereby individual tumours contain genetically and phenotypically distinct subpopulations, poses an added layer of complexity for treatment strategies (Sottoriva et al., 2013; Lathia et al., 2015). This diversity in cancer cell populations arises from tumour evolution under selective pressures from IR and TMZ, resulting in subclones with varied capacities for proliferation, therapeutic resistance and stemness which may provide a selective advantage for survival (Liau et al., 2017; Wang et al., 2017). Longitudinal transcriptomic analyses of pre-treatment and recurrent GB samples have shown that subtype identity is not fixed as only 55% of tumours retain their original molecular subtype upon recurrence, and up to 66% may undergo subtype switching (Wang et al., 2017). Proneural and classical tumours are more likely to transition into a mesenchymal phenotype under the selective pressures of conventional therapy. This shift towards the mesenchymal signature is believed to result from the enhanced survival and expansion of therapy-resistant stem-like subclones, further enhancing the malignancy of recurrent tumours (Liau et al., 2017).

Even prior to selective pressures imposed by treatment, BTSCs contribute to this heterogeneity via their capacity for persistent self-renewal, differentiation into multiple cell lineages, and dynamic adaptation to extrinsic cues (Lathia et al., 2015). This evolving and intrinsic plasticity poses a significant challenge to effective therapy and complicates clinical management (Sottoriva et al., 2013; Lathia et al., 2015). Single biopsies often fail to capture this heterogeneity; therefore, to more accurately classify the tumour, multi-region biopsies should be performed and integrated with comprehensive genetic, epigenetic and proteomic profiling (Sottoriva et al., 2013; Lathia et al., 2015). Understanding and addressing both intra- and inter-tumoural heterogeneity is essential for the development of patient tailored therapeutic strategies to prevent tumour recurrence (Neftel et al., 2019; Lathia et al., 2015).

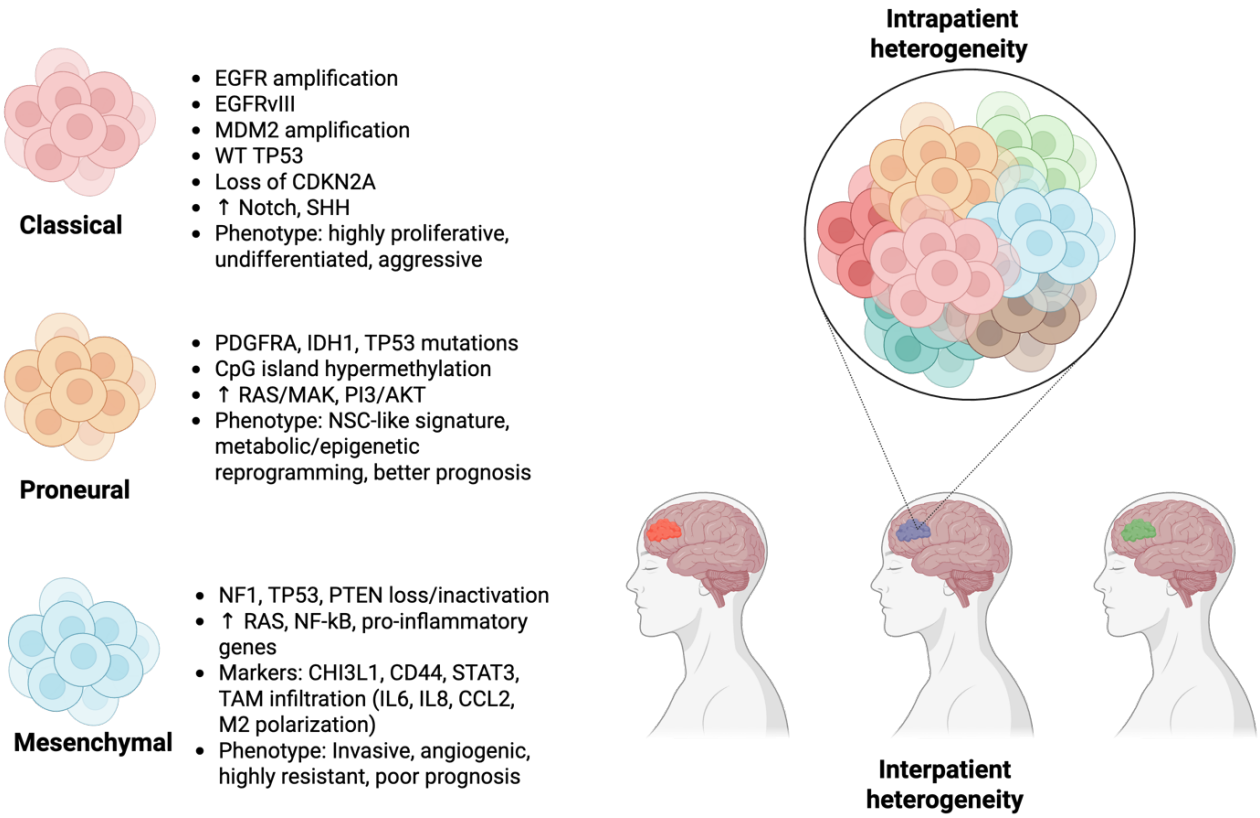

Figure 1. GB intrapatient and interpatient heterogeneity. GB displays significant interpatient and interpatient diversity, with tumours classified as classical, proneural, or mesenchymal subtypes, each defined by unique genetic, signalling, and phenotypic profiles. Major subtypes are shown with their defining gene alterations, signalling pathways, and clinical features. This heterogeneity is dynamic, as subtype identity is not fixed: only about 55% of tumours retain their original molecular subtype upon recurrence, while up to 66% undergo subtype switching, often transitioning towards the more aggressive, therapy-resistant mesenchymal phenotype. Created using Biorender.com.

1.1.4. Models of Heterogeneity

Multiple models have been proposed to explain the interpatient heterogeneity, intratumoural heterogeneity, and plasticity observed in GB (Greaves & Maley, 2012; Sottoriva et al., 2013). The clonal evolution model proposes that GB develops from single transformed progenitor cells that accumulate mutations over time, leading to genetically distinct subclones via natural selection (Greaves & Maley, 2012). Clones with the highest fitness tend to grow and dominate, driven by selective pressures of the environment, including oxygen level, nutrient level, pH level and immune cell infiltration (Sottoriva et al., 2013; Wang et al., 2016). Additionally, therapeutic interventions add another layer of selection pressure, often leading to the survival and expansion of treatment-resistant subclones (Lan et al., 2017; Wang et al., 2016). In contrast, the cancer stem cell (CSC) model proposes that a subset of self-renewing stem-like cells promote tumour heterogeneity by differentiating into multiple cell lineages with diverse transcriptional landscapes and varied sensitivities to conventional treatment (Chen et al., 2012; Suvà & Tirosh, 2020).

These two models may not be mutually exclusive, with emerging evidence supporting a hybrid model in which GB exhibits both clonal evolution and a degree of hierarchical organization, with CSC at the top of the hierarchy and more differentiated subclones at the bottom (Patel et al., 2014; Lan et al., 2017). Spatial analyses of GB tumours have revealed that different tumoural regions support varied cellular behaviours, with specific TME niches fostering invasive, proliferative, or therapy-resistant phenotypes, thereby supporting the clonal evolution model (Sottoriva et al., 2013; Wang et al., 2016). Studies using single-cell RNA sequencing and lineage tracing have also shown that GB cells are highly plastic and can shift between stem-like and differentiated states, driven by signals from the surrounding TME (Neftel et al., 2019; Suvà & Tirosh, 2020). This ability to switch identity from CSC to non-CSC contributes to therapeutic resistance and tumour recurrence, by allowing the cells to dynamically respond to environmental cues such as hypoxia, nutrient deprivation, and therapeutic stress (Lan et al., 2017; Neftel et al., 2019). Understanding these models of heterogeneity highlight the central role of CSC in driving GB heterogeneity, plasticity, and treatment resistance, setting the stage for a deeper understanding of their regulatory networks and clinical significance.

1.2. Brain Tumour Stem Cells

1.2.1. Developmental Origins

BTSCs are widely implicated in GB initiation, maintenance, and therapeutic resistance (Chen et al., 2012; Singh et al., 2003). According to the CSC hypothesis, BTSCs represent a subpopulation within the tumour that exhibit many features of neural stem cells (NSCs), including self-renewal, multilineage differentiation, persistent proliferation, and expression of neural stem cell markers such as prominin-1 (CD133), Nestin, and SRY-box transcription factor 2 (SOX2) (Bao et al., 2006; Rich & Eyler, 2009; Singh et al., 2003). These cells are thought to originate either from neural precursor cells that revert to a less differentiated state or from NSCs in the subventricular zone (SVZ) that acquire oncogenic mutations and migrate to other brain regions to initiate tumour formation (**Figure 2**) (Azzarelli et al., 2018; Valor & Hervás-Corpión, 2020). Lineage-tracing studies in mouse models have demonstrated that mutations in key tumour suppressor genes (TP53, PTEN) or oncogenes (EGFR) within NSCs are sufficient to initiate GB tumours, reinforcing the correlation between NSCs that undergo malignant transformation (Alcantara Laguno et al., 2015; Wang et al., 2019).

Although BTSCs have many molecular features in common with normal NSCs, they also harbour distinct genetic and epigenetic alterations that endow them with tumourigenic potential and therapeutic resistance (Singh et al., 2004; Bao et al., 2006). While NSCs tightly regulate their signalling networks, such as Notch, Wnt, and SHH, these pathways are often dysregulated in BTSCs, contributing to uncontrolled cell growth, inhibition of differentiation, maintenance of stemness, and tumour progression (Lathia et al., 2015; Liu et al., 2006). In addition to their

proliferative capabilities, BTSCs can adopt a dormant or slow-cycling state, allowing them to survive conventional therapies that target actively dividing cells (Bao et al., 2006). These quiescent cells can later re-enter the cell cycle to repopulate the tumour, giving rise to diverse cell types and contributing to recurrence (Rich & Eyler, 2009).

1.2.2. Role in Tumour Initiation, Progression, and Recurrence

BTSCs play a key role in GB tumour initiation, progression, and recurrence due to their capacity for persistent self-renewal, differentiation, and therapeutic resistance (**Figure 2**) (Singh et al., 2004; Chen et al., 2012). These cells possess higher tumourigenic potential compared to the bulk tumour cell population, as highlighted by their ability to initiate tumours when transplanted into immuno-compromised mice (Singh et al., 2004; Galli et al., 2004). Due to their genetic plasticity, BTSCs also give rise to the heterogeneous cellular landscape observed in GB tumours. During tumour progression, BTSCs contribute to intratumoural heterogeneity by differentiating into multiple non-stem-cell GB lineages, each with distinct genetic features, phenotypes, and varied sensitivities to therapies, while maintaining a pool of self-renewing BTSCs (Lathia et al., 2015; Sottoriva et al., 2013). This plasticity allows them to adapt and survive in the face of different environmental pressures, including hypoxia, lack of nutrients, IR and TMZ chemotherapy (Heddleston et al., 2009; Bao et al., 2006).

BTSCs are heavily implicated in tumour recurrence, as they are more resistant to conventional treatments compared to more differentiated GB cells (Bao et al., 2006; Lathia et al., 2015). Over 90% of GB tumours recur, despite multimodal treatment, with a median time to recurrence of 6.9 months post-therapy (Stupp et al., 2005; Weller et al., 2013). BTSCs contribute significantly to

this high recurrence rate by employing various intrinsic and adaptive resistance mechanisms, including upregulating DNA damage repair pathways, which leads to increased expression of radiation sensitive protein 51 (RAD51) and MGMT, enabling repair of DNA breaks and alkylation caused by IR and TMZ (Bao et al., 2006; Blough et al., 2011). BTSCs also upregulate ABC transporters, ABCG2 and ABCC1, which facilitate TMZ drug efflux out of the cell, thereby reducing drug accumulation and cytotoxicity (Bleau et al., 2009; Lathia et al., 2015). Furthermore, BTSCs upregulate anti-apoptotic pathways through increased expression of BCL-2 family proteins and NF-kB signalling, which block pro-apoptotic pathways, even in the presence of cytotoxic stress induced by IR and TMZ (Heddleston et al., 2009; Eyler & Rich, 2008). In response to therapy-induced stress, BTSCs can also enter a dormant or slow-cycling state, thereby evading conventional treatments which target actively dividing cells (Bao et al., 2006; Lathia et al., 2015). Once conditions become more favourable, these dormant BTSCs then reenter the cell cycle to undergo persistent self-renewal and differentiation to repopulate heterogeneous tumours with a higher population of treatment-resistant subclones with a more aggressive mesenchymal phenotype (Lathia et al., 2015; Hara et al., 2021).

1.2.2.1 Dormancy

BTSC dormancy refers to a state of quiescence characterized by reversible exit from the cell cycle under unfavourable conditions, such as exposure to IR and TMZ chemotherapy, while retaining the potential for self-renewal and differentiation upon reactivation under more favourable conditions (**Figure 2**) (Chen et al., 2012; Rehman et al., 2021). This dormant or slow-cycling state plays a key role in therapeutic resistance and high rates of recurrence, as conventional treatments for GB are designed to target actively dividing cells (Chen et al., 2012;

Rehman et al., 2021). Researchers have explored the intrinsic and extrinsic factors that enter and maintain BTSCs in a dormant state, and have proposed that several TME cues promote dormancy, including hypoxia, nutrient deprivation, low pH, and immunomodulatory signals (Heddleston et al., 2009). Researchers demonstrated that hypoxia-inducible factors (HIFs), such as HIF-1a and HIF-2a, are upregulated in hypoxic tumour regions and induce a quiescent phenotype in GB cells (Heddleston et al., 2009). HIF signalling inhibits key pathways that drive proliferation, such as the myelocytomatosis oncogene (Myc) pathway which normally promotes ribosomal biogenesis, as well as cyclin D1, cyclin-dependent kinase 4 (CDK4) and E2F Transcription Factor 1 (E2F1) expression which are necessary for cell cycle progression (Heddleston et al., 2009). HIFs promote the expression of max interactor 1 (MXI1), a potent Myc inhibitor, which impedes Myc's transcriptional activity and downregulates its target genes (Koshiji et al., 2004). Intrinsic mechanisms employed by dormant BTSCs include upregulation of cyclin-dependent kinase inhibitors (CDKIs), including p21Cip1 and p27Kip1, which block the transition from the G1 phase to the S phase of the cell cycle, keeping cells in a non-dividing dormant state (Harper et al., 2016; Rehman et al., 2021).

Lineage-tracing studies support the importance of BTSC dormancy in facilitating tumour recurrence. Researchers showed that a population of labelled stem-like cancer cells were slow-cycling during TMZ treatment, survived cytotoxic stress due to their drug-tolerance, and gave rise to tumours under more favourable conditions (Rehman et al., 2021). These dormant cancer cells also showed an upregulation of genes associated with resistance to cytotoxic stress, as well as anti-apoptotic signalling (Rehman et al., 2021. The ability of BTSCs to enter dormancy, survive treatment, and contribute to tumour recurrence presents a significant challenge for GB

treatment, underscoring the need for greater understanding of the regulatory mechanisms that are employed, such that more effective therapeutics can be developed (Chen et al., 2012).

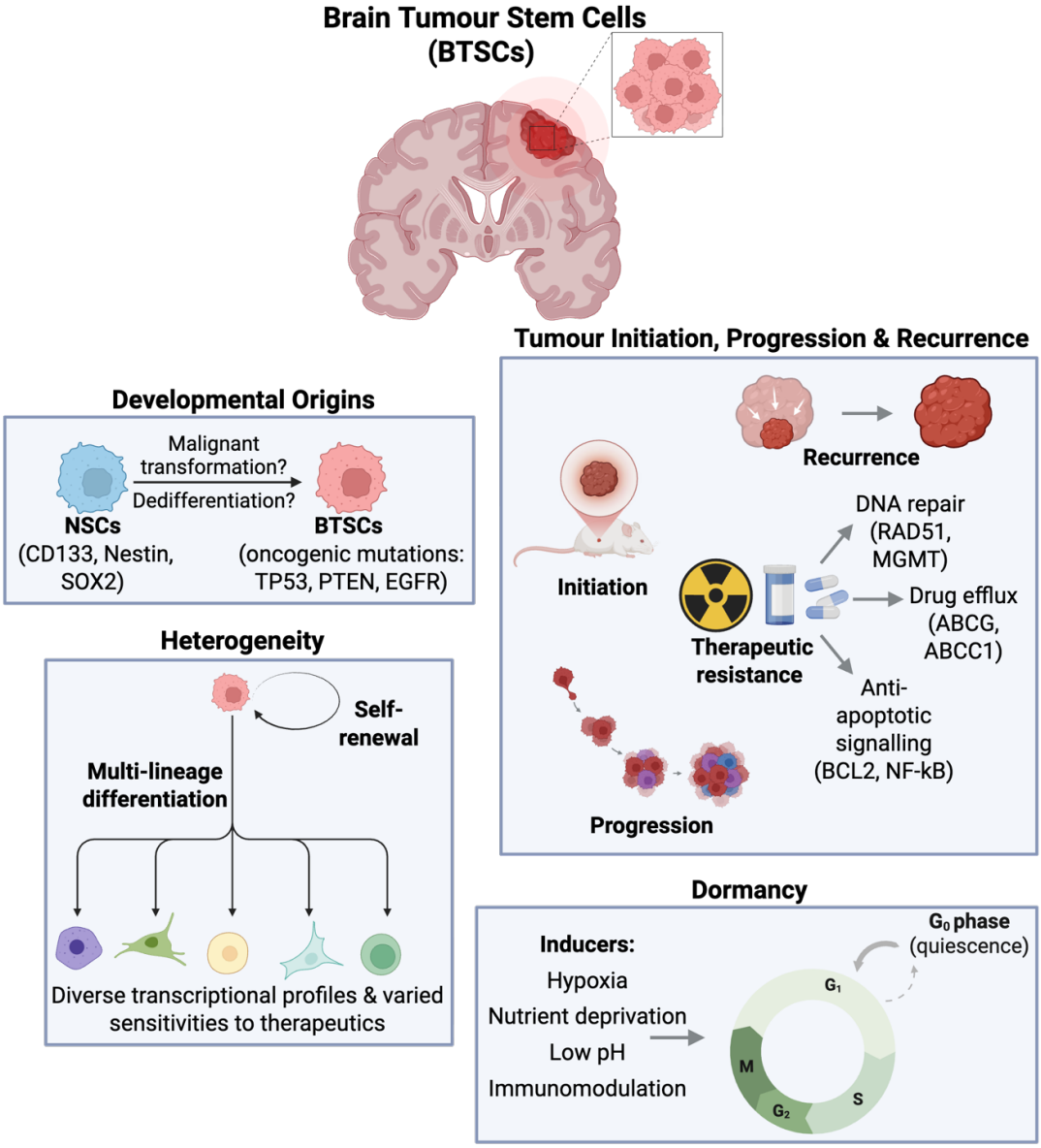

Figure 2. Developmental origins, features and roles of BTSCs in GB. BTSCs may originate from neural stem or precursor cells (NSC) via oncogenic mutations, acquire stemness and resistance features, and contribute to tumour initiation, heterogeneity, therapeutic resistance, and recurrence. Their survival is supported by dormancy, intrinsic defense mechanisms, and interactions with a tumour-permissive microenvironment. Created using Biorender.com.

1.2.3. EGFR/EGFRvIII/OSMR Signalling in BTSCs

EGFR signalling is one of the most frequently over-activated pathways in glioblastoma (GB) and plays a central role in regulating brain tumour stem cells (BTSCs) by promoting proliferation, survival, and self-renewal (Verhaak et al., 2010; Brennan et al., 2013; Li et al., 2023). Upon ligand binding, EGFR dimerizes and activates downstream signalling pathways, including PI3K/AKT, RAS/MAPK, and STAT, which collectively support BTSC maintenance, therapeutic resistance, and tumour progression (Taylor et al., 2012; Lee et al., 2018; Li et al., 2023). Despite extensive therapeutic efforts, targeting EGFR in GB has proven challenging due to pathway redundancy, compensatory signalling, and the presence of mutant receptor variants (Wen & Kesari, 2008; Gan et al., 2013).

EGFRvIII is a constitutively active, truncated EGFR variant present in approximately 20–30% of GB patients and is associated with aggressive tumour behaviour and reduced survival (Heimberger et al., 2005; Lorimer et al., 2025). Lacking part of the extracellular ligand-binding domain, EGFRvIII signals independently of ligand binding and persistently activates PI3K/AKT, RAS/MAPK, and STAT3 pathways, thereby enhancing BTSC proliferation, self-renewal,

invasion, and resistance to ionizing radiation and temozolomide (Huang et al., 1997; Heimberger et al., 2005; Shi et al., 2023). EGFRvIII also promotes angiogenesis and immune evasion through upregulation of VEGF and immunosuppressive cytokines such as IL-10 and TGF-β (Heimberger et al., 2008; Charles et al., 2012).

Further mechanistic insight revealed that EGFRvIII-driven oncogenic signalling is amplified through its interaction with the oncostatin M receptor (OSMR). OSMR is highly upregulated in EGFRvIII-expressing BTSCs and forms a complex with phosphorylated EGFRvIII or wild-type EGFR, leading to enhanced STAT3 activation and establishment of a feed-forward signalling loop that sustains tumourigenic signalling (Jahani-Asl et al., 2016). This EGFR/EGFRvIII/OSMR–STAT3 axis is critical for maintaining BTSC stemness, immune evasion, and therapeutic resistance, while also promoting a tumour-permissive microenvironment (Jahani-Asl et al., 2016; Yuan et al., 2025).

Notably, activation of this signalling axis induces expression of galectin-1 via direct STAT3 binding to the LGALS1 promoter (Sharanek et al., 2021). Galectin-1 subsequently interacts with the HOXA5 transcription factor to drive tumourigenic transcriptional programs that promote BTSC self-renewal, mesenchymal transformation, therapeutic resistance, and immune evasion (Sharanek et al., 2021). Disruption of galectin-1 genetically or pharmacologically impairs HOXA5 DNA binding and transcriptional activity, highlighting galectin-1 as a key downstream effector of EGFRvIII/STAT3 signalling in BTSCs, though the precise molecular mechanisms regulating this axis remain incompletely understood (Sharanek et al., 2021).

1.3. HOXA5

1.3.1. Structure and Mechanisms of Transcriptional Activity

HOXA5 is a member of the homeobox family of transcription factors, encoded by the HOXA5 gene located on human chromosome 7 (Pearson et al., 2005; Shah & Sukumar, 2010). It is characterized by a highly conserved 61-amino acid homeodomain responsible for DNA binding to specific genomic regions containing homeobox response elements within their promoters (**Figure 3**) (Pearson et al., 2005; Shah & Sukumar, 2010). This homeodomain, which contains a helix-turn-helix motif enables HOXA5 to precisely regulate gene transcription in a temporally and spatially coordinated manner during embryogenesis, organogenesis, and tissue homeostasis (McGinnis & Krumlauf, 1992).

Beyond its DNA-binding region, HOXA5 contains domains that facilitate the recruitment of transcriptional co-regulators, including chromatin modifiers and histone-modifying enzymes, thereby functioning as either a transcriptional activator or repressor depending on the cellular context (Shah & Sukumar, 2010; Bhatlekar et al., 2014). The N-terminal region of HOXA5 (amino acids 1-75) is essential for its regulatory function, primarily by mediating protein-protein interactions that enable the formation of transcriptional complexes (Ritesh et al., 2024). During embryonic development, HOXA5 interacts with suppressed cAMP-inducible POU (SCIP), a neural transcription factor, through this N-terminal domain to cooperatively regulate gene expression (Ritesh et al., 2024). This function aligns with findings in other HOX proteins, such as HOXC9, whose N-terminal arm binds the mad homology 1 (MH1) domain of mothers against

decapentaplegic homolog 4 (Smad4), a key TGF-B signalling mediator, critical for transcriptional modulation (Zhou et al., 2008).

Adjacent to the N-terminus is a predicted intrinsically disordered region (amino acids 75-175), which lacks a fixed 3D structure, enabling flexible binding to multiple partners (De Kumar & Darland, 2021). This region contains a hexapeptide (YPWM) domain facilitating transient interactions with pre-B-cell leukemia transcription factors (PBX) cofactors from the three-amino acid loop extension homeodomain (TALE) homeodomain family, altering DNA-binding specificity and enabling fine-tuned gene expression regulation (De Kumar & Darland, 2021). Such intrinsically disordered regions are frequently targeted by post-translational modifications like phosphorylation, acetylation, or ubiquitination, further regulating HOXA5's transcriptional activity (De Kumar & Darland, 2021). The most well-characterized region is its homeobox domain (amino acids 195-257) enabling sequence-specific DNA binding to promoters of key genes such as TP53, cyclin-dependent kinase inhibitor 1A (CDKN1A), and protein tyrosine phosphatase receptor type Z1 (PTPRZ1), thereby regulating cell cycle arrest, apoptosis, and DNA repair (Gendronneau et al., 2010; He et al., 2022; Jeannotte et al., 2016). Collectively, the N-terminal, disordered, and homeobox domains mediate protein interactions, modulate DNA-binding specificity, and enable target gene recognition.

HOXA5 function is modulated by post-translational modifications such as phosphorylation, which influence its activity and interactions. It also cross-talks with tumour suppressors like p53, enhancing p53-mediated cell cycle arrest and apoptosis in some cancer contexts (Raman et al., 2000; Bhatlekar et al., 2014). In GB, however, HOXA5 is frequently overexpressed and appears

oncogenic. This overexpression is in part a result of gene amplification due to gain of chromosome 7, which is common in isocitrate dehydrogenase (IDH) wild-type GB, contributing to tumour aggressiveness and poor prognosis (Cimino et al., 2018). Epigenetic mechanisms, such as promoter hypermethylation and histone modifications, also regulate HOXA5 expression, especially in IDH-mutant GB, where overexpression coexists with promoter hypermethylation linked to worse outcomes (Mamatjian et al., 2023; Ding et al., 2021).

Importantly, HOXA5's oncogenic activity in GB depends on its interaction with galectin-1, a protein upregulated downstream of EGFRvIII/OSMR/STAT3 signalling (Sharanek et al., 2021). Galectin-1 binds HOXA5, redirecting its genomic binding to drive transcriptional programs supporting BTSC self-renewal, mesenchymal transformation, immune evasion, and therapy resistance (Sharanek et al., 2021). Loss of galectin-1 impairs HOXA5's regulation of these gene networks, making the HOXA5/galectin-1 axis a promising therapeutic target in EGFRvIII-positive GB (Sharanek et al., 2021).

1.3.2 Physiological Functions

1.3.2.1. Role in Embryogenesis

HOXA5 plays a central role in embryonic development and tissue homeostasis by regulating genes involved in proliferation and differentiation (**Figure 3)** (Krumlauf, 1994; Mallo et al., 2010). HOXA5 spatially and temporally regulates specific genes that direct proper anterior-posterior axis formation and organogenesis at the correct developmental stages (Krumlauf, 1994;

Mallo et al., 2010). During early embryogenesis, HOXA5 expression is tightly regulated such that it is restricted to regions that will form the axial skeleton, respiratory tract, lungs, and gastrointestinal system (Warot et al., 1997; Mallo et al., 2010). This regulation is controlled by morphogen gradients such as retinoic acid and by transcriptional repressors and activators that restrict HOXA5 expression to specific body regions (Warot et al., 1997; Packer et al., 2000; Mallo et al., 2010). Spatiotemporal control is further achieved via enhancer elements and chromatin modifications that limit HOXA5 transcription to defined embryonic locations (Boucherat et al., 2009). Experimental knockout models in mice demonstrate that loss of HOXA5 results in abnormal skeletal patterning, defective lung development, and malformations of the trachea and esophagus, underscoring its essential role in normal organogenesis (Warot et al., 1997; Manley & Capecchi, 1998).

At the molecular level, HOXA5 regulates genes involved in cell cycle arrest such as p21 and TP53 to coordinate cellular proliferation and differentiation timing, thereby ensuring proper tissue patterning and organ formation (Raman et al., 2000). It also promotes epithelial cell differentiation and epithelial integrity by upregulating E-cadherin and suppressing epithelial-to-mesenchymal transition (EMT) (Bhatlekar et al., 2014; Teo et al., 2016). Furthermore, HOXA5 contributes to vascular development by regulating VEGF expression that directs angiogenesis and circulatory system formation during embryogenesis (Jeannotte et al., 2016). Together, these findings highlight HOXA5 as a key developmental regulator whose precise spatial and temporal control is essential for normal organogenesis and tissue differentiation.

1.3.2.2. Role in Hematopoiesis

HOXA5 continues to regulate cellular proliferation and differentiation in adult tissues within the hematopoietic system (**Figure 3)**. HOXA5 regulates hematopoietic stem and progenitor cell (HSPC) lineage commitment by binding to promoter and enhancer regions of key hematopoietic genes to control their self-renewal, survival, proliferation, and differentiation, thereby maintaining hematopoietic homeostasis (Yang et al., 2015; Jeannotte, 2016). HOXA5 tightly regulates the balance between self-renewal and differentiation into myeloid and lymphoid lineages through the regulation of other lineage-specifying transcription factors (Steens & Klein 2022; Jeannotte, 2016).

Abnormal HOXA5 expression correlates with dysregulated hematopoiesis and malignant transformation. In acute myeloid leukemia (AML), HOXA5 overexpression is frequently observed and associated with blocked differentiation, therapeutic resistance, and worse patient outcomes (Argiropoulos & Humphries, 2007; Yang et al., 2021; Jeannotte, 2016). HOXA5 overexpression contributes to the failure of HSPCs to properly differentiate into mature blood cells, leading to the accumulation of immature blasts, a hallmark of AML, contributing to impaired blood cell formation and weakened immune function (Argiropoulos & Humphries, 2007). Moreover, elevated HOXA5 levels have been implicated in promoting resistance to conventional therapies due to over-activation of survival pathways and inhibition of apoptotic pathways in AML cells (Argiropoulos & Humphries, 2007; Yang et al., 2021). Consequently, patients with HOXA5 overexpression tend to experience more aggressive cancer progression and worse clinical outcomes, underscoring the importance of HOXA5's tight regulation of its target

genes in maintaining normal hematopoiesis and preventing malignant transformation (Yang et al., 2021).

1.3.3. Pathological Functions

HOXA5 plays important roles in various pathological states, including cancer, morphological abnormalities, and metabolic disease. In cancer, HOXA5 functions in a context-specific manner wherein it can act as a tumour suppressor or oncogene depending on the cancer type (Bhatlekar et al., 2014; Shah & Sukumar, 2010). When acting as a tumour suppressor, HOXA5 promotes p53-driven differentiation and apoptosis (Raman et al., 2000; Bhatlekar et al., 2014). Conversely, as an oncogene, it supports transcriptional programs involving cell cycle progression, DNA repair, and stemness by modulating key pathways, including Wnt/B-catenin and Notch signalling (Ding et al., 2021; Fan et al., 2022). HOXA5's tissue-specific expression can be epigenetically regulated, with silencing by promoter hypermethylation or overexpression via gene amplification (Shah & Sukumar, 2010; Cimino et al., 2018).

In breast carcinoma, HOXA5 usually functions as a tumour suppressor by directly binding and driving transcription of TP53 (Raman et al., 2000; Fan et al., 2022). In breast cancer cell lines, HOXA5 was shown to interact with the oncogenic transcription factor Twist, thereby impeding Twist-mediated suppression of p53 target genes (Stasinopoulos et al., 2005). HOXA5 expression is typically downregulated in breast cancers due to hypermethylation of its promoter, correlating with more aggressive tumour phenotypes and poorer prognoses (Raman et al., 2000; Stasinopoulos et al., 2005).

Similarly, in non-small-cell lung cancer (NSCLC), HOXA5 acts as a tumour suppressor where higher expression is linked to reduced invasion, metastasis, and improved patient survival (Fan et al., 2022). HOXA5 impairs cytoskeletal remodelling by downregulating genes such as actin-related protein 2/3 complex (Arp 2/3,) paxillin (PXN), and PAK1, and cooperates with p53 to suppress MMP2, limiting tumour invasion (Fan et al., 2022). Promoter hypermethylation-mediated silencing of HOXA5 has also been reported in gastric and colorectal cancers, contributing to tumour progression (Fan et al., 2022). In gastric cancer, HOXA5 inhibits proliferation by upregulating p21 and suppressing PI3/AKT signalling (Fan et al., 2022; Peng et al., 2018). In colorectal cancer, it promotes differentiation by antagonizing Wnt/β-catenin signalling, reducing CSC features and tumour growth (Fan et al., 2022).

In contrast, HOXA5 is frequently overexpressed and acts as an oncogene in GB. HOXA5 overexpression correlates with IDH wild-type status, unmethylated MGMT, enhanced proliferation, radioresistance, and worse survival, attributable to activation of DNA repair pathways and dysregulated cell cycle (Ding et al., 2021). Similarly, in acute myeloid leukemia (AML), elevated HOXA5 expression is associated with higher blast counts and poorer outcomes (Yang et al., 2021; Argiropoulos & Humphries, 2007).

Beyond cancer, HOXA5 has significant roles in non-malignant states, particularly in development and metabolism. During embryogenesis, HOXA5 is essential for proper lung and respiratory tract formation. Mice deficient in HOXA5 exhibit perinatal lethality from respiratory distress due to defective tracheal and lung development (Warot et al., 1997; Boucherat et al., 2009). These mice also show abnormalities in diaphragm innervation and, if they survive,

develop emphysema-like lung pathology and goblet cell metaplasia, indicating ongoing roles for HOXA5 in pulmonary homeostasis post-development (Boucherat et al., 2009). Thyroid gland development is also affected in HOXA5-deficient mice, which display abnormal follicles and hypothyroidism (Meunier et al., 2003; Boucherat et al., 2009). In the gastrointestinal tract, HOXA5 regulates epithelial differentiation to maintain a balance between secretory and absorptive cells, crucial for gut homeostasis; loss of HOXA5 leads to goblet cell hyperplasia and diminished zymogenic cells, impairing GI function and contributing to tumourigenesis (Thompson et al., 2018; Bhatlekar et al., 2014). Furthermore, HOXA5 exerts protective effects in metabolic disease by promoting M2 macrophage polarization, thereby suppressing inflammation during obesity-associated adipose tissue expansion (Cao et al., 2019). Overall, the diverse roles of HOXA5 in both malignant and non-malignant states highlight its importance as a tightly regulated transcriptional factor, whose dysregulation can significantly influence development, cellular homeostasis, and disease progression.

1.3.3.1. Role in BTSCs of GB

HOXA5 is a critical oncogenic driver in GB, especially in IDH wild-type tumours where the HOXA5 gene is often amplified (**Figure 3**) (Cimino et al., 2018). The degree of HOXA5 overexpression correlates with tumour aggressiveness and predicts a worse prognosis and lower patient survival (Cimino et al., 2018; Ding et al., 2021). Researchers have shown that impaired HOXA5 expression also impedes tumour-sphere formation, lowers invasiveness, and limits the self-renewal capacity of BTSCs (He et al., 2022; Suva et al., 2014). In contrast, HOXA5 overexpression enhances tumour-sphere size and self-renewal capacity, highlighting the role of HOXA5 in regulating stem cell characteristics (He et al., 2022; Suva et al., 2014).

Mechanistically, researchers showed that HOXA5 can directly bind to the promoter region of the PTPRZ1 gene, which encodes a receptor-type protein tyrosine phosphatase, upregulating its expression which drives BTSC self-renewal and invasive behavior (He et al., 2022). PTPRZ1-overexpressing BTSCs cells exhibit higher expression of stem-cell markers, enhanced tumour-sphere formation, and increased tumour initiating potential in mouse models (He et al., 2022). PTPRZ1 also promotes BTSC invasiveness in response to modulation by its ligand, pleiotrophin (PTN), which is secreted by TAMs of the TME. This event results in downstream activation of B-catenin and PI3K/AKT pathways, which promotes cytoskeletal remodelling and upregulation of MMPs, thereby enhancing cellular motility and degradation of the ECM which facilitate BTSC invasion (Papadimitriou et al., 2023).

Furthermore, researchers have shown that HOXA5 overexpression in murine models accelerates tumour growth and increases proliferation, as indicated by elevated Ki-67 staining. HOXA5 overexpression also upregulates transcriptional programs that promote cell cycle progression and DNA damage repair, thereby shortening survival rates in mice (He et al., 2022). Additionally, *in-vitro* studies using glioma cell lines indicate that HOXA5 promotes radioresistance, as cells exhibiting HOXA5 overexpression proliferated more quickly after exposure to IR and had reduced γ-H2AX levels, reflecting fewer double stranded breaks in DNA due to enhanced DNA repair (Cimino et al., 2018). These cells also had reduced activation of apoptosis and checkpoint regulators, including p53, p21, and Bcl2-associated X apoptosis regulator (BAX), indicating that HOXA5 increases survival in the face of cytotoxic stress from IR (Cimino et al., 2018). HOXA5 overexpression often results from gene amplification due to the gain of whole chromosome 7, which is an early and common event in IDH wild-type GB (Cimino et al., 2018). This indicates

that HOXA5 amplification confers a selective advantage, correlating with increased tumour aggressiveness, faster disease progression, and lower patient survival (Cimino et al., 2018; Ding et al., 2021). Together, these findings highlight HOXA5 as a key regulator of BTSC characteristics, making it a promising therapeutic target to disrupt BTSC-mediated tumour maintenance, invasion, and therapeutic resistance.

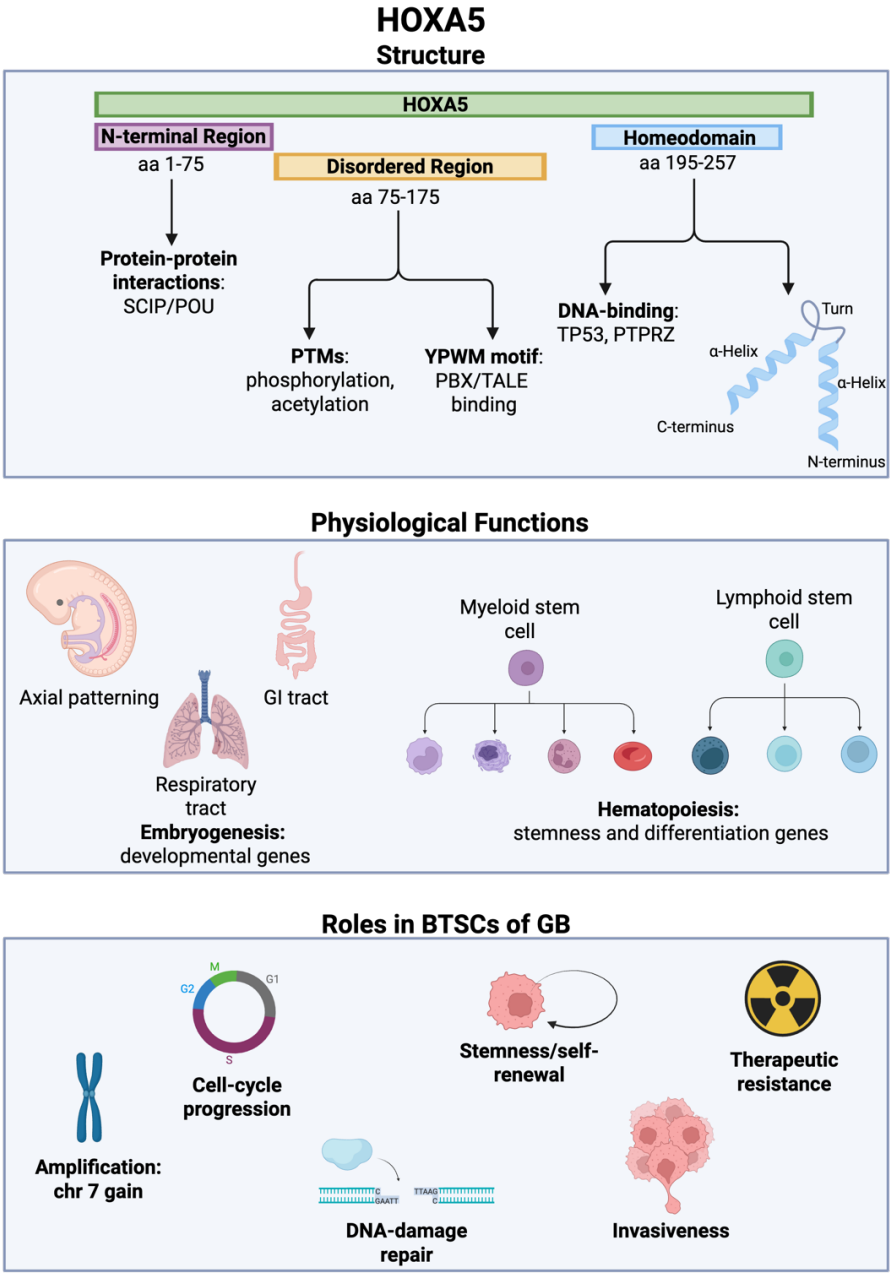

Figure 3. Structure and multifaceted roles of HOXA5. HOXA5 contains three main functional domains: an N-terminal protein interaction region, an intrinsically disordered cofactor-binding domain, and a conserved homeobox DNA-binding domain. It regulates gene expression by binding key target promoters involved in cell cycle, apoptosis, and differentiation. Under physiological conditions, HOXA5 regulates embryonic development and hematopoiesis. In GB, it functions as an oncogene, where it enhances BTSC proliferation, DNA repair, stemness, and radioresistance. Created using Biorender.com.

1.4. Galectin-1

1.4.1. Structure

Galectin-1 is a lectin protein characterized by a conserved carbohydrate recognition domain (CRD) that binds B-galactoside sugars on glycoproteins and glycolipids (**Figure 4**) (Camby et al., 2006). Galectin-1 has various roles in both normal and pathological conditions, including immune regulation, inflammation, nervous tissue regeneration, and cancer (Camby et al., 2006). Structurally, galectin-1 functions mainly as a non-covalent homodimer, with each monomer consisting of approximately 135 amino acids forming a B-sandwich fold that mediates binding to glycans (Barondes et al., 1994; Camby et al., 2006). Studies propose that galectin-1 functions as a homodimer for much of its biological activity, with its dimerization enabling interactions with glycoproteins as well as influencing receptor binding within the context of intracellular signalling (Stillman et al., 2006). This homodimeric structure is also essential for cross-linking with cell surface glycoconjugates, which facilitates cell-cell and cell-ECM interactions.

Galectin-1 dimerizes via non-covalent interactions occurring at the N and the C termini of constituent monomers positioned at the dimer interface (Cho & Cummings, 1995). Specifically, B-strands 1 and 11 from each monomer align to form an extended 12-stranded B-sheet interface (Porciúncula-González et al., 2021). This dimer interface is stabilized by a combination of hydrophobic interactions from nonpolar amino acids, hydrogen bonding between backbone atoms and polar side chains, and van der Waals forces that help maintain close packing (Porciúncula-González et al., 2021).

While galectin-1 typically functions as a homodimer, it can also naturally exist as a monomer in cells under certain conditions (Cho & Cummings, 1995; Miura et al., 2004). A notable example is galectin-1B, a naturally occurring truncated isoform lacking the first six N-terminal amino acid residues, which remains monomeric and exhibits distinct biological functions, such as promoting axonal regeneration (Miura et al., 2004). Additionally, studies have shown that galectin-1 is initially synthesized as a monomer in the cytosol and can remain in this form, particularly in environments lacking sufficient glycan ligands or under oxidative conditions that prevent dimerization (Cho & Cummings, 1995). These findings highlight the functional versatility of galectin-1's oligomeric state within specific cellular contexts.

Specific mutations introduced into LGALS1, the gene encoding galectin-1, can alter two critical amino acid residues to disrupt homodimerization, while retaining its carbohydrate-binding activity (Cho & Cummings, 1995). Specifically, cysteine at position 2 is replaced with serine, and valine at position 5 is replaced with aspartic acid (Cho & Cummings, 1995). These changes

impair interactions at both the N and C-termini of galectin-1 monomers, leading to destabilization and dissociation of the homodimer (Cho & Cummings, 1995). However, the oligomeric state of galectin-1 which is necessary for its functional interaction with HOXA5 has not been elucidated.

1.4.2. Physiological Functions

Under physiological states, galectin-1 plays important roles in immune regulation, tissue repair, and angiogenesis (Figure 5). It mediates its effects via its carbohydrate-binding domain (CBD), which interacts with cell surface glycoconjugates to initiate downstream signalling (Rabinovich et al., 2002). It induces apoptosis in activated pro-inflammatory Th1 and Th17 T cells by cross-linking CD7, CD43, and CD45 glycoproteins, thereby triggering downstream caspase cascades. This culminates in the downregulation of the anti-apoptotic Bcl-2 protein, permeabilization of mitochondrial membranes, cytochrome c release, and caspase activation leading to programmed cell death to maintain immune homeostasis and peripheral tolerance (Perillo et al., 1995; Rabinovich et al., 2002). Galectin-1 therefore limits immune system over-activation which could lead to autoimmunity or chronic inflammation, as well as clearing self-reactive immune cells. In contrast, anti-inflammatory regulatory T cells (Tregs) display different cell surface glycosylation patterns, which makes them less sensitive to galectin-1 mediated apoptosis, thereby promoting an anti-inflammatory state (Rabinovich et al., 2002; Toscano et al., 2007).

Galectin-1 also regulates myofibroblast activation and ECM remodelling to promote wound healing. It binds neuropilin-1 (NRP1) receptors on fibroblasts, which activates downstream

signalling that results in Smad3 phosphorylation and upregulation of NADPH oxidase 4 (NOX4) [AJ1] enzyme. NOX4 drives ROS production, which in turn activates redox-sensitive transcription factors that upregulate genes involved in fibroblast proliferation, cytoskeletal and matrix remodelling, migration, and expression of alpha smooth muscle actin (a-SMA), which promotes tissue formation and wound contraction (Lin et al., 2015). Furthermore, galectin-1 stimulates angiogenesis during development and wound healing. It interacts with glycosylated vascular endothelial growth factor receptor 2 (VEGFR-2) and neuropilin-1 complexes on endothelial cells to modulate intracellular signalling pathways that promote endothelial cell proliferation (Thijssen et al., 2010). Overall, galectin-1 serves as a key regulator of immune balance, tissue repair, and angiogenesis, with its precise regulation being essential for maintaining physiological homeostasis.

1.4.3. Pathological Functions

In pathological states such as cancer, galectin-1 is often overexpressed and associated with increased tumour aggressiveness and worse prognosis (Camby et al., 2006; Cedeno-Laurent et al., 2012). In GB, galectin-1 levels correlate with higher tumour grade and a more invasive phenotype, as galectin-1 binds to glycosylated cell-surface integrins to activate FAK and SRC kinase-mediated signalling pathways which activate Rho GTPases to modulate the cytoskeleton and ECM to promote cellular migration and invasion (Cousin et al., 2016; Croci et al., 2014). Within the TME, galectin-1 dampens anti-tumoural immune responses by promoting anti-inflammatory signalling pathways (Huang et al., 2021; Li et al., 2021). This results in apoptosis of pro-inflammatory effector T cells and increased polarization macrophages towards the

tumour-permissive M2 phenotype, thereby allowing GB cells to evade immune surveillance (Huang et al., 2021; Li et al., 2021).

Additionally, due to its ability to stimulate angiogenesis, galectin-1 supports tumour vascularization, which is crucial to sustain nutrient and oxygen supply, promote invasion to surrounding brain tissue and create perivascular niches that support cell survival and therapeutic resistance (Thijssen et al., 2010; Camby et al., 2006). Furthermore, galectin-1 has been shown to promote metabolic reprogramming in GB cells, shifting them in favour of glycolysis over oxidative phosphorylation (OXPHOS) (Guda et al., 2022). This Warburg effect has been proposed to allow GB cells to survive under hypoxic conditions, sustain rapid proliferation, as well as allowing for acidification of the TME which aids in immune evasion (Guda et al., 2022). Galectin-1 achieves this by physically interacting with and upregulating the expression of carbonic anhydrase IX (CA-IX), a hypoxia-responsive enzyme that supports glycolytic metabolism and suppresses OXPHOS (Guda et al., 2022).

Galectin-1 also plays important roles in various other cancers, fibrotic disorders, autoimmune disorders and infections (Camby et al., 2006; Cedeno-Laurent et al., 2012). In lung, pancreatic, prostate, breast, and skin cancer, galectin-1 is often overexpressed, promoting tumour aggressiveness and worse patient outcomes (Camby et al., 2006; Cedeno-Laurent et al., 2012; Chung et al., 2012; Orozco et al., 2018; Kim et al., 2025). In these cancers, galectin-1 has been proposed to enhance cell migration, invasion, angiogenesis, and promotes EMT (Croci et al., 2014; Camby et al., 2006; Cedeno-Laurent et al., 2012; Chung et al., 2012; Orozco et al., 2018; Kim et al., 2025). Galectin-1 also enhances immune evasion by inducing apoptosis in activated T

cells (Perillo et al., 1995; Rabinovich et al., 2002). In pancreatic cancer, galectin-1 is produced by both tumour cells and pancreatic stellate cells (PSCs), where it facilitates the generation of fibrotic tissue around the tumour (Martinez-Bosch et al., 2018;). This desmoplasia is a common feature of pancreatic cancer, whereby the tumour becomes protected from therapeutics and drug delivery is impeded (Martinez-Bosch et al., 2018; Orozco et al., 2018). Similarly, in breast and prostate cancer, galectin-1 contributes to tumour aggressiveness and therapeutic resistance by activating pro-survival and pro-metastatic signalling cascades via its interactions with cell-surface integrins (Wang et al., 2017; Liu et al., 2018; Kim et al., 2025).

Within the context of fibrotic disorders, including pulmonary fibrosis and liver cirrhosis, galectin-1 upregulation in stromal cells promotes aberrant ECM remodelling which leads to excess deposition of collagen (Novák et al., 2025; Hermenean et al., 2022). This galectin-1-mediated stiffening of the ECM disrupts normal lung and liver tissue structure and function, thereby worsening the fibrotic process in these disorders (Novák et al., 2025; Hermenean et al., 2022). Studies also propose that galectin-1 plays a protective role in neuroinflammatory disorders, via its anti-inflammatory effects on the environment (Starossom et al., 2012). Finally, in viral infections, including human immunodeficiency virus (HIV) infection, galectin-1 enhances viral entry by facilitating the attachment of the HIV particle to CD4+ T cells via its direct interaction with glycans on the viral envelope and host cell (St-Pierre et al., 2011). Overall, the dysregulation of galectin-1 expression and its complex roles in various pathological states highlight its central role in promoting tumour progression, immune evasion, angiogenesis, and pathological tissue remodelling, making it a promising target for therapeutic intervention.

1.4.3.1. Role in BTSCs of GB

Clinically, high galectin-1 expression correlates with advanced GB tumour grade and shorter patient survival, suggesting a critical role in promoting BTSC-driven tumour progression (Camby et al., 2006; Huang et al., 2021; Li et al., 2021). Notably, silencing of the LGALS1 gene in BTSCs reduces sphere formation and invasive capacity, as well as inducing apoptosis, highlighting galectin-1 importance in BTSC maintenance (**Figure 4**) (Sharanek et al., 2021). Galectin-1 promotes cytoskeletal remodelling and cellular motility by binding and activating glycosylated integrins on the surface of BTSCs, thereby modulating FAK and SRC kinase signalling pathways, which in turn activate Rho GTPases to drive invasion (Cousin et al., 2016; Croci et al., 2014). Additionally, galectin-1 promotes a tumour-permissive immunosuppressive TME by inducing apoptosis in effector T cells and driving M2-polarization in TAMs, facilitating BTSC immune evasion (Huang et al., 2021; Li et al., 2021). Furthermore, galectin-1 facilitates neovascularization and the creation of perivascular niches that support BTSC survival via its activation of angiogenic signalling pathways (Thijssen et al., 2010). Together, galectin-1 plays a critical role in BTSC regulation through its ability to promote metabolic reprogramming, maintenance, invasion, angiogenesis, immune evasion, and resistance to therapy, highlighting its potential as a therapeutic target in GB (Camby et al., 2006; He et al., 2022; Huang et al., 2021; Li et al., 2021).

Galectin-1

Structure

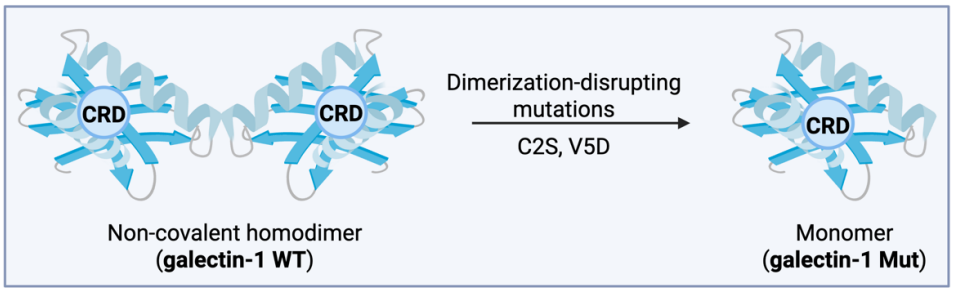

Physiological Functions

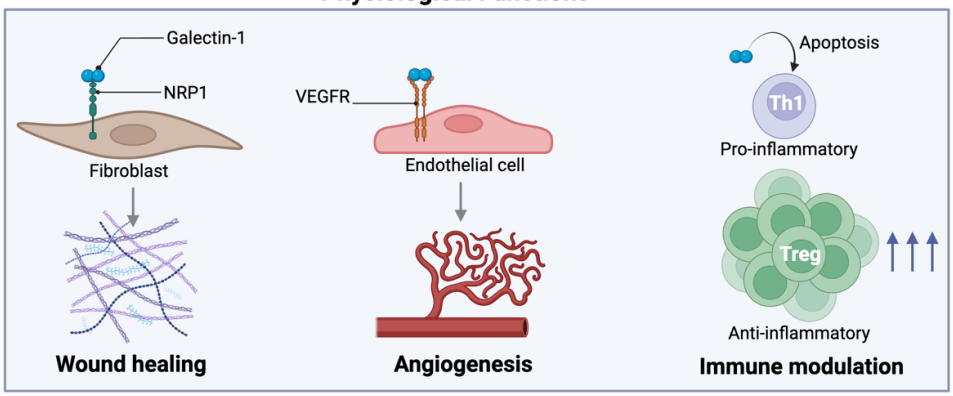

Roles in BTSCs of GB

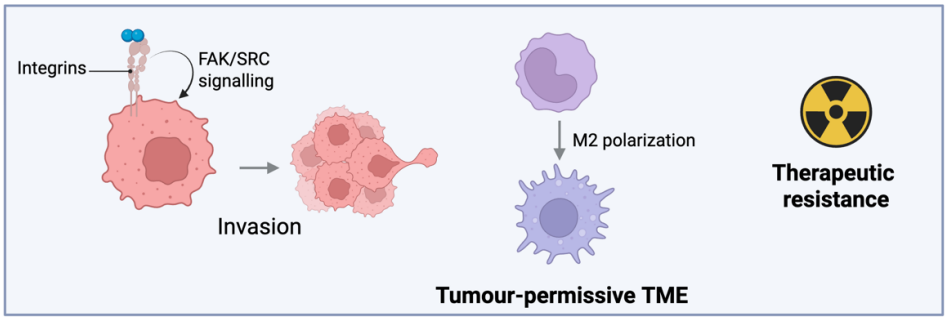

Figure 4. Structure and multifaceted roles of galectin-1. Galectin-1 functions primarily as a homodimer, with each monomer featuring a beta-sandwich fold and a carbohydrate recognition domain (CRD) critical for glycan binding. It modulates immune responses by inducing apoptosis in pro-inflammatory T cells while regulatory T cells (Tregs) survive and proliferate. It also promotes M2 polarization in TAMs, promoting a tumour-suppressive environment. Galectin-1 promotes wound healing via fibroblast activation and stimulates angiogenesis through interactions with endothelial receptors. In GB, galectin-1 is frequently overexpressed to enhance tumour cell invasion, immune evasion, and therapeutic resistance. Created using Biorender.com.

1.5. HOXA5/galectin-1 Regulation of BTSCs

Researchers have identified a HOXA5 signalling pathway that reprograms the transcriptional landscape of BTSCs to promote self-renewal, radioresistance and differentiation into the most aggressive GB subtype (Sharanek et. al, 2021). Using EGFRvIII mutant BTSCs, they showed that STAT3 transcriptionally activates the LGALS1, leading to galectin-1 expression which forms a complex with HOXA5 to regulate its target genes (Sharanek et. al, 2021). Genetic and pharmacological inhibition of HOXA5/galectin-1 signalling inhibited BTSC self-renewal, increased susceptibility to IR and downregulated the expression of genes associated with the mesenchymal subtype of GB (Sharanek et. al, 2021). Although studies have shown that HOXA5/galectin-1 inhibition significantly impairs BTSC survival and tumourigenic capacity, the mechanisms by which this axis regulates BTSCs have not been fully characterized.

A critical unanswered question is whether galectin-1's oligomeric state influences its functional interaction with HOXA5 in BTSCs. Studies suggest that galectin-1 primarily functions as a

homodimer, with dimerization enabling key biological functions, although it can also exist as a monomer under certain contexts and may have different functions from its homodimeric form (Stillman et al., 2006; Miura et al., 2004). The homodimeric form exhibits increased binding affinity for B-galactoside sugars, which facilitates the crosslinking of cell-surface receptors and ECM components (Miura et al., 2004; Stillman et al., 2006). This crosslinking event facilitates receptor clustering and stabilization of signaling complexes, leading to the regulation of cellular processes, such as adhesion, migration, immune modulation, angiogenesis, and intracellular signalling across multiple cell types (Miura et al., 2004; Stillman et al., 2006). Studies also suggests that galectin-1 homodimer localizes to the cytoplasm and nucleus, where it engages in glycan-independent protein-protein interactions that influence transcriptional regulation, redox-sensitive signalling pathways, or protein stability (Miura et al., 2004; Stillman et al., 2006). However, galectin-1 exists in a dynamic monomer/dimer equilibrium and can adopt a monomeric state under specific cellular conditions, including low protein concentration, intracellular reducing environments, or genetic mutations that impair dimerization (Cho & Cummings, 1995; Miura et al., 2004). In contrast to the homodimer, monomeric galectin-1 displays reduced glycan-binding affinity and impaired capacity to crosslink receptors, suggesting that many of its regular biological functions are diminished in this form (Stillman et al., 2006). Using lectin-binding assays, receptor aggregation analyses, and signalling readouts, researchers demonstrated that homodimeric galectin-1 efficiently promoted glycoprotein lattice formation and stabilized receptor complexes, whereas the monomeric form failed to induce comparable receptor clustering (Stillman et al., 2006). carbohydrate-binding assays also revealed that monomeric galectin-1 binds lactose and other galactosides with significantly lower affinity

compared to the homodimer, resulting from the loss of the multivalent interactions required for stable glycan binding (Stillman et al., 2006).

Notably, galectin-1B, a naturally occurring monomeric truncated isoform lacking the first six N-terminal amino acids, has been shown to exhibit distinct biological activity from the homodimer (Miura et al., 2004). Galectin-1B has been reported to promote axonal regeneration, supporting the concept that monomeric galectin-1 can mediate glycan-independent intracellular functions (Miura et al., 2004). Researchers showed that expression or exogenous delivery of galectin-1B significantly enhanced axonal regeneration following nerve injury, and that galectin-1B associates with cytoskeletal and signalling proteins involved in neuronal growth cone dynamics (Miura et al., 2004). Collectively, these findings indicate that galectin-1's oligomeric state shapes molecular interactions and functional outcomes; however, the oligomeric state of galectin-1 which is necessary for its functional interaction with HOXA5 in BTSCs has not been established. Similarly, HOXA5 is composed of distinct functional domains, including an N-terminal protein interaction region, an intrinsically disordered region that mediates cofactor binding, and a highly conserved homeobox domain responsible for DNA binding (Ritesh et al., 2024; De Kumar & Darland, 2021; Pearson et al., 2005; Shah & Sukumar, 2010). Although these domains likely have coordinated roles in regulating BTSC transcriptional programs, their individual contributions to BTSC self-renewal and proliferation remain uncharacterized. Collectively, these knowledge gaps underscore the need to explore both the structural requirements of galectin-1 and the domain-specific functions of HOXA5 in BTSC regulation. Addressing these questions will provide greater mechanistic understanding of BTSC regulation and may uncover novel therapeutic targets.

1.6. Hypothesis and Objectives

Hypothesis: I hypothesize that homodimeric galectin-1 is required for HOXA5's regulation of BTSCs, and that disruption of galectin-1 dimerization alters HOXA5 chromatin engagement and downstream transcriptional programs that govern BTSC self-renewal and growth. This hypothesis is based on evidence that galectin-1 primarily functions as a homodimer to mediate protein interactions and cellular signalling, while monomeric galectin-1 exhibits distinct context-dependent functions, and on the established role of HOXA5 as a transcription factor regulating BTSC pathways.

Objectives: The overall objective of this thesis is to determine how monomeric and homodimeric Galectin-1 impact BTSCs self-renewal and growth. In addition, I will address which HOXA5 domains are indispensable for these processes. The results obtained will direct future studies to assess their mode of interaction in BTSC regulation.

1. Assess Galectin-1 homodimer (WT) vs monomer (Mut) effects on BTSC characteristics.

2. Investigate the effects of HOXA5 structural domains on BTSC characteristics.

2. Materials and Methods

2.1. Patient-derived BTSC culture

Primary human BTSC lines, BTSC30, BTSC73, and BTSC147, were derived from glioblastoma patient tumour specimens obtained during surgical resection with informed consent. The lines were generously provided by Dr. Samuel Weiss (University of Calgary) and have been previously described (Chesnelong et al., 2019; Cusulin et al., 2015). Each line was characterized for hallmark glioblastoma mutations, including EGFRvIII, p53, PTEN, and IDH1 status (Jahani-Asl et al., 2016). BTSC73 and BTSC147 harbor endogenous EGFRvIII mutations, while BTSC30 does not, and were selected accordingly for this study. Neurospheres were enzymatically dissociated and cultured in neurosphere conditions using ultra-low-attachment flasks (Corning) and complete BTSC medium composed of NeuroCult NS-A basal medium (StemCell Technologies, #05750) supplemented with 2 µg/mL heparin (#07980), 20 ng/mL human EGF (Miltenyi Biotec, #130-093-825), 10 ng/mL human FGFb (Miltenyi Biotec, #130-093-838), and penicillin-streptomycin (1:100, Sigma Aldrich, #P4333). Cells were passaged every 3-4 days or when spheroids reached 200-250 µm to avoid necrosis. Passaging involved gentle dissociation with 200 µL ACCUMAX (Innovative Cell Technologies, #AM105) for 10 minutes at 37°C, followed by quenching with 800 µL of BTSC medium. Single-cell suspensions were generated by gentle pipetting and viability assessed with 0.4% Trypan Blue (Gibco, #15250-061). Cell plating density was adjusted based on flask size and experimental timelines. Prior to experimental use, BTSCs were thawed from cryopreservation stocks maintained in 10% dimethyl sulfoxide (DMSO) (Sigma-Aldrich) and recovered under identical culture conditions.

Table 1. BTSC donor information and mutational status

Line	Age (years)	Sex	EGFR	TP53	PTEN	IDH1	NF1	CDK2A
BTSC30	67	Male	WT	WT	Mut	WT	N/A	N/A
BTSC73	52	Male	vIII	Mut	Mut	WT	N/A	Homo del
BTSC147	55	Male	vIII	Mut	Mut	WT	WT	Homo del

Wild-type (WT) or mutant (Mut) variations of key genes often mutated in GB in the different BTSC lines used. Homozygous deletion (Homo del), not applicable (N/A) and EGFR variant III (vIII) indicated.

2.2. Electroporation

To generate a transient expression of galectin-1 WT and galectin-1 Mut in patient derived BTSCs, plasmids carrying either WT LGALS1 gene or Mut LGALS1 gene (cysteine at position 2 is replaced with serine, and valine at position 5 is replaced with aspartic acid, preventing dimerization) were used. 1 million cells were processed into a single cell suspension and subsequently mixed with the plasmids at a concentration of 100 nM. The cells were co-transfected with a GFP plasmid to enable subsequent FACS sorting for GFP-positive cells. The plasmids were delivered using the BTX™ Gemini X2 Electroporation System set at 250 volts, resistance 1050 Ω, capacitance 250 uF, and an electrode gap of 2 mm. Electroporated cells were plated in a T-25 culture flask containing BTSC media and incubated at 37°C and 5% CO2. Cells were plated for ELDA and sphere growth assay 24 hours after electroporation.

2.3. Gene expression analysis

Total RNA was extracted using the TRIzol reagent-based protocol. Briefly, cell pellets were lysed in 1 mL of TRIzol (Invitrogen, #15596026) and incubated at room temperature for 5 minutes to ensure complete dissociation of nucleoprotein complexes. Phase separation was achieved by adding 200 µL of chloroform (Sigma Aldrich, #288306), followed by vigorous shaking for 20 seconds and a 2-3 minute incubation at room temperature. Samples were centrifuged at 12,000 × g for 15 minutes at 4°C, after which the upper aqueous layer (500 µL) was transferred to a fresh tube and mixed with an equal volume of isopropanol. RNA precipitation was carried out by incubating the mixture at room temperature for 15 minutes, followed by centrifugation at 12,000 × g for 10 minutes at 4°C. The resulting pellet was sequentially washed with 75% and 100% ethanol, each followed by centrifugation at 7,500 × g for 5 minutes. After air-drying for 10-15 minutes, RNA was resuspended in 20 µL of RNase-free water and incubated at 55-60°C for 10-15 minutes to aid in dissolution. cDNA synthesis was performed using the 5X All-In-One RT MasterMix (abm, #G492) according to the manufacturer's instructions. Quantitative real-time PCR (RT-qPCR) was subsequently carried out using SYBR Green dye (Bio-Rad, #1725271) on a QuantStudio™ 7 Flex Real-Time PCR System (Applied Biosystems). Each 10 µL reaction contained 5 µL SYBR Green master mix, 1 µL each of 5 µM forward and reverse primers (sequences listed in Table 3), and 3 µL of cDNA template (30 ng). Amplification specificity and efficiency were confirmed via melt curve analysis. Gene expression levels were normalized to the housekeeping gene GUSB (β-glucuronidase) using the ΔΔCt method.

Table 2. qPCR primers used for gene expression analysis

Gene	Forward Primer Sequence	Reverse Primer Sequence
GUSB	GCGTTCCTTTTGCGAGGAGA	GGTGGTATCAGTCTTGCTCAA
LGALS1	AACCTGGAGAGTGCCTTCGA	GTAGTTGATGGCCTCCAGGT
HOXA5	AGATCTACCCCTGGATGCGC	CCTTCTCCAGCTCCAGGGTC
PTN	GAGATCTGGCTTTGCACTCATTGAA	GCATATGGAGAATGGGAGGGAATGA
KCNK2	CGTGGATGCTTCGTGTGTAA	TTCAGGAAGAAATTCCCTGATT
CDH1	AAAATTAGGCCGCTCGAGGC	GTATTTTTAGTACAGACGGGGT
DSCAM	AAGGGGCTATATGTTTGGGATT	CTCCTTCCAAATCCTTGCTG
TP53	CCTCAGCATCTTATCCGAGTGG	TGGATGGTGGTACAGTCAGAGC
HBB	CTGTTTGAGGTTGCTAGTG	TCATCACTTAGACCTCACC
HOXA5-GFP	AGGAGGGGCCTTCCGTC	TTCCGTCGACCTTGTCATCG

2.4. Immunoblotting

BTSCs were lysed in ice-cold 1X RIPA buffer (Thermo Fisher Scientific, #89900) supplemented with a protease and phosphatase inhibitors (Thermo Fisher Scientific, #A32959) to preserve protein integrity. Lysates were clarified by brief centrifugation, and protein concentration was quantified using the Bradford protein assay (Bio-Rad) according to the manufacturer's instructions. Equal amounts of total protein were resolved by SDS-PAGE on 10% polyacrylamide gels, followed by electrotransfer onto 0.45 μm nitrocellulose membranes (Bio-

Rad, #1620115) using a two-step voltage protocol: 80 V for 15 min, then 120 V for 1 hour minutes to ensure efficient transfer. Membranes were blocked in 5% bovine serum albumin (BSA) in 1X TBST to minimize non-specific antibody binding, and then incubated overnight at 4°C with primary antibodies diluted in blocking buffer. The following day, membranes were washed and probed with HRP-conjugated secondary antibodies (diluted in 5% BSA) for 1 hour at room temperature. Chemiluminescent detection was carried out using Clarity™ Western ECL Substrate (Bio-Rad, #170-5060), and protein signals were visualized and documented using the Bio-Rad ChemiDoc Imaging System. Antibodies used in this study are listed: β-Actin (1:1000, Cell Signalling, mouse), Galectin-1 (1:2000, Cell Signalling, D608T, rabbit), GAPDH (1:1000, Cell Signalling, #2118, rabbit), GFP (1:1000, Abcam, ab1218, mouse), HA (1:5000, Abcam, ab9110, rabbit), HOXA5 (1:5000, Thermo Fisher, PA6-80045, rabbit), HOXA5 (1:500, Abcam,140636, rabbit), HOXA5 (1:500, Abnova, H00003202-M14, mouse), HOXA5 (1:100, Santa Cruz, sc-365784, mouse), Ubiquitin (1:500, Cell Signalling, #91112, rabbit).

2.5. Extreme limiting dilution assay

Extreme limiting dilution assays (ELDA) were conducted to assess self-renewal capacity of BTSCs. Neurospheres were enzymatically dissociated into single-cell suspensions, which were then serially diluted in complete BTSC medium composed of serum-free NeuroCult NS-A (StemCell Technologies, #05750), supplemented with 100 U/mL penicillin and 100 µg/mL streptomycin (Sigma Aldrich, #P4333), 2 µg/mL heparin (StemCell Technologies, #07980), 20 ng/mL human EGF (Miltenyi Biotec, #130-093-825), and 10 ng/mL human FGF (Miltenyi Biotec, #130-093-838). Diluted single-cell suspensions (100 µL per well) were seeded into 96-well ultra-low attachment plates at limiting dilutions of 25, 12, 6, 3, and 1 cell(s) per well, with

12 replicate wells per condition. Plates were incubated at 37°C with 5% CO_2 for 7 days, after which wells were scored for the presence or absence of neurospheres. Sphere formation data were analyzed using the ELDA software tool (https://bioinf.wehi.edu.au/software/elda/), which calculates stem cell frequency (SCF) and provides statistical estimates for the minimum number of cells required to initiate sphere formation under each condition.

2.6. Sphere growth assay

Sphere growth assays were conducted to assess proliferative capacity of BTSCs. Neurospheres were enzymatically dissociated into single-cell suspensions, which were then serially diluted in complete BTSC medium composed of serum-free NeuroCult NS-A (StemCell Technologies, #05750), supplemented with 100 U/mL penicillin and 100 µg/mL streptomycin (Sigma Aldrich, #P4333), 2 µg/mL heparin (StemCell Technologies, #07980), 20 ng/mL human EGF (Miltenyi Biotec, #130-093-825), and 10 ng/mL human FGF (Miltenyi Biotec, #130-093-838). Diluted single-cell suspensions (100 µL per well) were seeded into 96-well ultra-low attachment plates at limiting dilutions of 200, 100, 50, 25, 12, and 6 cell(s) per well, with 3 replicate wells per condition. Plates were incubated at 37°C with 5% CO_2 for 7 days, after which wells were scored for the number of neurospheres present.

2.7. Immunostaining

For immunofluorescence staining, BTSCs were seeded onto Lab-Tek II CC2-treated chamber slides (Thermo Fisher Scientific, #154941) using complete BTSC medium. To promote optimal cell adherence, residual ACCUMAX was removed via an additional centrifugation step at 120 × g for 10 minutes prior to plating. Once adhered, cells were gently rinsed with pre-warmed 1X

PBS and fixed in freshly thawed 4% paraformaldehyde (PFA) at 37°C for 10 minutes. Following fixation, cells were permeabilized with 0.5% Triton X-100 (Sigma Aldrich, #T8787) for 20 minutes and subsequently blocked with 5% normal horse serum (NDS) in 1X PBS for 1 hour at room temperature. Primary antibody incubation was performed overnight at 4°C using the following antibodies: HA (1:500, Abcam, ab9110, rabbit). The following day, cells were washed three times with 1X PBS (5 minutes each), then incubated for 1 hour at room temperature with species-specific secondary antibodies: Alexa Fluor 488 goat anti-mouse (1:500, Thermo Fisher Scientific, #A32740) and Alexa Fluor 594 goat anti-mouse (1:500, Thermo Fisher Scientific, #A11032). Nuclei were counterstained using 2 mg/mL DAPI (Thermo Fisher Scientific, #D1306), and slides were mounted with ProLong Gold Antifade Mountant (Thermo Fisher Scientific, #P36934). Fluorescence imaging was performed on a Zeiss Axio Observer 7 microscope using 40× or 100× oil-immersion objectives.

2.8. Chromatin immunoprecipitation

Cells were pre-washed in cold PBS supplemented with protease inhibitors (Thermo Fisher Scientific, #A32959) to preserve protein integrity prior to fixation. Crosslinking was performed by incubating cells in 1% formaldehyde in PBS for 10 minutes at room temperature with gentle rotation, followed by quenching with 0.125 M glycine in PBS for 5 minutes to halt the crosslinking reaction. All fixation and quenching steps were carried out in 15 mL Falcon tubes under continuous rotation at room temperature. After quenching, cells were washed twice with ice-cold PBS containing protease inhibitors, and cell pellets were collected by centrifugation at 150 × g for 10 minutes at 4°C. Pellets were lysed in ice-cold ChIP lysis buffer (40 mM Tris-HCl pH 8.0, 1% Triton X-100, 4 mM EDTA, 300 mM NaCl) supplemented with protease inhibitors.

Chromatin was fragmented to an average size of ~500 base pairs using a Bioruptor water bath sonicator (Diagenode) at 4°C. Lysates were clarified by centrifugation at 12,000 × g for 15 minutes at 4°C, and the supernatant was diluted 1:1 with ChIP dilution buffer (40 mM Tris-HCl pH 8.0, 4 mM EDTA) containing protease inhibitors. Immunoprecipitation was performed using a ChIP-grade HA antibody (10 µg, ab9110), or rabbit IgG isotype control (10 µg, Cell signalling, #3900S). Immune complexes were captured, sequentially washed, and eluted, followed by reversal of cross-links as previously described (Soleimani et al., 2013). Immunoprecipitated DNA was quantified by qPCR, and binding enrichment was calculated as a percentage of input DNA. Primer sequences used for qPCR analysis are listed in Table 1.

2.9. Generation of stable transgenic BTSCs

Transgenic *HOXA5-overexpressing* BTSCs were generated via lentivirus carrying different *HOXA5* plasmids (OriGene, puromycin resistant) or a non-targetting control construct. Lentivirus was produced in HEK293T cells using a three-plasmid system consisting of the transfer vector, psPAX2 packaging plasmid, and pMD2.G envelope plasmid at a 4:3:1 mass ratio. HEK293T cells were seeded at 80% confluence and transfected using polyethyleneimine (PEI), and viral supernatants were collected at 48 and 72 hours post-transfection. The combined supernatants were cleared by centrifugation, passed through a 0.45 µm filter, and stored at -80 °C in single-use aliquots. BTSC Neurospheres were enzymatically dissociated into single-cell suspensions, and 1 million cells were suspended in complete BTSC medium composed of serum-free NeuroCult NS-A (StemCell Technologies, #05750), supplemented with 100 U/mL penicillin and 100 µg/mL streptomycin (Sigma Aldrich, #P4333), 2 µg/mL heparin (StemCell Technologies, #07980), 20 ng/mL human EGF (Miltenyi Biotec, #130-093-825), and 10 ng/mL

human FGF (Miltenyi Biotec, #130-093-838) and cultured in neurosphere conditions using ultra-low-attachment flasks (Corning). Lentiviral supernatant was added, and after 12-16 hours, the viral medium was replaced with fresh growth medium, and cells were allowed to recover for 48-72 hours before puromycin selection. Puromycin was added at a concentration of 0.5 µg/mL for 7-10 days with medium changes every 48 hours such that all non-transduced cells were eliminated. Transduction efficiency and stable overexpression were confirmed by RT-qPCR for HOXA5 mRNA, Western blotting, and immunofluorescence staining. Control lines were generated in parallel using the non-targeting control lentivirus under identical production, transduction, and selection conditions. All lentiviral work was conducted under biosafety level 2 (BSL-2) containment.

2.10. Subcloning

The LGALS1 gene was subcloned into a lentiviral backbone using restriction enzyme cloning, with mCherry used as the reporter to permit co-expression studies with HA-tagged HOXA5-GFP plasmids. The GFP sequence in the lentiviral backbone was replaced with the mCherry coding sequence derived from a donor plasmid. Both the lentiviral backbone and mCherry donor plasmid were digested with BamHI and BsrGI to excise the GFP cassette and release the mCherry insert, respectively. Digested products were resolved by agarose gel electrophoresis, and the correct vector backbone and mCherry fragments were purified and ligated using T4 DNA ligase. The ligation mixture was transformed into chemically competent *E. coli*, and four colonies were selected for downstream validation. Plasmid DNA was isolated from each clone and transfected into HEK-293 cells using polyethyleneimine (PEI) to assess reporter expression. The confirmed mCherry-positive vector was then used as the recipient backbone for LGALS1

insertion. Full-length LGALS1 WT and LGALS1 Mut coding sequences were PCR-amplified and subcloned into the mCherry-expressing lentiviral backbone using XhoI and SmaI restriction sites. Ligation products were transformed into competent *E. coli*, and colony PCR was performed using LGALS1-specific primers to screen for positive clones. Colonies yielding PCR amplicons of the expected size (400 bp) were cultured for plasmid isolation and purification. Positive plasmids were subjected to Sanger sequencing to verify full-length LGALS1 sequence identity, confirm that no off-target mutations were introduced, and ensure that mCherry, Flag-tag, and P2A sequences were in-frame. Sequencing further verified the specific amino acid substitutions differentiating Galectin-1 WT from Galectin-1 Mut (C2S and V5D).

2.12. *In-vitro* binding assay

Single BL21 colonies harboring GST or GST-HOXA5 were grown overnight in LB (37 °C), diluted 1:10 into fresh LB, cultured 2 h at room temperature, induced with 0.5 mM IPTG, and incubated a further 4-5 h at room temperature. Pellets were stored at -80 °C (2 months). For purification, pellets were resuspended in Buffer A(GST) (HEPES 25-50 mM pH 7.3-7.5, NaCl 50-100 mM, $MgCl_2$ 12.5 mM, KCl 12.5 mM, DTT 1-2 mM, EDTA 1 mM, protease inhibitors) supplemented with 1% Triton X-100. Cells were sonicated on ice (20 s bursts), clarified (14,000 x g, 30 min, 4 °C), and supernatants were incubated with 30 µl glutathione-Sepharose 4B (GSH) beads for 2 hr at 4 °C. Beads were washed 3× with Buffer B(GST) (HEPES 50 mM pH 7.3-7.5, NaCl 1 M, Triton X-100 1%, DTT 1 mM, EDTA 1 mM). Bead-bound GST or GST-HOXA5 was used directly for pull-down. BL21 cultures expressing His-Gal1 WT or His-Gal1 Mut were grown and induced as above, then pellets from 200-500 ml cultures were resuspended in Ni-NTA Buffer A(His) (1xPBS, NaCl 100 mM, NP-40 0.5%, imidazole 20 mM, DTT 1 mM,

EDTA-free protease inhibitors). Lysates were sonicated on ice and clarified (15,000 rpm, 30 min). Supernatants were incubated with 1-2 ml Ni-NTA agarose for 2 hr at 4 °C. Resin was washed 3x with Ni-NTA Buffer B(His) (1xPBS, NaCl 1 M, NP-40 1%, imidazole 20 mM, DTT 1 mM) and eluted stepwise with Ni-NTA Buffer C(His) (1xPBS, imidazole 300 mM; 200-500 µl x 3-5 elutions). Protein yield was monitored by Bradford assay. Eluates were buffer-exchanged into GST binding Buffer A(pull-down) before use. 5 µg GST or GST-HOXA5 was incubated with 5 µg His-Gal1 WT or His-Gal1 Mut in 400 µl Buffer A(pull-down) for 2 hr at 4 °C with rotation. Buffer A(pull-down): 25 mM Tris-HCl pH 7.5, 150 mM NaCl, 1 mM EDTA, 1 mM DTT, 0.5% Triton X-100, protease inhibitors. Complexes were retrieved by adding 20 µl GSH-Sepharose and incubating 1 hr at 4 °C, followed by centrifugation. Beads were washed 3-5x with Buffer B(pull-down) (25 mM Tris-HCl pH 7.5, 300 mM NaCl, 1 mM EDTA, 1 mM DTT, 0.5% Triton X-100; typically, without protease inhibitors for final washes). Bound proteins were eluted by boiling in a 2x SDS sample buffer for 5 min. Eluates and input controls (5-10% of each protein) were resolved by SDS-PAGE and transferred to PVDF. Membranes were probed with anti-galectin-1 (detects WT and Mut) to assess prey binding and anti-GST to confirm bait recovery. Total protein on the gel was visualized by Coomassie blue as a loading/bead-recovery control. Negative controls included GST-only bait with each His-Gal1 variant and beads-only. All pull-downs were performed in 3 independent experiments. Where indicated, densitometry of galectin-1 signals was normalized to GST bait signal (anti-GST) or total lane protein.

2.13. Statistical analyses

All experiments were performed with three independent biological replicates (n = 3). Data are presented as mean +/- standard deviation (SD). Statistical analyses and graphing were performed

using GraphPad Prism. For comparisons between two experimental groups, statistical significance was assessed using an unpaired Student's t-test. For experiments involving three or more groups, statistical significance was assessed using one-way analysis of variance (ANOVA) followed by post hoc multiple comparison testing to account for multiple pairwise comparisons. For RT-qPCR, relative mRNA expression was calculated using the ΔΔCt method, with target gene expression normalized to the GUSB housekeeping gene. For ChIP-qPCR, enrichment values were expressed as % input, with qPCR technical replicates averaged within each biological replicate before statistical testing. Statistical comparisons across conditions were performed as one-way ANOVA with post hoc testing. For extreme limiting dilution analysis (ELDA), self-renewal frequency was estimated from limiting dilution data by fitting the single-hit model to the fraction of negative wells across cell densities plated. Statistical testing was performed using one-way ANOVA. For sphere growth assays, the first readout was the number of spheres per well across densities cell densities plated. Statistical comparisons were performed using one-way ANOVA. For immunostaining analyses, signal intensity and subcellular localization were quantified from confocal microscopy images acquired using identical acquisition settings (exposure time, gain, and laser intensity) across all conditions within each experiment. For each condition, multiple random fields of view were imaged per biological replicate. Mean fluorescence intensity of the antibody signal was measured after background subtraction (signal from an unstained or secondary antibody-only control).

3. Results

3.1. Structural models predict distinct modes of interaction between HOXA5 and galectin-1 WT vs Mut

Galectin-1 functions as a homodimer for much of its biological activities (Stillman et al., 2006). Our lab has conducted a protein interaction analysis to explore the structural basis of Galectin-1 and HOXA5's interaction. Protein-protein docking models were generated using ClusPro 2.0 and High Ambiguity Driven protein–protein DOCKing version 4.0 (HADDOCK 4.0). Docking of Galectin-1 wild-type (WT) homodimer with HOXA5, predicts an interaction between Galectin-1 WT and the N-terminal region of HOXA5 (**Figure 5**). This interaction appears to promote flexibility of the homeobox domain, potentially enhancing HOXA5's ability to bind to DNA. In contrast, docking simulations with the Galectin-1 Mut monomer suggest that the mutant interacts directly with the homeobox domain of HOXA5 (**Figure 5**). This binding appears to restrict conformational flexibility within the homeobox domain, potentially impeding its ability to bind DNA. These structural models suggest that the monomeric form of Galectin-1 (Mut) may bind to the DNA-binding domain of HOXA5, potentially hindering its ability to bind and regulate its target genes. While these models provide a framework to explain the differences in galectin-1 WT versus Mut regulation of HOXA5 based on differential binding, they remain predictive and require experimental validation. Furthermore, HOXA5/galectin-1 interactions in the nuclear environment may be influenced by additional cofactors, post-translational modifications, or chromatin context that are not captured by docking models.

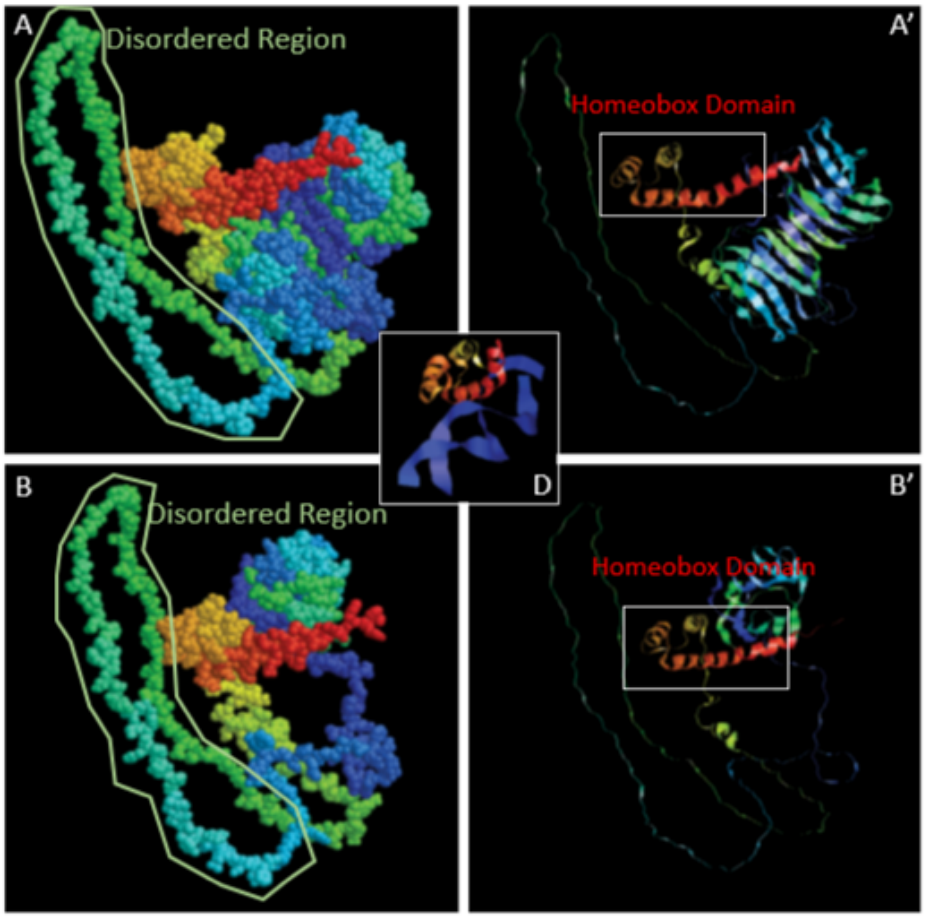
A
Disordered Region
A'
Homeobox Domain
D
B
Disordered Region
B'
Homeobox Domain

Figure 5. Predicted docking models of galectin-1 and HOXA5. A and A' represent the docking of galectin-1 WT homodimer and HOXA5 predicted by ClusPro2.0. The N-terminal region of HOXA5 interacts with galectin-1 WT homodimer, leading to flexibility of the DNA-binding region (homeobox domain) of HOXA5 which facilitates binding to DNA. A and A', the protein-protein docking between galectin-1 and HOXA5 is presented with space fill and ribbon models, respectively. B and B' represent the docking of galectin-1 Mut monomer and HOXA5 predicted by HADDOCK4.0. In this model, the galectin-1 Mut monomer interacts with the homeobox domain of HOXA5, causing inflexibility of this domain, which impedes HOXA5 binding to DNA. B and B', the protein-protein docking between galectin-1 and HOXA5 is presented with space fill and ribbon models, respectively. D, 3D structures from 6FQQ. Homeobox domain (60 amino acids composed of 3-alpha helices) binds to double-strand DNA (Blue). This figure was generated by Dr. Dianbo Qu.

3.2. Sequencing and expression assays validate galectin-1 WT and Mut constructs and confirm dimerization-disrupting mutations

To confirm the integrity of the Galectin-1 plasmid constructs, Sanger sequencing was performed on both the WT and Mut LGALS1 inserts (**Figure 6a**). Chromatogram analysis verified full-length sequence identity with the intended constructs and showed no off-target mutations within the coding regions. As expected, the Galectin-1 Mut plasmid contains two amino acid substitutions relative to the WT; cysteine at position 2 is replaced with serine, and valine at position 5 is replaced with aspartic acid. These substitutions were designed to disrupt dimerization.

To assess the functional impact of these mutations on protein oligomerization, both constructs were transfected into HEK293T cells, and native PAGE was used to examine their migration profiles (**Figure 6b**). Galectin-1 WT band exists at a higher molecular weight, consistent with homodimer formation, whereas the Mut protein appears as a lower molecular weight band, indicative of its monomeric form. Importantly, SDS-PAGE analysis showed that both WT and Mut proteins were expressed at comparable levels, confirming equivalent transfection efficiency and protein production. These results indicate that the amino acid substitution mutations disrupt Galectin-1 homodimerization while maintaining comparable protein expression. However, native PAGE provides an indirect assessment of oligomeric state and does not exclude the presence of transient or weak dimerization under specific cellular conditions. Furthermore, these analyses were performed in HEK293T cells, and the oligomeric state of galectin-1 WT and Mut may differ in BTSCs or within the nuclear environment, where additional binding partners or post-translational modifications could influence dimerization.

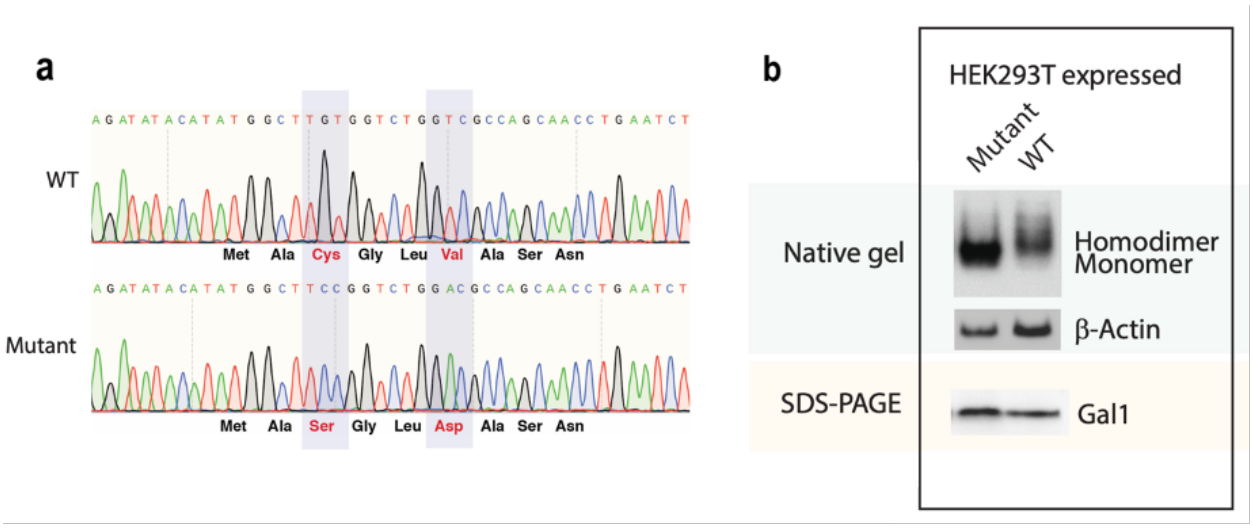
a
WT
Met Ala Cys Gly Leu Val Ala Ser Asn
Mutant
Met Ala Ser Gly Leu Asp Ala Ser Asn
b
HEK293T expressed
Mutant
WT
Native gel
Homodimer
Monomer
β-Actin
SDS-PAGE
Gal1

Figure 6. Sanger sequencing confirmation of galectin-1 WT and Mut plasmid constructs and validation of protein expression and oligomerization status in HEK293T cells.

(a) Sanger sequencing confirms sequence integrity of LGALS1 WT and Mut constructs, with the intended amino acid substitutions at positions 2 and 5 in the Mut plasmid. (b) Native gel analysis shows galectin-1 WT migrating at a higher molecular weight consistent with homodimer formation, whereas the Mut protein migrates at a lower molecular weight indicative of a monomeric state. SDS-PAGE demonstrates comparable expression levels of WT and Mut galectin-1. Data are representative of n = 3 independent biological replicates. This figure was generated by Dr. Dianbo Qu.

3.3. Galectin-1 Mut binds HOXA5 *in-vitro*

Previous research has shown that galectin-1 WT binds to HOXA5 (Sharanek et al., 2021). To investigate whether galectin-1 Mut also associates directly with HOXA5, we performed a GST pull-down using recombinant GST-HOXA5 (bait) or GST alone (negative control) incubated with purified His-tagged galectin-1 WT or the dimerization-deficient Mut (**Figure 7**). After washing, bound proteins were analyzed by western blot using an anti-galectin-1 antibody which also detects galectin-1 Mut. A clear galectin-1 signal was observed in the GST-HOXA5 pull-down for both WT and Mut, whereas binding to GST alone was negligible, indicating that HOXA5 directly binds galectin-1 independent of its oligomeric state. Anti-GST antibody was used to verify comparable recovery of GST-HOXA5 and GST across conditions, and Coomassie blue staining confirmed equal bait loading and the presence of the His-galectin-1 inputs. Together, this data demonstrates that HOXA5 binds galectin-1 *in-vitro* and that the dimerization-deficient Mut retains HOXA5-binding capacity. However, this approach does not indicate the specific binding interface, binding affinity, or the influence of cellular context on the interaction. Thus, complementary assays in BTSCs will be required to define how galectin-1 oligomeric state modulates HOXA5 binding and function.

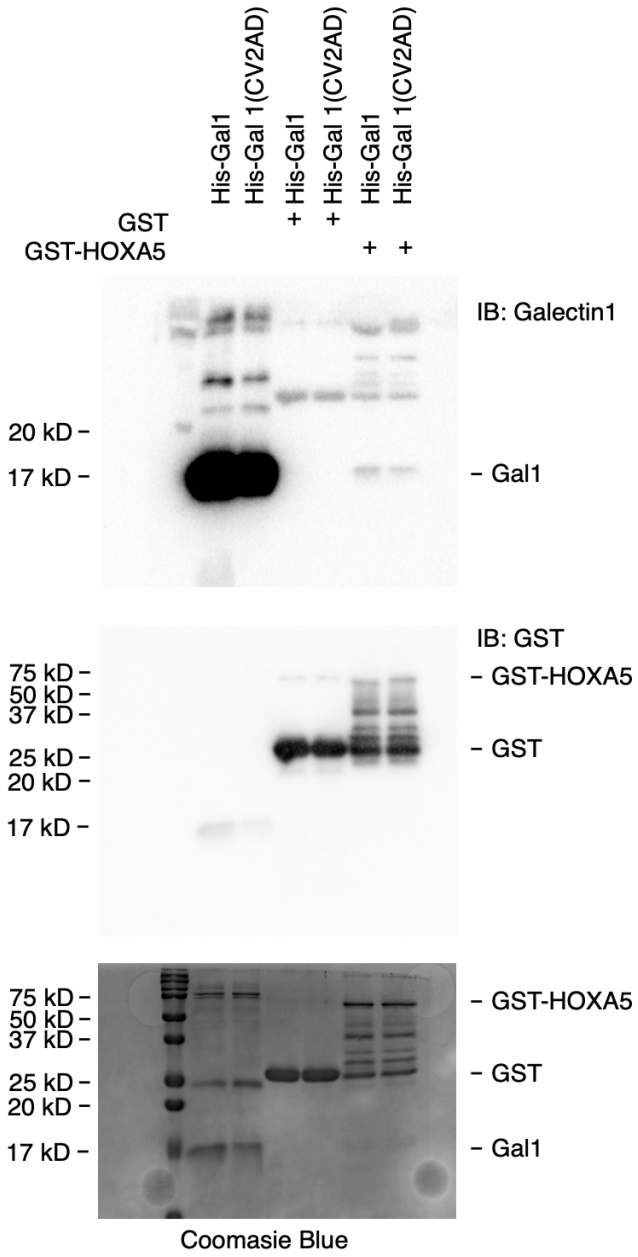
His-Gal1
His-Gal 1(CV2AD)
+ His-Gal1
+ His-Gal 1(CV2AD)
His-Gal1
His-Gal 1(CV2AD)
GST
GST-HOXA5
+ +
IB: Galectin1
20 kD
17 kD
Gal1
IB: GST
75 kD
50 kD
37 kD
25 kD
20 kD
17 kD
GST-HOXA5
GST
75 kD
50 kD
37 kD
25 kD
20 kD
17 kD
GST-HOXA5
GST
Gal1
Coomasie Blue

Figure 7. Galectin-1 WT and Mut binds HOXA5 *in-vitro*. Recombinant GST-HOXA5 or GST (bait) incubated with purified His-tagged galectin-1 WT (His-Gal1 WT) or galectin-1 Mut (His-Gal1 Mut; CV2AD). Bound proteins were analyzed by western blot with anti-galectin-1 (top panel) and anti-GST (middle panel). Total protein is shown by Coomassie Blue staining (bottom panel). Lanes (left to right): (1) GST + His-Gal1 WT; (2) GST + His-Gal1 Mut; (3) GST-HOXA5 + His-Gal1 WT; (4) GST-HOXA5 + His-Gal1 Mut; (5) His-Gal1 WT input; (6) His-Gal1 Mut input. A specific galectin-1 band (17 kDa) was observed with GST-HOXA5 for both galectin-1 WT and Mut, whereas binding to GST alone was negligible. Anti-GST blotting shows comparable recovery of GST-HOXA5 (65 kDa) and GST (26 kDa) across conditions, and Coomassie blue assay confirms equivalent bait loading and galectin-1 inputs. Data are representative of n = 3 independent biological replicates. This figure was generated by Dr. Dianbo Qu.

3.4. Galectin-1 WT supports HOXA5-mediated BTSC self-renewal and sphere growth, while galectin-1 Mut impairs both

To validate our predicted protein interaction model (**Figure 5**), which suggests that the galectin-1 Mut disrupts HOXA5's DNA-binding activity, we assessed the effects of galectin-1 Mut on self-renewal and sphere growth. If galectin-1 Mut impairs HOXA5's ability to bind DNA and regulate transcription, we would expect to observe reduced self-renewal capacity and diminished sphere growth in the galectin-1 Mut BTSC lines. To test this, we co-transfected BTSCs with galectin-1 WT and galectin-1 Mut plasmids and a separate GFP plasmid via electroporation and employed fluorescence-activated cell sorting (FACS) to collect GFP-positive cells. We then performed extreme limiting dilution analysis (ELDA) and sphere growth analysis in 3 different patient-derived BTSC cell lines to assess the functional significance of galectin-1 WT homodimer and galectin-1 Mut monomer in maintaining BTSC self-renewal (**Figure 8**) and sphere growth (**Figure 9**). These cell lines harbor distinct mutations in key GB genes, modeling different molecular subtypes and enabling us to test whether the effects of galectin-1 oligomeric state are conserved across genetically diverse BTSCs (**Table 1**).

Preliminary results suggest that galectin-1 WT homodimer enhances BTSC self-renewal and growth, while the Mut monomer form may impair these functions by potentially interfering with HOXA5's DNA-binding function and gene regulation. This phenotype is consistent across these cell lines, suggesting that galectin-1 homodimerization may play a key role in HOXA5-mediated transcriptional regulation and BTSC maintenance, independent of their mutational background. Using LGALS1 CRISPR BTSCs previously generated in our lab (Sharanek et al., 2021), which lack endogenous galectin-1 expression, we isolated the effects of exogenous galectin-1 (**Figure**

8d). We observed a consistent decrease in self-renewal and sphere growth when galectin-1 Mut was introduced, relative to galectin-1 WT. An empty vector control (CTL) was included to establish baseline self-renewal and sphere growth in the absence of galectin-1 expression in LGALS1 CRISPR cells. Compared with this control, exogenous galectin-1 Mut showed a slight but non-significant reduction in self-renewal, and in sphere assays did not significantly reduce growth across seeding densities of 200, 25, and 12 cells per well (Figure 9d). These patterns suggest that galectin-1 Mut behaves similarly to the absence of galectin-1, as its effects on self-renewal and sphere growth closely resembles that of the CTL, indicating a loss of functional activity relative to galectin-1 WT. Methodologically, low electroporation efficiency produced few GFP+ cells after FACS, preventing reliable Western blot quantification of galectin-1, and because galectin-1 plasmids lacked a fluorescent tag we performed co-transfection with a separate GFP reporter plasmid. Thus, GFP positivity does not guarantee uniform plasmid delivery or matched expression of galectin-1 WT vs Mut. Consequently, differences in abundance between WT and Mut cannot be excluded, and the lack of significance versus CTL may reflect under-expression of Mut compared to endogenous galectin-1. Notably, exogenous galectin-1 WT significantly increased self-renewal over CTL, reinforcing the importance of galectin-1 dimerization for BTSC self-renewal and sphere growth.

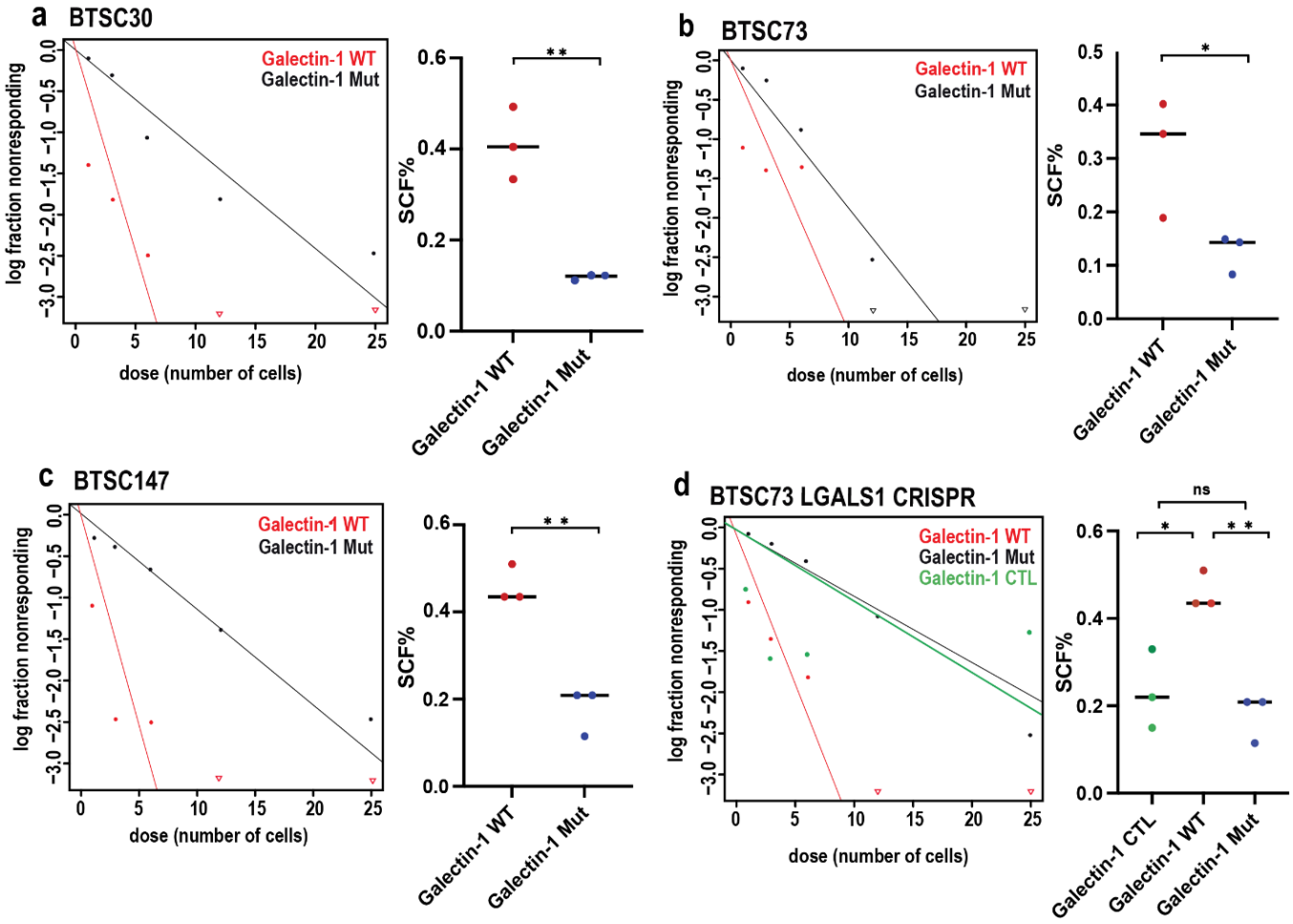
a
BTSC30
Galectin-1 WT
Galectin-1 Mut
log fraction nonresponding
dose (number of cells)
SCF%
**
Galectin-1 WT
Galectin-1 Mut
b
BTSC73
Galectin-1 WT
Galectin-1 Mut
log fraction nonresponding
dose (number of cells)
SCF%
*
Galectin-1 WT
Galectin-1 Mut
c
BTSC147
Galectin-1 WT
Galectin-1 Mut
log fraction nonresponding
dose (number of cells)
SCF%
**
Galectin-1 WT
Galectin-1 Mut
d
BTSC73 LGALS1 CRISPR
Galectin-1 WT
Galectin-1 Mut
Galectin-1 CTL
log fraction nonresponding
dose (number of cells)
SCF%
ns
*
**
Galectin-1 CTL
Galectin-1 WT
Galectin-1 Mut

Figure 8. Galectin-1 WT and Mut effects on BTSC self-renewal. (a-d) Extreme limiting dilution analysis (ELDA) of cells expressing galectin-1 WT or Mut plasmids. Graphs show the log fraction of wells without spheres plotted against the number of cells plated per well, with solid lines representing the fitted linear regression for each condition. Statistical analysis was performed using using one-way ANOVA. Data are represented as the means ± SD.*p-value<0.05; **p-value<0.01; ***p-value<0.001; ns: non-significant. Data are representative of n = 3 independent biological replicates.

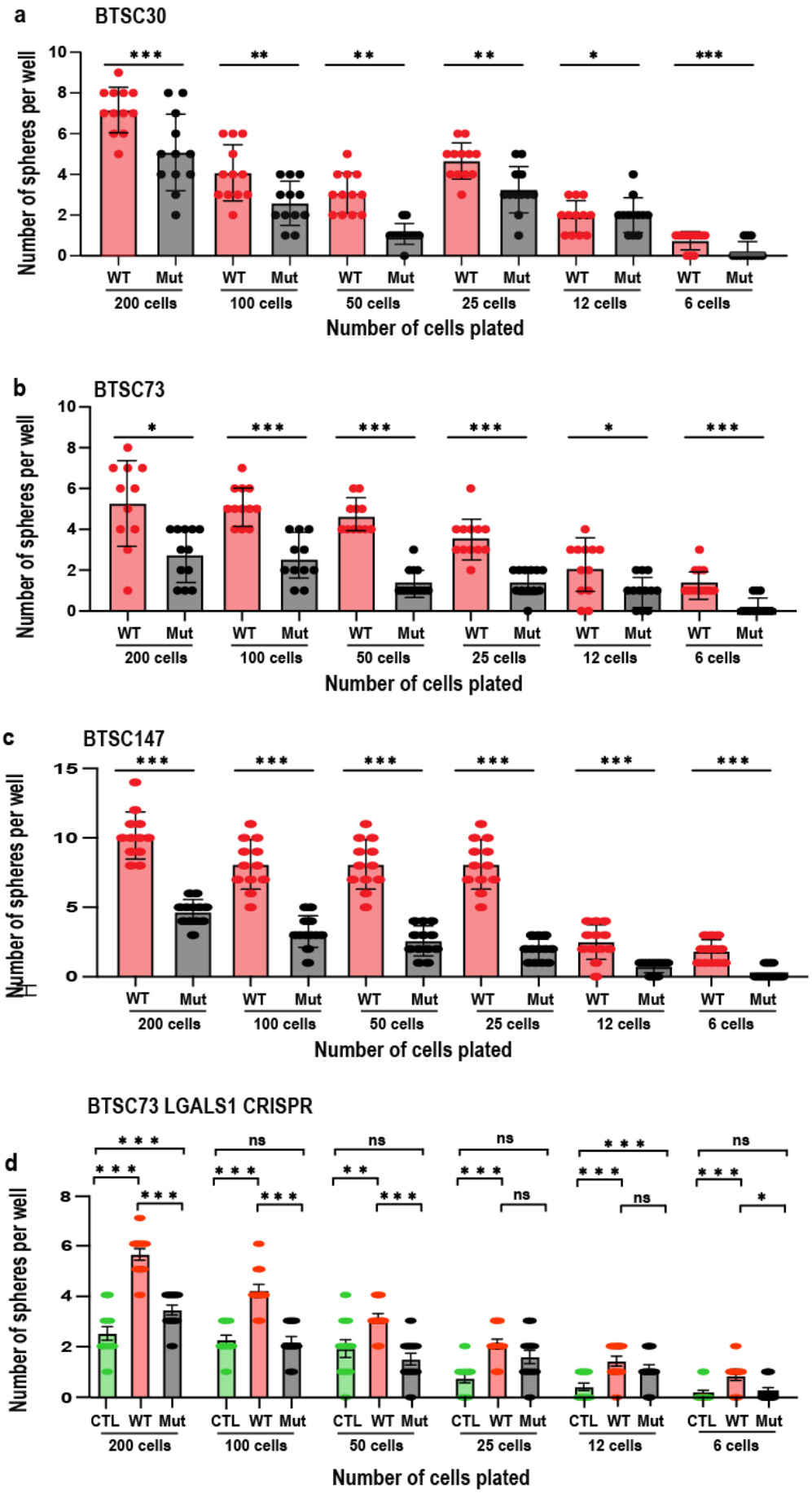
a
BTSC30
Number of spheres per well
WT
Mut
200 cells
100 cells
50 cells
25 cells
12 cells
6 cells
Number of cells plated
b
BTSC73
c
BTSC147
d
BTSC73 LGALS1 CRISPR
CTL

Figure 9. Galectin-1 WT and Mut plasmid effects on BTSC sphere growth. Limiting dilution analysis (LDA) of cells expressing galectin-1 WT or Mut plasmids. The x-axis represents the number of cells seeded per well, while the y-axis shows the number of spheres formed per well. Statistical analysis was performed using one-way ANOVA. Data are represented as the means ± SD.*p-value<0.05; **p-value<0.01; ***p-value<0.001; ns: non-significant. Data are representative of n = 3 independent biological replicates.

3.5. Galectin-1 WT enhances HOXA5 occupancy at target genes, while galectin-1 Mut impairs HOXA5 DNA-binding

To assess the effect of galectin-1 on HOXA5's transcriptional activity, we probed for enrichment at the promoter of known HOXA5 target genes: Tumour protein p53 (TP53), pleiotrophin (PTN), cadherin-1 (CHD1), Potassium channel subfamily K member 2 (KCNK2) and Down Syndrome cell adhesion molecule (DSCAM) (**Figure 10**). Hemoglobin subunit beta (HBB) locus was used as a negative control. In HEK293T cells co-expressing HOXA5 WT and galectin-1 WT, we observed a significant increased enrichment of HOXA5 at the promoter of PTN, CHD1, KCNK2 and DSCAM target genes, consistent with active DNA-binding. However, in cells expressing HOXA5 WT and galectin-1 Mut, a significantly reduced enrichment at the same HOXA5 target genes was observed, suggesting impaired interaction between HOXA5 and DNA. Statistical significance was not achieved when the TP53 target gene was used, however the trend of reduced enrichment in the presence of galectin-1 Mut held consistent. Additionally, an empty vector control was also co-expressed with HOXA5 WT to establish the baseline level of HOXA5 DNA occupancy in the absence of exogenous galectin-1, such that any differences can be attributable to galectin-1 WT versus Mut. HBB acted as an off-target control to account for background non-specific binding, and a significant increase in enrichment was noted for the galectin-1 WT condition for PTN, CHD1, KCNK2 and DSCAM targets. Galectin-1 Mut has increased enrichment compared to HBB for CHD1 and PTN, while it had non-significant comparable levels for KCNK2 and DSCAM, indicating galectin-1 Mut reduces HOXA5 enrichment to background levels. These findings point to a model in which galectin-1 dimerization may facilitate HOXA5's ability to bind chromatin, potentially by stabilizing its conformation, aiding in nuclear localization, or by facilitating interactions with necessary co-

factors. Disruption of galectin-1 dimerization may attenuate HOXA5's transcriptional function. One possibility is that the galectin-1 Mut may aberrantly bind to the homeobox domain of HOXA5, sterically hindering its access to DNA or by disrupting the conformation required for stable DNA-binding. These findings thus warrant complementary functional assays to further elucidate the role of galectin-1's oligomeric state in regulating HOXA's DNA-binding and transcriptional activity.

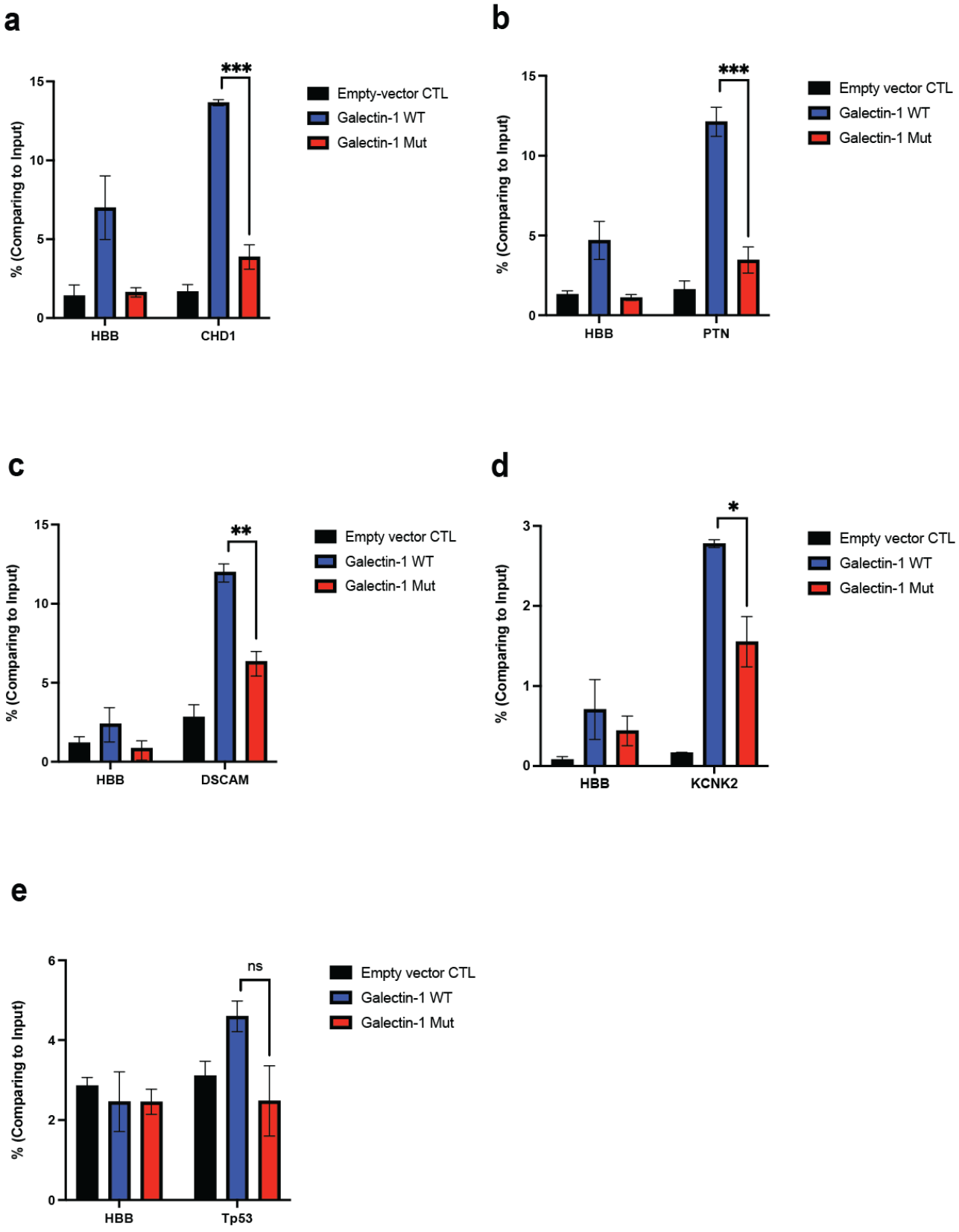
a
***
15
10
5
0
% (Comparing to Input)
HBB
CHD1
Empty-vector CTL
Galectin-1 WT
Galectin-1 Mut
b
***
15
10
5
0
% (Comparing to Input)
HBB
PTN
Empty vector CTL
Galectin-1 WT
Galectin-1 Mut
c
**
15
10
5
0
% (Comparing to Input)
HBB
DSCAM
Empty vector CTL
Galectin-1 WT
Galectin-1 Mut
d
*
3
2
1
0
% (Comparing to Input)
HBB
KCNK2
Empty vector CTL
Galectin-1 WT
Galectin-1 Mut
e
ns
6
4
2
0
% (Comparing to Input)
HBB
Tp53
Empty vector CTL
Galectin-1 WT
Galectin-1 Mut

Figure 10. Galectin-1 dimerization may promote HOXA5 DNA-binding at target genes. Chromatin immunoprecipitation followed by qPCR (ChIP-qPCR) was performed using an anti-HA antibody to assess HOXA5 binding at TP53, PTN, CHD1, KCNK2, and DSCAM promoters (known HOXA5 target genes) and the HBB promoter was used as an off-target negative control. qPCR values are expressed as % input. Data are represented as the means ± SD.*p-value<0.05; **p-value<0.01; ***p-value<0.001; ns: non-significant. Statistical analysis was performed using one-way ANOVA followed by post hoc multiple-comparison testing. Data are representative of n = 3 independent biological replicates.

3.6. LGALS1 (WT and Mut) was successfully subcloned in a lentiviral backbone to enable stable expression

To faciliate future investigation of HOXA5 interactions with galectin-1 homodimers vs monomers, we subcloned LGALS1 into a lentiviral vector using restriction enzyme cloning. This lentiviral system provides more efficient and consistent gene delivery in BTSCs compared to electroporation, while supporting stable transgene expression. This strategy sets the stage for future mechanistic studies on how galectin-1's oligomeric state influences its mode of binding and transcriptional cooperation with HOXA5.

To generate lentiviral constructs for stable expression of galectin-1 WT and Mut, we first replaced the GFP reporter in a lentiviral backbone with mCherry (**Figure 11a**). This facilitates co-transfection of HA-tagged HOXA5 plasmids which contain a GFP reporter, with galectin-1 plasmids. The mCherry coding sequence came from a donor plasmid and was inserted into a lentiviral backbone via restriction enzyme digestion and ligation. The ligation mixture was transformed into competent bacteria, and four colonies were selected for downstream screening. Plasmid DNA from each clone was purified and used for PEI transfection into HEK-293T cells to validate successful reporter replacement by fluorescence microscopy (**Figure 11b**). Three of the four clones exhibited mCherry fluorescence, indicating successful substitution with mCherry, while one retained GFP expression, suggesting an unsuccessful replacement.

The confirmed mCherry-positive vector was used for subcloning with either PCR-amplified Galectin-1 WT or galectin-1 Mut coding sequences (**Figure 11c**). To confirm successful incorporation of the LGALS1 gene, we performed screening using colony PCR (**Figure 11d**).

Colony PCR showing the expected band size were selected for plasmid isolation and purification. Plasmids from positive clones were sent for Sanger sequencing, which confirmed that there is no mutation introduced in the full-length LGALS1 gene, and that mCherry, Flag-tag and P2A sequences were in frame (**Figure 11e**). This final step validated that the galectin-1 WT and Mut constructs were accurately inserted into the mCherry-tagged lentiviral vector, ready for downstream viral packaging and functional studies in BTSCs.

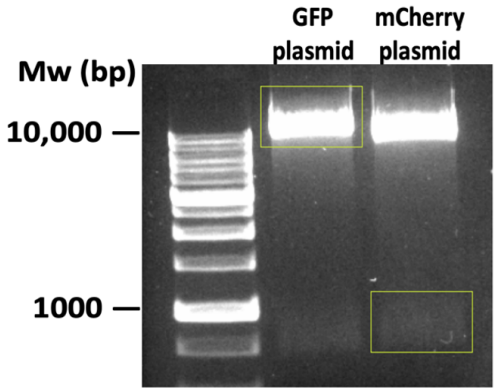
GFP plasmid
mCherry plasmid
Mw (bp)
10,000
1000

Figure 11a. Restriction digestion of GFP-expressing lentiviral backbone and mCherry donor plasmid. Plasmids were digested with BamHI and BSRGI to remove the GFP insert from the lentiviral backbone and to isolate the mCherry fragment from the donor plasmid. DNA gel electrophoresis confirmed successful digestion, with two distinct bands visible in each lane: one representing the vector backbone and the lower band representing the excised GFP or mCherry insert.

Incomplete digestion

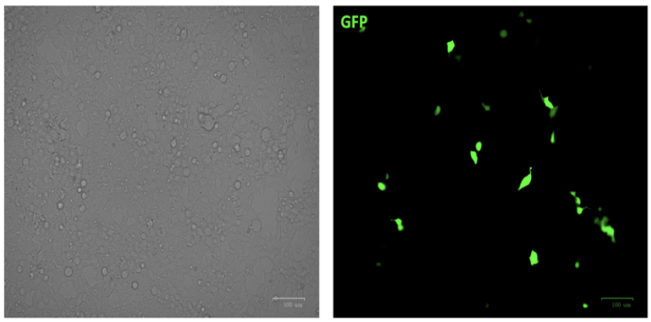

Complete digestion

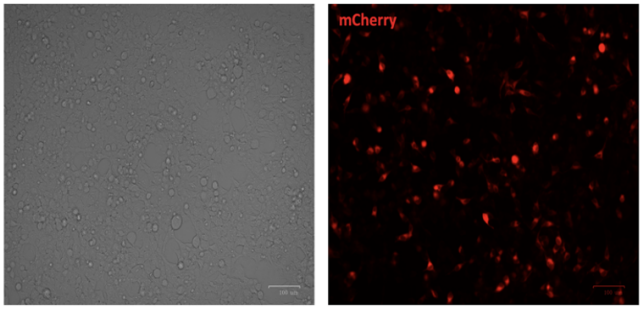

Figure 11b. Fluorescence microscopy of HEK-293 cells transfected with candidate mCherry-replacement clones. Four bacterial clones from the mCherry ligation were screened by PEI transfection into HEK-293 cells. Fluorescence microscopy revealed that three clones expressed mCherry, confirming successful replacement of GFP, while one clone retained GFP signal, indicating failed substitution, and was excluded from follow up analysis.

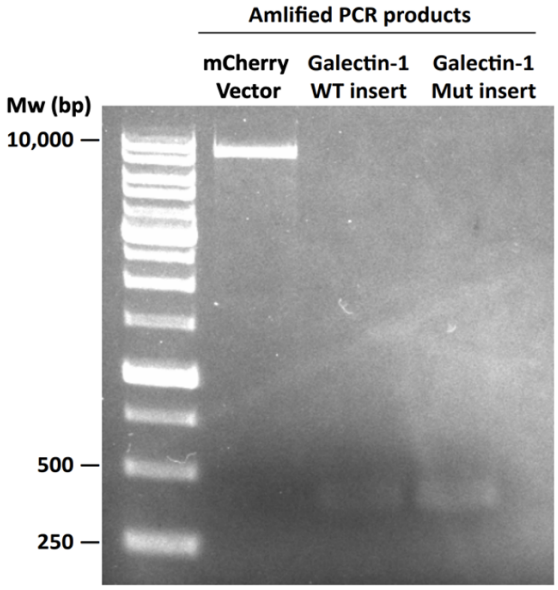
Amlified PCR products
mCherry Vector
Galectin-1 WT insert
Galectin-1 Mut insert
Mw (bp)
10,000
500
250

Figure 11c. Restriction digestion and PCR amplification for Galectin-1 subcloning.

Following successful mCherry replacement, Galectin-1 WT and Mut sequences were PCR-amplified and subcloned into the mCherry-expressing lentiviral backbone using Xho1 and Smal1 restriction enzymes. DNA gel electrophoresis shows successful amplification of LGALS1 WT and Mut inserts and digestion of the recipient vector.

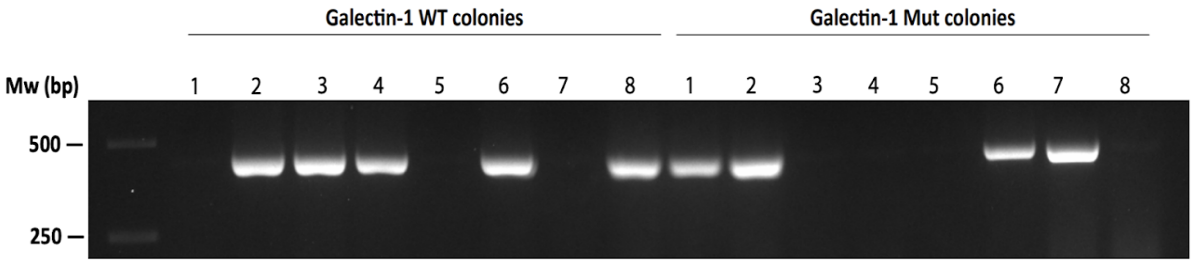
Galectin-1 WT colonies
Galectin-1 Mut colonies
Mw (bp)
1 2 3 4 5 6 7 8 1 2 3 4 5 6 7 8
500
250

Figure 11d. Colony PCR screening for Galectin-1 (LGALS1) insertion into lentiviral plasmids. Bacterial colonies transformed with ligation products were screened via colony PCR using LGALS1-targetting primers. Gel electrophoresis confirmed the presence of the LGALS1 insert in selected clones, as indicated by the expected amplicon size around 400 bp.

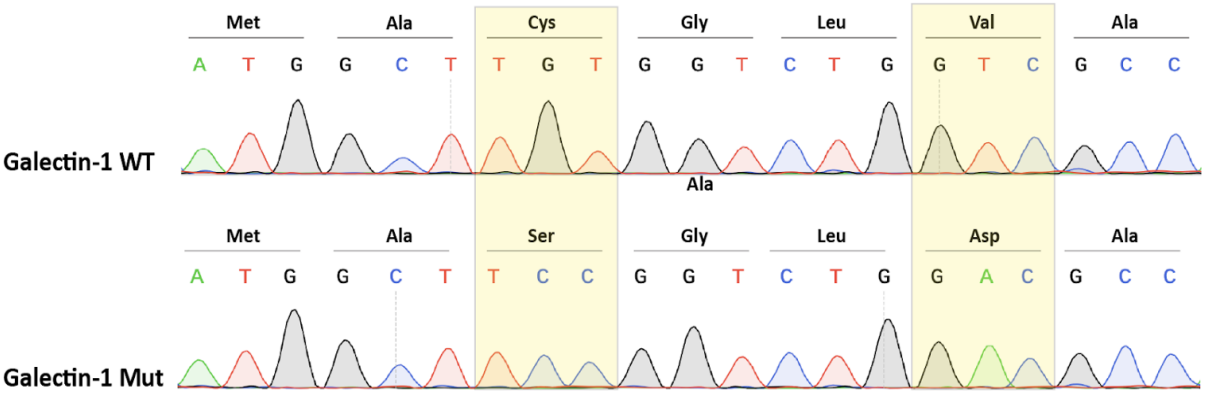
Met
Ala
Cys
Gly
Leu
Val
Ala
A T G G C T T G T G G T C T G G T C G C C
Galectin-1 WT
Ala
Met
Ala
Ser
Gly
Leu
Asp
Ala
A T G G C T T C C G G T C T G G A C G C C
Galectin-1 Mut

Figure 11e. Sanger sequencing confirmation of Galectin-1 WT and Mutant plasmid constructs. Plasmids from positive colony PCR clones were sequenced to verify the presence and integrity of LGALS1 WT and Mut inserts. Chromatograms confirmed full-length sequence identity and absence of unintended mutations in the coding region. Amino acid substitutions differentiating Galectin-1 WT from Galectin-1 Mut plasmids are observed at positions 2 and 5, wherein cysteine and valine in the WT sequence are replaced with serine and aspartic acid in the Galectin-1 Mut plasmid.

3.7. Anti-HOXA5 antibodies lack specificity in BTSCs

We sought to identify an anti-HOXA5 antibody that binds endogenous HOXA5 with high specificity, suitable for downstream genetic and functional assays. Using HOXA5 CRISPR and wild-type control (CTL) BTSCs, we tested four commercially available anti-HOXA5 antibodies by Western blot and immunostaining (**Figure 12**). However, none of the antibodies demonstrated adequate specificity, as non-specific signals were detected in control lines compared to CRISPR lines. These limitations led us to pursue an alternative strategy: generating BTSCs expressing HA-tagged HOXA5 via lentiviral transduction, enabling reliable detection and downstream functional analysis using anti-HA antibodies.

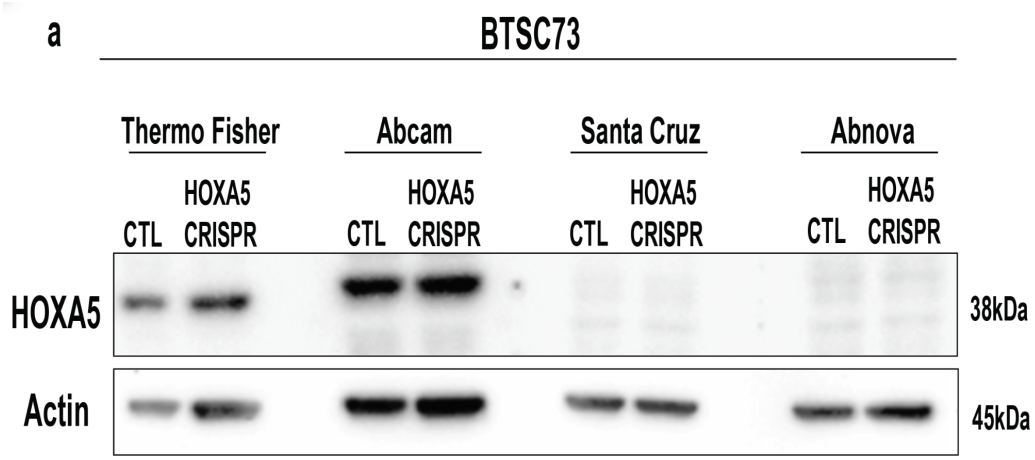
a
BTSC73
Thermo Fisher
Abcam
Santa Cruz
Abnova
CTL
HOXA5 CRISPR
CTL
HOXA5 CRISPR
CTL
HOXA5 CRISPR
CTL
HOXA5 CRISPR
HOXA5
38kDa
Actin
45kDa

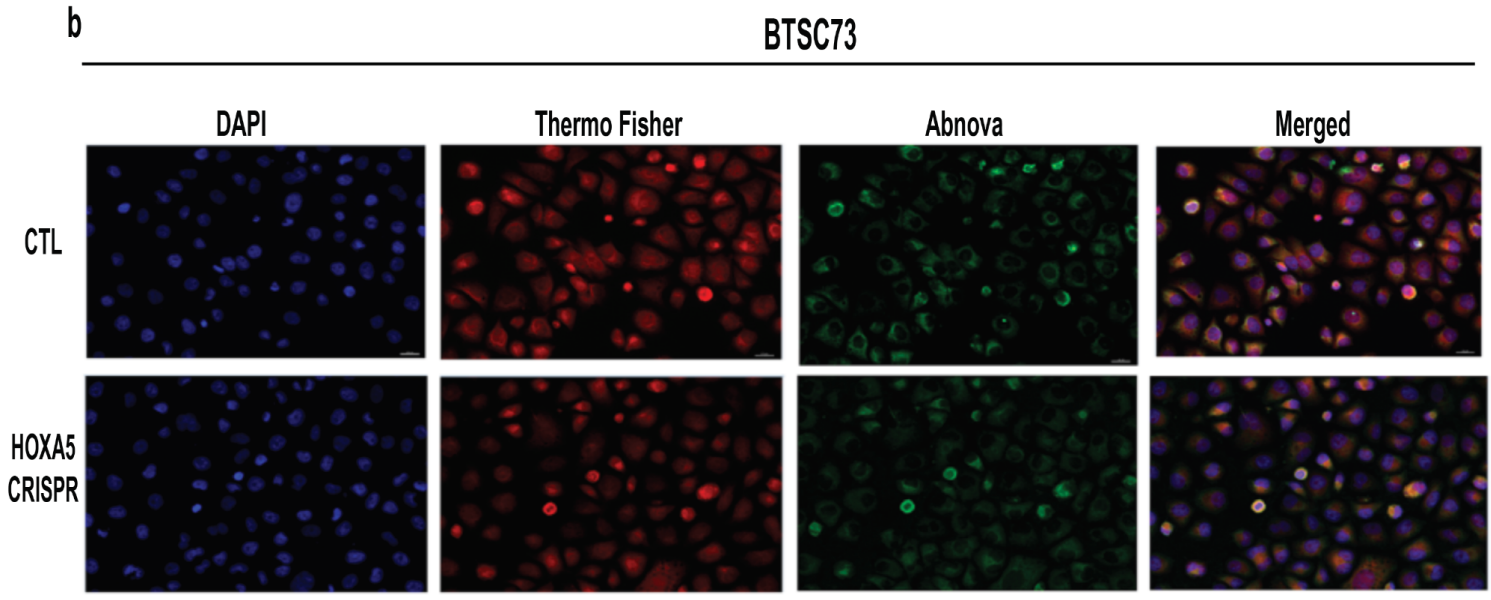
b
BTSC73
DAPI
Thermo Fisher
Abnova
Merged
CTL
HOXA5 CRISPR

Figure 12. Evaluation of anti-HOXA5 antibody specificity in BTSCs. To identify a high-specificity anti-HOXA5 antibody suitable for genetic and functional assays, four commercially available antibodies were tested by (a) Western blot and (b) immunostaining in HOXA5 CRISPR and wild-type control (CTL) BTSCs. None of the antibodies demonstrated adequate specificity, as comparable signals were observed in both CRISPR and CTL samples, indicating non-specific binding. Data are representative of n = 3 independent biological replicates.

3.8. Generation of lentiviral HA-tagged HOXA5 WT and domain-deletion BTSC lines to enable reliable detection and domain-specific functional dissection

To enable downstream studies on galectin-1 WT vs Mut interaction with HOXA5, we first aimed to establish reliable tools for detecting endogenous HOXA5 in BTSCs. We were unable to identify a high-specificity anti-HOXA5 antibody, so we used an alternative approach by generating BTSCs expressing HA-tagged HOXA5 via lentiviral transduction, allowing for reliable detection and downstream functional studies using anti-HA antibodies. In addition to generating BTSCs expressing HA-tagged WT HOXA5, we introduced a series of HOXA5 mutant constructs via lentiviral transduction to investigate the functional contribution of specific HOXA5 domains to BTSC characteristics of self-renewal and sphere growth (**Figure 13**). These mutants were designed to dissect the role of different structural regions of the protein: the first HOXA5 mutant contains a deletion of the N-terminal region (ΔN-terminal: aa 2-75); the second mutant construct contains deletion of the intrinsically disordered region (Δdisordered region: aa 75-193); and the third mutant lacks the homeobox DNA-binding domain (Δhomeobox domain: aa 175-259). These lines will enable future studies comparing the effects of these mutants with WT HOXA5, with the aim of elucidating the contributions of individual HOXA5 domains to BTSC characteristics.

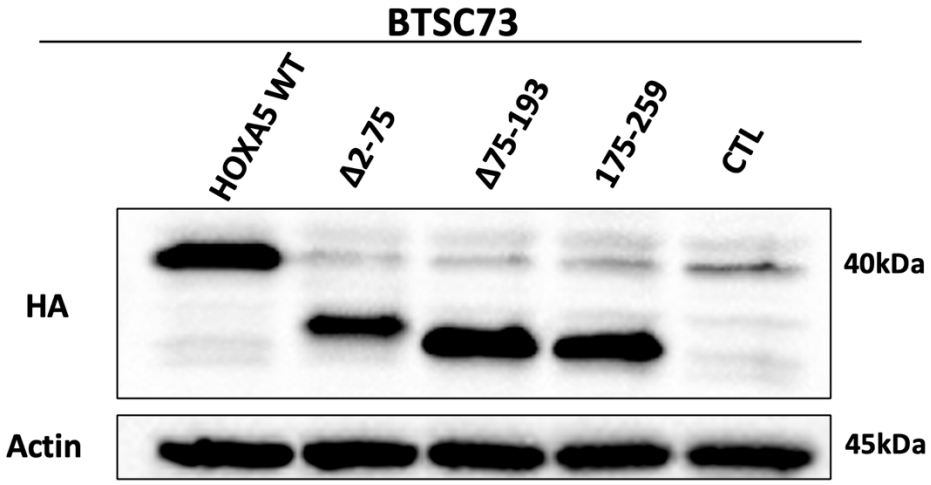
BTSC73
HOXA5 WT
Δ2-75
Δ75-193
175-259
CTL
HA
40kDa
Actin
45kDa

Figure 13. Characterization of HA-tagged HOXA5 WT and mutant over-expressing BTSCs. BTSCs were transduced with lentiviral plasmids encoding HA-tagged wild-type (WT) HOXA5 or one of three deletion mutants to investigate the functional contribution of distinct HOXA5 domains. The first HOXA5 mutant lacks the N-terminal region (ΔN-terminal: aa 2-75), the second mutant has a deletion within the intrinsically disordered region (Δdisordered region: aa 75-193), and the third mutant lacks the homeobox DNA-binding domain (Δhomeobox domain: aa 175-259). The expression of each construct was confirmed by fluorescence microscopy using GFP reporter and western blot using anti-HA antibody. Western blot analysis reveals no detectable band for the empty control (CTL) vector, while a distinct band at approximately 40 kDa corresponds to HA-tagged HOXA5 WT. The three truncated HOXA5 mutant constructs display bands slightly below 38 kDa, and β-actin serves as a loading control. Data are representative of n = 3 independent biological replicates. This figure was generated by Dr. Behnaz Nateghi and Chelsea Leduc.

4. Discussion and Future Directions

4.1. Differential HOXA5 engagement by Galectin- 1 WT and Galectin-1 Mut: implications for DNA binding and BTSC transcriptional regulation

The predictive docking models reveal different modes of interaction between HOXA5 and homodimeric WT galectin-1 versus monomeric Mut galectin-1, with possible implications for HOXA5's DNA-binding and transcriptional activity. Consistent with previous literature demonstrating that galectin-1 acts primarily as a homodimer to mediate much of its biological functions (Stillman et al., 2006), our ClusPro 2.0-based model predicts that the galectin-1 WT homodimer preferentially binds the N-terminal region of HOXA5. This interaction is proposed to promote flexibility in the homeobox domain of HOXA5, which in turn may facilitate binding to its target genes. The conformational flexibility of the homeodomain could allow HOXA5 to efficiently scan chromatin, interact with binding sites with high affinity, and recruit cofactors for transcriptional regulation. In contrast, docking simulations using HADDOCK 4.0 predict that galectin-1 Mut binds to HOXA5's homeodomain, which may reduce the structural flexibility of this DNA-binding region, potentially impeding its ability to bind DNA. This proposed inhibitory mode of galectin-1 binding indicates that its oligomeric state may modulate both its own biological activity and that of its binding partners. The docking data aligns with our hypothesis that galectin-1 dimerization may be required for optimal HOXA5-mediated transcriptional control of BTSC fate. Thus, the disruption of galectin-1 dimerization may lead to decreased DNA-binding efficiency and altered regulation of HOXA5 target genes involved in BTSC maintenance, proliferation, and therapeutic resistance.

While these models provide a framework to explain the differences in galectin-1 WT versus Mut regulation of HOXA5 in BTSCs based on differential binding, it is a predictive model which requires experimental validation. Additionally, given the complexity of protein-protein interactions in the nuclear environment, the interactions between galectin-1 WT vs Mut and HOXA5 may be influenced by additional cofactors, post-translational modifications, or the chromatin context, which the docking models do not accounted for. To validate these predicted models, co-immunoprecipitation (Co-IP) in BTSCs expressing WT or Mut galectin-1, along with additional HOXA5 domain-specific deletion mutants, could refine our understanding of their modes of binding. Additionally, proximity ligation assay (PLA) could be used to visualize these interactions and nuclear co-localization in situ. Functional rescue experiments could assess whether restoring galectin-1 dimerization recovers HOXA5 activity and BTSC phenotypes. These studies can further elucidate whether altered modes of galectin-1 binding impact HOXA5's regulatory function in BTSCs, setting the stage for disrupting galectin-1 dimerization as a potential therapeutic target in GB.

4.2. Validated galectin-1 WT and Mut constructs show oligomerization-independent HOXA5 binding

The sequencing and protein expression analyses performed in this study confirm the structural and functional integrity of the galectin-1 WT and Mut constructs, setting the stage for downstream functional assays. Sanger sequencing verified that both constructs contained the correct full-length LGALS1 sequence without mutations in the coding region, ensuring that any observed phenotypic differences in downstream assays can be attributed to the dimerization-

deficient galectin-1 Mut. Sequencing also verified that the galectin-1 Mut construct carries the two targeted substitutions, C2S and V5D, which literature has reported to disrupt the disulfide bond and hydrophobic interactions necessary for dimerization (Cho & Cummings, 1996).

Native PAGE analysis further supported the functional consequence of these substitutions, with galectin-1 WT migrating at a molecular weight consistent with homodimer formation, while the Mut protein migrated as a monomer. These findings are consistent with previous research that the cysteine at position 2 plays a key role in maintaining galectin-1's dimer interface, and that disruption of early N-terminal residues impairs stable dimerization without destabilizing the monomer itself (Cho & Cummings, 1996). SDS-PAGE analysis also demonstrated that galectin-1 WT and Mut proteins were expressed at comparable levels following transfection into HEK293T cells, excluding differences in protein production or transfection efficiency as confounding factors.

While these findings support indicate that the introduced amino acid substitutions disrupt stable galectin-1 homodimer formation, the assessment of oligomeric state using native PAGE is indirect. Since native PAGE separates proteins based on molecular weight, charge, and conformation, it cannot be used definitively exclude the presence of weak, transient, or context-dependent dimerization that may not be maintained during electrophoresis. Additionally, these experiments were conducted in HEK293T cells, which may not fully capture the intracellular environment of BTSCs, where factors such as protein concentration, redox state, post-translational modifications, and the presence of specific binding partners could influence galectin-1 oligomerization status. Consequently, while these data indicates that the Mut construct disrupts stable galectin-1 homodimerization, complementary experiments in BTSCs would be required to fully characterize the oligomeric state of galectin-1 under physiologically relevant

conditions, including size-exclusion chromatography, crosslinking, or proximity ligation assays (PLA).

Our *in-vitro* pulldown assay shows that recombinant HOXA5 directly binds both galectin-1 WT and the dimerization-deficient Mut, establishing that galectin-1's physical interaction with HOXA5 may not require dimerization. This finding indicates that galectin-1 oligomerization modulates how galectin-1 cooperates with HOXA5 rather than dictating whether or not it binds it. This also supports our protein docking predictions, which proposes that galectin-1 WT and Mut both bind HOXA5, however, to validate whether the Mut binds the homeodomain, additional binding assays must be conducted. Future domain-mapping experiments are required, such as Co-IP/GST pulldown with isolated HOXA5 domains, or site-directed mutagenesis of HOXA5 domains followed by Co-IP/GST pulldown. Thus, while this data confirms direct physical association between galectin-1 Mut and HOXA5, it does not identify the binding site or binding-affinity, and it does not mimic the cellular conditions of BTSCs, which may influence protein binding. In BTSCs, HOXA5 and galectin-1 operate in a nuclear environment which is shaped by a distinctive chromatin landscape, abundance of co-factors and chromatin remodelers (PBX/MEIS, p300/CBP) that typically interact with and stabilize HOXA5, post-translational modifications (PMTs) (phosphorylation/acetylation of HOXA5) as well as a distinct redox environment which dictates galectin-1 homodimer vs monomer equilibrium. Thus, domain mapping in BTSCs using HOXA5 point mutants followed by Co-IP/PLA, as well as BTSC chromatin-context assays (ChIP-qPCR) will be required to determine how BTSC-specific conditions modulate galectin-1/HOXA5 interaction.

4.3. Galectin-1 oligomeric status impacts BTSC characteristics

Our results demonstrate that galectin-1's oligomeric state has functional consequences for BTSC self-renewal and sphere growth capacity (**Figure 14**). These effects are consistent across genetically diverse patient-derived BTSC lines. Galectin-1 WT consistently enhanced both self-renewal (ELDA) and sphere growth (LDA), whereas galectin-1 Mut was associated with a trend toward reduced function in both assays. These results support our docking predictions, which suggest that WT galectin-1 interacts with the N-terminal region of HOXA5 which may promote conformational flexibility in the homeodomain, thereby enhancing DNA-binding. In contrast, galectin-1 Mut may interact directly with the homeodomain in a manner that may restrict its conformational flexibility, potentially impeding DNA-binding and transcriptional regulation. We used three BTSC lines representing distinct GB mutational profiles: BTSC30 (EGFR WT, TP53 WT, PTEN Mut), BTSC73 (EGFRvIII, TP53 Mut, PTEN Mut, CDKN2A Mut), and BTSC147 (EGFRvIII, TP53 Mut, PTEN Mut, CDKN2A Mut, NF1 WT). This enabled us to evaluate whether this phenotype is context-specific or broadly observed. Notably, the consistent impairment observed with galectin-1 Mut suggests that the requirement for galectin-1 dimerization in HOXA5-mediated transcription is independent of EGFR or TP53 status. We also used LGALS1 CRISPR cell lines, which lack endogenous galectin-1 expression, which allowed us to isolate the impact of the exogenous galectin-1 on self-renewal and growth, without the potential confounding influence of endogenous galectin-1 crosstalk or interference. These cell lines also exhibit a similar pattern, whereby decreased self-renewal and growth is observed when galectin-1 Mut. Additionally, when comparing sphere growth in the presence of exogenous galectin-1 Mut vs endogenous galectin-1 WT (CTL), the Mut did not have reduced sphere growth capacity at all cell doses. At 200, 25 and 12 cells plated, the Mut had increased sphere

growth compared to the CTL. This suggests that endogenous homodimeric galectin-1 is sufficient in maintaining stemness and sphere growth, and that the Mut monomer is either non-functional or ineffective at dampening stemness and sphere growth programs at the achieved expression levels, compared to endogenous galectin-1 homodimeric expression levels. Due to low electroporation efficiency, a low cell number of GFP+ BTSCs were collected after FACS, giving insufficient protein for reliable Western blot analysis of expression levels. Additionally, since the galectin-1 plasmids did not carry a fluorescent reporter, we co-transfected a separate GFP plasmid. Thus, sorting for GFP+ does not guarantee uniform co-delivery or matched expression of the galectin-1 constructs, and we cannot exclude unequal uptake or expression between WT and Mut galectin-1. Consequently, we cannot adequately compare galectin-1 WT versus Mut protein abundance in these experiments, as the effects observed could reflect reduced Mut expression rather than a true biological effect.

Additionally, exogenous galectin-1 WT overexpression produces a significant increase in self-renewal capacity compared to endogenous galectin-1 WT levels, indicating that homodimeric galectin-1 may be a limiting factor for BTSC maintenance and that increasing its expression levels may further promote stemness programs. This is consistent with the signalling axis in which galectin-1 homodimers enhance HOXA5-dependent transcriptional programs (Sharanek et al., 2021) and that galectin-1 overexpression correlates with increased GB aggressiveness (Camby et al., 2006; Huang et al., 2021; Li et al., 2021). Together, these results point to the importance of galectin-1 dimerization in driving BTSC self-renewal and growth, while highlighting that the monomeric Mut confers a possible dampening effect. These results point towards a model where interfering with the dimerization of galectin-1 monomers may disrupt HOXA5/galectin-1 complex formation and BTSC tumourigenicity.

Future experiments can employ galectin-1 constructs which have a fluorescent tag on the same promoter, and FACS sort based on matched reporter intensity, and confirm protein expression by Western blot analysis using antibodies against the fluorescent tag, to exclude endogenous galectin-1 expression. Additionally stable lentiviral delivery would ensure comparable galectin-1 WT and Mut expression and allow for comparisons of transient vs stable expression on BTSC characteristics. Additionally, future studies may focus on transcriptomic profiling of BTSCs expressing galectin-1 WT or Mut which could reveal the broader impact on galectin-1 Mut on HOXA5-regulated gene networks. Finally, *in-vivo* xenograft experiments using BTSCs expressing galectin-1 WT versus Mut would determine whether these *in-vitro* phenotypes translate into differences in tumour initiation and growth, ultimately assessing the therapeutic potential of targeting galectin-1 dimerization in GB.

Galectin-1 homodimer (WT)

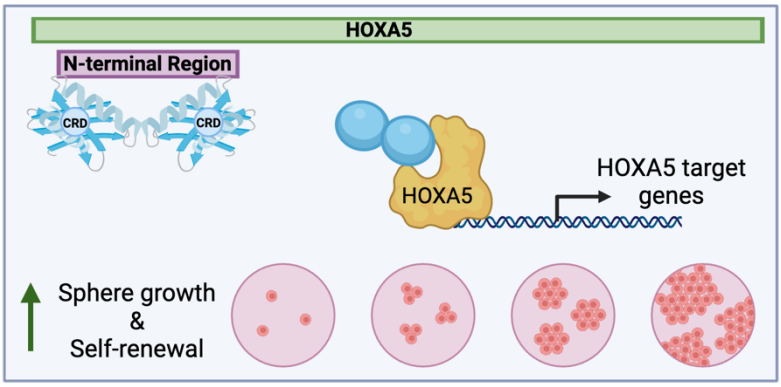

Galectin-1 monomer (Mut)

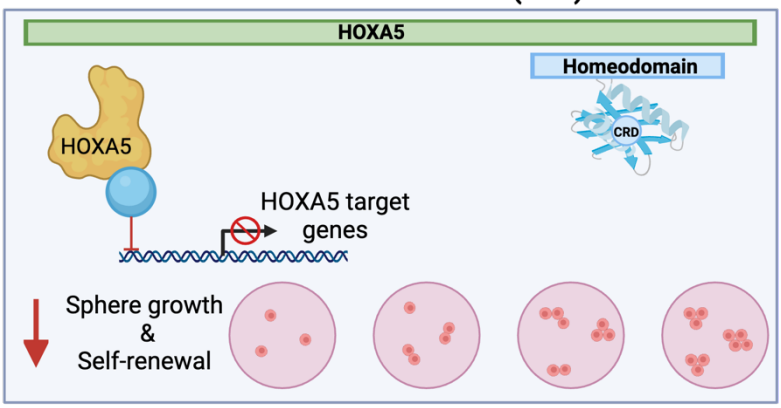

Future directions

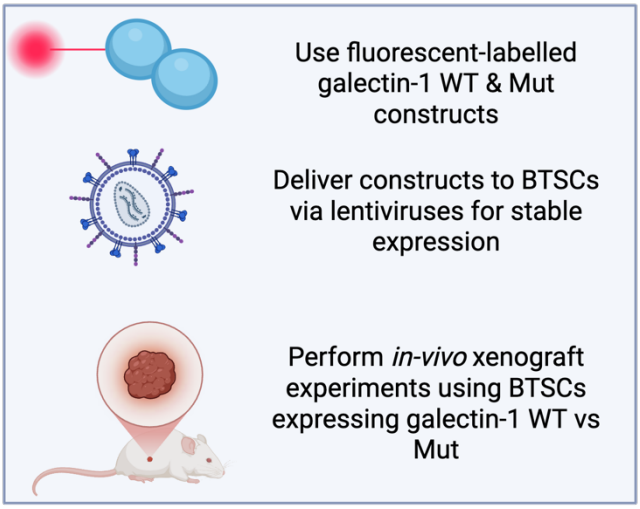

Figure 14. Galectin-1 oligomeric status modulates BTSC self-renewal and growth via HOXA5 interaction. Galectin-1 WT enhances BTSC self-renewal and sphere formation by potentially promoting conformational flexibility of the HOXA5 homeodomain, thereby facilitating transcriptional regulation. In contrast, galectin-1 Mut may bind to the homeodomain itself, thereby impairing DNA-binding and reducing stemness and sphere growth across genetically diverse BTSC lines. These findings suggest that galectin-1 dimerization is critical for HOXA5-dependent transcription of BTSCs, pointing to oligomerization disruption as a potential therapeutic strategy. Limitations in construct expression levels warrant future studies with stable, fluorescently tagged galectin-1 variants and in vivo models. Created using Biorender.com.

4.4. Galectin-1 oligomeric status influences HOXA5 occupancy at target genes

ChIP-qPCR analysis indicates that galectin-1's oligomeric state may affect HOXA5's occupancy at target gene promoters (**Figure 15**). In HEK293T cells co-expressing HOXA5 and galectin-1 WT, enrichment at promoters of known HOXA5 target genes including PTN, CHD1, KCNK2, and DSCAM was significantly higher than in cells co-expressing the dimerization-deficient galectin-1 Mut. This pattern may support our structural model, which predicts that the interaction of galectin-1 WT with HOXA5 facilitates HOXA5-mediated regulation of its targets.

Moreover, since enrichment was reduced but not completely impaired in the presence of galectin-1 Mut, this suggests that HOXA5 retains some intrinsic DNA-binding capacity independent of galectin-1, but that galectin-1 dimerization enhances this interaction, possibly by stabilizing HOXA5 on chromatin or aiding in its recruitment to specific DNA regions. This effect was observed across multiple HOXA5 target genes involved in neurodevelopment

(DSCAM, PTN), cell adhesion (CHD1), and ion channel regulation (KCNK2), suggesting a broad impact on HOXA5's transcriptional regulation. Another possibility is the presence of alternate co-factors, which upon binding to HOXA5 may still modulate its binding to DNA to maintain basal transcriptional activity. However, taken together, our data suggests that galectin-1 dimerization enhances HOXA5 promoter engagement across multiple gene targets, while the monomeric Mut attenuates binding toward background levels. Empty vector control co-expression with HOXA5 established the baseline of HOXA5 occupancy in the absence of exogenous galectin-1, confirming that the observed differences are attributable to WT versus Mut galectin-1.

However, significance was not achieved for one of the targets, the TP53 gene, although we observed a consistent trend of higher enrichment with galectin-1 WT and reduced occupancy with Mut. This may be attributable to cell-type context, whereby HEK293T may have a different chromatin landscape from BTSCs which potentially alters HOXA5's access to TP53 regulatory elements. Additionally, HOXA5 may act at distal enhancers, or alternative TP53 promoter regions not captured by our primers, giving an underestimate of true occupancy, closer to background levels. Furthermore, HOXA5 binding and stabilization at the TP53 gene may require BTSC-specific co-factors which may be absent or limited in HEK293T cells.

HEK293T cells were used for these initial assays due to the low electroporation efficiency of galectin-1 constructs in BTSCs, which limited the feasibility of obtaining high expression which is necessary for ChIP-qPCR. While HEK293T cells offer high transfection efficiency, they lack the endogenous chromatin landscape and co-factor composition present in BTSCs. Thus, additional biological replicates and validation in BTSCs will be necessary to confirm the biological relevance of these findings in future studies. It would be also important to assess

global HOXA5 binding at a genome-wide scale using ChIP-seq in BTSCs expressing galectin-1 WT or Mut to establish whether dimerization-dependent effects extend to the broader HOXA5 regulatory network. Furthermore, co-immunoprecipitation and mass spectrometry (Co-IP/MS) could reveal whether galectin-1 dimerization promotes the recruitment of chromatin-modifying or transcriptional co-activators to the HOXA5 complex. A luciferase reporter assays linking HOXA5 promoter occupancy to transcriptional activation is also essential to provide functional evidence of whether differences in HOXA5 binding translate to changes in gene expression. This would link the ChIP-qPCR data and downstream effects on BTSC self-renewal and sphere growth, establishing a mechanistic link between binding events and transcriptional regulation.

ChIP-qPCR analysis:
Galectin-1 dimerization promotes HOXA5 DNA occupancy

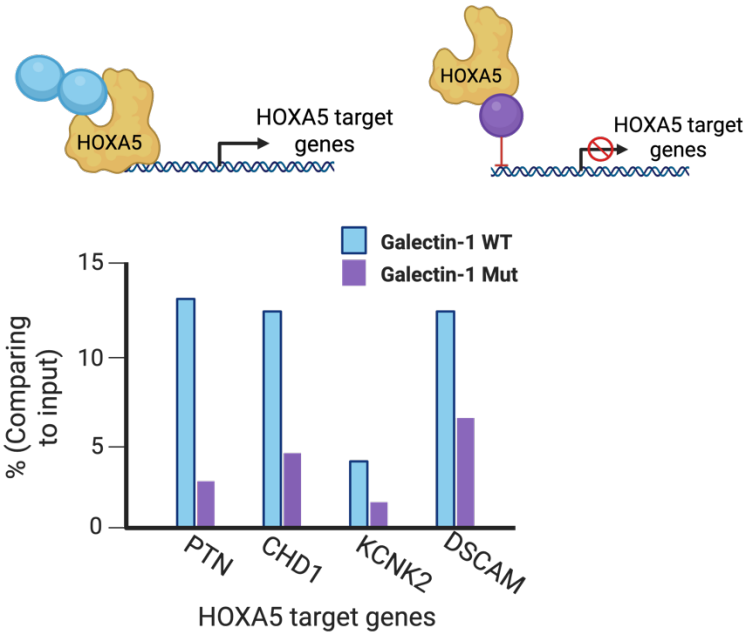

Future directions:

- Validate ChIP-qPCR in BTSCs
- Perform ChIP-seq to assess galectin-1 WT vs Mut impact on genome-wide HOXA5 occupancy
- Co-IP/MS to identify co-factors
- Luciferase assay to measure promoter activity

Figure 15. Galectin-1 dimerization enhances HOXA5 occupancy at target gene promoters. ChIP-qPCR analysis in HEK293T cells demonstrates that co-expression of galectin-1 WT increases HOXA5 enrichment at the promoters of key target genes involved in neurodevelopment (DSCAM, PTN), cell adhesion (CHD1), and ion channel regulation (KCNK2), compared to co-expression with dimerization-deficient galectin-1 Mut or empty vector controls. The reduced but not abolished occupancy in the presence of Mut suggests HOXA5's intrinsic DNA-binding ability, which is augmented by galectin-1 dimerization likely via stabilization and enhanced recruitment to chromatin. Further validation in BTSCs via genome-wide assays and functional studies will clarify the broader regulatory impact of galectin-1 WT vs Mut on HOXA5 function. Created using Biorender.com.

4.5. Generation of HA-tagged HOXA5 WT and domain-deletion mutant BTSC lines

BTSC lines overexpressing HA-tagged HOXA5 WT and domain-specific deletion mutants were generated to enable HOXA5 detection in the absence of a commercially available high-specificity anti-HOXA5 antibody. The HA-tagged constructs addressed antibody specificity issues by enabling detection with reliable anti-HA antibodies. These lines can be used in future studies to dissect the functional contributions of distinct HOXA5 domains to its transcriptional regulation, nuclear localization, and the maintenance of BTSC characteristics.

4.6. Conclusion

Collectively, our findings suggest that galectin-1's oligomeric state regulates HOXA5-mediated transcriptional regulation of BTSCs (**Figure 16**). Predictive docking models suggest that galectin-1 homodimers engage the N-terminal region of HOXA5 to promote homeodomain flexibility and enhance DNA-binding, while monomeric galectin-1 binds the homeodomain itself, potentially restricting its conformational flexibility and impeding DNA-binding. These structural predictions are supported by functional assays showing binding of galectin-1 WT and Mut to HOXA5, and impairment of BTSC self-renewal and growth in the presence of the monomeric form across genetically diverse patient-derived cell lines. Preliminary ChIP-qPCR data in HEK293T cells further indicate that galectin-1 dimerization enhances HOXA5 occupancy at multiple target gene promoters, reinforcing the model that oligomerization facilitates HOXA5's regulatory activity. In future experiments, the generation of stable lentiviral systems for co-expression of galectin-1 WT or Mut with HOXA5 in BTSCs will be required to further investigate this interaction under physiologically relevant conditions. Together, this data proposes a mechanistic framework in which galectin-1 dimerization facilitates HOXA5's transcriptional activity and tumourigenic potential, highlighting the disruption of this interaction as a promising therapeutic strategy in BTSCs of GB.

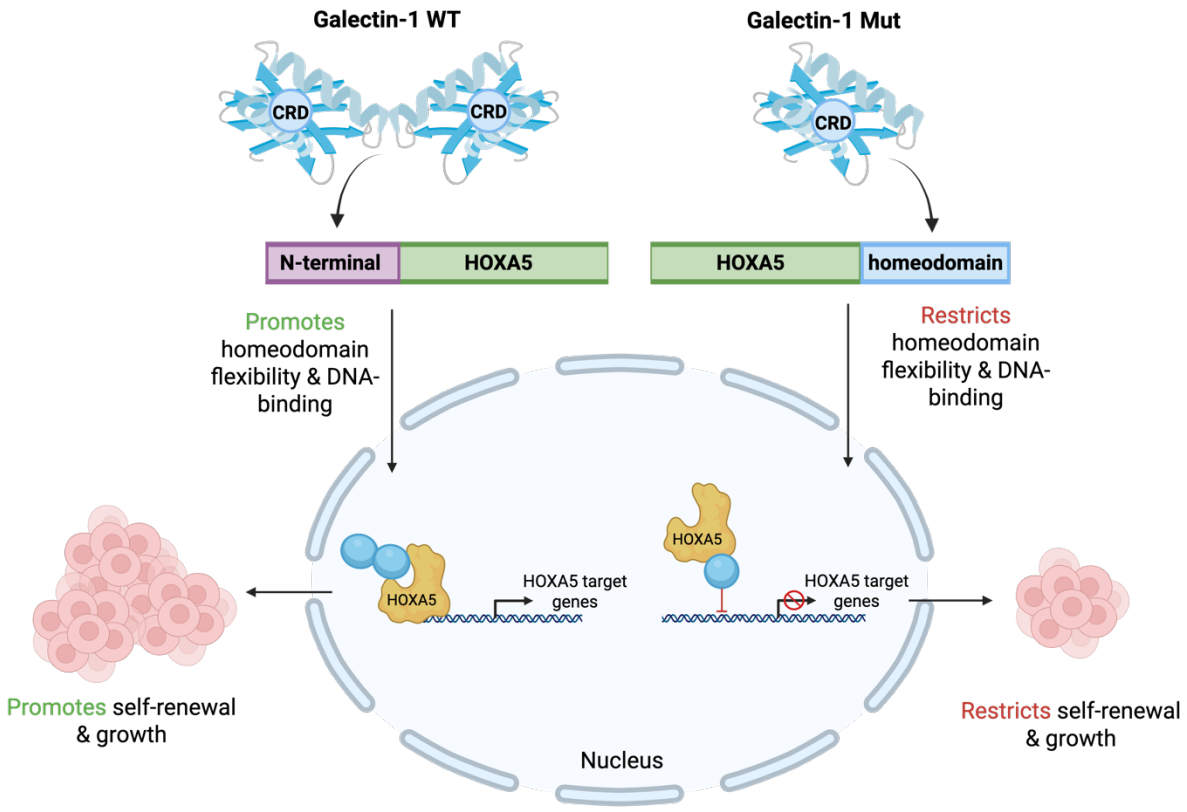
Galectin-1 WT
Galectin-1 Mut
CRD
CRD
CRD
N-terminal
HOXA5
HOXA5
homeodomain
Promotes
homeodomain
flexibility & DNA-
binding
Restricts
homeodomain
flexibility & DNA-
binding
HOXA5
HOXA5 target
genes
HOXA5
HOXA5 target
genes
Promotes self-renewal
& growth
Restricts self-renewal
& growth
Nucleus

Figure 16. Galectin-1 oligomerization modulates HOXA5 transcriptional activity in BTSCs. Structural docking models predict that galectin-1 homodimeric WT binds the N-terminal region of HOXA5, enhancing homeodomain flexibility and DNA-binding, whereas monomeric galectin-1 Mut interacts with the homeodomain itself, restricting its conformational flexibility and reducing DNA-binding. Experimental binding assays confirm association of both galectin-1 WT and mutant forms with HOXA5, and functional assays reveal impaired BTSC self-renewal and growth when galectin-1 Mut is present across diverse patient-derived BTSC lines. Complementary ChIP-qPCR in HEK293T cells shows that galectin-1 dimerization increases HOXA5 occupancy at multiple target gene promoters, supporting a model where galectin-1 oligomerization is critical for HOXA5-mediated transcriptional regulation of BTSCs. Created using Biorender.com.

References

Alcantara Llaguno, S., Chen, J., Kwon, C. H., Jackson, E. L., Li, Y., Burns, D. K., Alvarez-Buylla, A., & Parada, L. F. (2009). Malignant astrocytomas originate from neural stem/progenitor cells in a somatic tumour suppressor mouse model. Cancer Cell, 15(1), 45-56. https://doi.org/10.1016/j.ccr.2008.12.006

Argiropoulos, B., & Humphries, R. K. (2007). Hox genes in hematopoiesis and leukemogenesis. Oncogene, 26(47), 6766-6776. https://doi.org/10.1038/sj.onc.1210760

Azzarelli, R., Simons, B. D., & Philpott, A. (2018). The developmental origin of brain tumours: a cellular and molecular framework. Development, 145(10), dev162693. https://doi.org/10.1242/dev.162693

Bao, S., Wu, Q., McLendon, R. E., Hao, Y., Shi, Q., Hjelmeland, A. B., Dewhirst, M. W., Bigner, D. D., & Rich, J. N. (2006). Glioma stem cells promote radioresistance by preferential activation of the DNA damage response. Nature, 444(7120), 756-760. https://doi.org/10.1038/nature05236

Barondes, S. H., Cooper, D. N., Gitt, M. A., & Leffler, H. (1994). Galectins. Structure and function of a large family of animal lectins. Journal of Biological Chemistry, 269(33), 20807-20810. PMID: 8063692

Begicevic, R. R., & Falasca, M. (2017). ABC transporters in cancer stem cells: Beyond chemoresistance. International Journal of Molecular Sciences, 18(11), 2362. https://doi.org/10.3390/ijms18112362

Bhat, K. P. L., Balasubramaniyan, V., Vaillant, B., Ezhilarasan, R., Hummelink, K., Hollingsworth, F., ... & Aldape, K. (2013). Mesenchymal differentiation mediated by NF-κB promotes radiation resistance in glioblastoma. Cancer Cell, 24(3), 331-346. https://doi.org/10.1016/j.ccr.2013.08.001

Bhatlekar, S., Fields, J. Z., & Boman, B. M. (2014). HOX genes and their role in the development of human cancers. Journal of Molecular Medicine, 92(8), 811-823. https://doi.org/10.1007/s00109-014-1181-y

Bleau, A.-M., Hambardzumyan, D., Ozawa, T., Fomchenko, E. I., Huse, J. T., Brennan, C. W., & Holland, E. C. (2009). PTEN/PI3K/Akt pathway regulates the side population phenotype and ABCG2 activity in glioma tumour stem-like cells. Cell Stem Cell, 4(3), 226-235. https://doi.org/10.1016/j.stem.2009.01.007

Blough, M. D., Westgate, M. R., Beauchamp, D., Kelly, J. J., Stechishin, O., Ramirez, A. L., Weiss, S., & Cairncross, J. G. (2010). Sensitivity to temozolomide in brain tumour initiating cells. Neuro-Oncology, 12(7), 756-760. https://doi.org/10.1093/neuonc/noq032

Boucherat, O., Guillou, F., Aubin, J., & Jeannotte, L. (2009). Hoxa5: un maître d'oeuvre à multiples facettes [Hoxa5: a master gene with multifaceted roles]. Med Sci (Paris), 25(1), 77-82. https://doi.org/10.1051/medsci/200925177

Brar, G., Weissman, J. Ribosome profiling reveals what, when, where and how of protein synthesis. *Nat Rev Mol Cell Biol* 16, 651-664 (2015). https://doi.org/10.1038/nrm4069

Brennan, C. W., Verhaak, R. G. W., McKenna, A., Campos, B., Noushmehr, H., Salama, S. R., Zheng, S., Chakravarty, D., Sanborn, J. Z., Berman, S. H., Beroukhim, R., Bernard, B., et al. (2013). The somatic genomic landscape of glioblastoma. Cell, 155(2), 462-477. https://doi.org/10.1016/j.cell.2013.09.034

Broekman, M. L., Maas, S. L. N., Abels, E. R., et al. (2018). Multidimensional communication in the microenvirons of glioblastoma. Nature Reviews Neurology, 14, 482-495. https://doi.org/10.1038/s41582-018-0025-8

Calabrese, C., Poppleton, H., Kocak, M., Hogg, T. L., Fuller, C., Hamner, B., ... Gilbertson, R. J. (2007). A perivascular niche for brain tumour stem cells. Cancer Cell, 11(1), 69-82. https://doi.org/10.1016/j.ccr.2006.11.020

Carro, M. S., Lim, W. K., Alvarez, M. J., Bollo, R. J., Zhao, X., Snyder, E. Y., Sulman, E. P., Anne, S. L., Doetsch, F., Colman, H., Lasorella, A., Aldape, K., Califano, A., & Iavarone, A. (2011). The transcriptional network for mesenchymal transformation of brain tumours. Nature, 463(7279), 318-325. https://doi.org/10.1038/nature08712

Carruthers, R. D., Ahmed, S. U., Ramachandran, S., Strathdee, K., Kurian, K. M., Hedley, A., Gomez-Roman, N., Kalna, G., Neilson, M., Gilmour, L., Stevenson, K. H., Hammond, E. M., & Chalmers, A. J. (2018). Replication stress drives constitutive activation of the DNA damage response and radioresistance in glioblastoma stem-like cells. Cancer Research, 78(17), 5060-5071. https://doi.org/10.1158/0008-5472.CAN-18-0569

Charles, N., Ozawa, T., Squatrito, M., Bleau, A. M., Brennan, C. W., Hambardzumyan, D., & Holland, E. C. (2010). Perivascular nitric oxide activates notch signalling and promotes stem-like character in PDGF-induced glioma cells. Cell Stem Cell, 6(2), 141-152. https://doi.org/10.1016/j.stem.2010.01.001

Charles, N. A., Holland, E. C., Gilbertson, R., Glass, R., & Kettenmann, H. (2012). The brain tumour microenvironment. Glia, 60(3), 502-514. https://doi.org/10.1002/glia.21264

Chen, J., Li, Y., Yu, T.-S., McKay, R. M., Burns, D. K., Kernie, S. G., & Parada, L. F. (2012). A restricted cell population propagates glioblastoma growth after chemotherapy. Nature, 488(7412), 522-526. https://doi.org/10.1038/nature11287

Cimino, P. J., Kim, Y., Wu, H. J., Alexander, J., Wirsching, H. G., Szulzewsky, F., Pitter, K., Ozawa, T., Wang, J., Vazquez, J., Arora, S., Rabadan, R., Levine, R., Michor, F., & Holland, E. C. (2018). Increased HOXA5 expression provides a selective advantage for gain of whole chromosome 7 in IDH wild-type glioblastoma. Genes & Development, 32(7-8), 512-523. https://doi.org/10.1101/gad.312157.118

Camby, I., Le Mercier, M., Lefranc, F., & Kiss, R. (2006). Galectin-1: A small protein with major functions. Glycobiology, 16(11), 137R-157R. https://doi.org/10.1093/glycob/cwl025

Cao, W., Zhang, T., Feng, R., Xia, T., Huang, H., Liu, C., & Sun, C. (2019). Hoxa5 alleviates obesity-induced chronic inflammation by reducing ER stress and promoting M2 macrophage polarization in mouse adipose tissue. Journal of Cellular and Molecular Medicine, 23(10), 7029-7042. https://doi.org/10.1111/jcmm.14600

Cedeno-Laurent, F., & Dimitroff, C. J. (2012). Galectins and their ligands: Negative regulators of anti-tumour immunity. Glycoconjugate Journal, 29(8-9), 619-625. https://doi.org/10.1007/s10719-012-9379-0

Cho, M., & Cummings, R. D. (1995). Galectin-1, a beta-galactoside-binding lectin in Chinese hamster ovary cells. I. Physical and chemical characterization. Journal of Biological Chemistry, 270(10), 5198-5206. https://doi.org/10.1074/jbc.270.10.5198

Chung, L. Y., Tang, S. J., Sun, G. H., Chou, T. Y., Yeh, T. S., Yu, S. L., & Sun, K. H. (2012). Galectin-1 promotes lung cancer progression and chemoresistance by upregulating p38 MAPK, ERK, and cyclooxygenase-2. Clinical Cancer Research, 18(15), 4037-4047. https://doi.org/10.1158/1078-0432.CCR-11-3348

Cousin, J. M., & Cloninger, M. J. (2016). The role of Galectin-1 in cancer progression, and synthetic multivalent systems for the study of Galectin-1. International Journal of Molecular Sciences, 17(9), 1566. https://doi.org/10.3390/ijms17091566

Croci, D. O., Cerliani, J. P., Dalotto-Moreno, T., Méndez-Huergo, S. P., Mascanfroni, I. D., Dergan-Dylon, S., Toscano, M. A., Caramelo, J. J., García-Vallejo, J. J., Ouyang, J., Mesri, E. A., Junttila, M. R., Bais, C., Shipp, M. A., Salatino, M., & Rabinovich, G. A. (2014). Glycosylation-dependent lectin-receptor interactions preserve angiogenesis in anti-VEGF refractory tumours. Cell, 156(4), 744-758. https://doi.org/10.1016/j.cell.2014.01.043

Dang, L., White, D. W., Gross, S., Bennett, B. D., Bittinger, M. A., Driggers, E. M., ... & Thompson, C. B. (2009). Cancer-associated IDH1 mutations produce 2-hydroxyglutarate. Nature, 462(7274), 739-744. https://doi.org/10.1038/nature08617

Davis, M. E. (2016). Glioblastoma: Overview of disease and treatment. Clinical Journal of Oncology Nursing, 20(5 Suppl), S2-S8. https://doi.org/10.1188/16.CJON.S1.2-8

Deeken, J. F., & Löscher, W. (2007). The blood-brain barrier and cancer: transporters, treatment, and Trojan horses. Clinical Cancer Research, 13(6), 1663-1674. https://doi.org/10.1158/1078-0432.CCR-06-2854

De Kumar, B., & Darland, D. C. (2021). The Hox protein conundrum: The "specifics" of DNA binding for Hox proteins and their partners. Developmental Biology, 477, 284-292. https://doi.org/10.1016/j.ydbio.2021.06.002

Ding, F., Chen, P., Bie, P., Piao, W., & Cheng, Q. (2021). HOXA5 is recognized as a prognostic-related biomarker and promotes glioma progression through affecting cell cycle. Frontiers in Oncology, 11, 633430. https://doi.org/10.3389/fonc.2021.633430

Dunn, J., Baborie, A., Alam, F., Joyce, K., Moxham, M., Sibson, R., ... & Walker, C. (2009). Extent of MGMT promoter methylation correlates with outcome in glioblastomas given temozolomide and radiotherapy. British Journal of Cancer, 101(1), 124-131. https://doi.org/10.1038/sj.bjc.6605127

Eyler, C. E., & Rich, J. N. (2008). Survival of the fittest: cancer stem cells in therapeutic resistance and angiogenesis. Journal of Clinical Oncology, 26(17), 2839-2845. https://doi.org/10.1200/JCO.2007.15.1829

Fan, F., Mo, H., Zhang, H., Dai, Z., Wang, Z., Qu, C., Liu, F., Zhang, L., Luo, P., Zhang, J., Liu, Z., Cheng, Q., & Ding, F. (2022). HOXA5: A crucial transcriptional factor in cancer and a potential therapeutic target. Biomedicine & Pharmacotherapy, 155, 113800. https://doi.org/10.1016/j.biopha.2022.113800

Galli, R., Binda, E., Orfanelli, U., Cipelletti, B., Gritti, A., De Vitis, S., Fiocco, R., Foroni, C., Dimeco, F., & Vescovi, A. (2004). Isolation and characterization of tumourigenic, stem-like neural precursors from human glioblastoma. Cancer Research, 64(19), 7011-7021. https://doi.org/10.1158/0008-5472.CAN-04-1364

Gan, H. K., Cvrljevic, A. N., & Johns, T. G. (2013). The epidermal growth factor receptor variant III (EGFRvIII): where wild things are altered. FEBS Journal, 280(21), 5350-5370. https://doi.org/10.1111/febs.12393

Gendronneau, G., Lemieux, M., Morneau, M., Paradis, J., Têtu, B., Frenette, N., Aubin, J., & Jeannotte, L. (2010). Influence of Hoxa5 on p53 tumourigenic outcome in mice. American Journal of Pathology, 176(2), 995-1005. https://doi.org/10.2353/ajpath.2010.090499

Gotti, F., Jeannotte, L., & Landry-Truchon, K. (2016). Hoxa5: A key player in development and disease. Journal of Developmental Biology, 4(2), 13. https://doi.org/10.3390/jdb4020013

Greaves, M., & Maley, C. C. (2012). Clonal evolution in cancer. Nature, 481(7381), 306-313. https://doi.org/10.1038/nature10762

Grochans, S., Cybulska, A. M., Simińska, D., Korbecki, J., Kojder, K., Chlubek, D., & Baranowska-Bosiacka, I. (2022). Epidemiology of glioblastoma multiforme-literature review. Cancers, 14(10), 2412. https://doi.org/10.3390/cancers14102412

Guda, M. R., Tsung, A. J., Asuthkar, S., & Velpula, K. K. (2022). Galectin-1 activates carbonic anhydrase IX and modulates glioma metabolism. Cell Death & Disease, 13(6), 574. https://doi.org/10.1038/s41419-022-05024-z

Hambardzumyan, D., Gutmann, D. H., & Kettenmann, H. (2016). The role of microglia and macrophages in glioma maintenance and progression. Nature Neuroscience, 19(1), 20-27. https://doi.org/10.1038/nn.4185

Hanif, F., Muzaffar, K., Perveen, K., Malhi, S. M., & Simjee, S. U. (2017). Glioblastoma multiforme: A review of its epidemiology and pathogenesis through clinical presentation and

treatment. Asian Pacific Journal of Cancer Prevention, 18(1), 3-9. https://doi.org/10.22034/APJCP.2017.18.1.3

Hara, T., Chanoch-Myers, R., Mathewson, N. D., Myskiw, C., Atta, L., Bussema, L., ... & Tirosh, I. (2021). Interactions between cancer cells and immune cells drive transitions to mesenchymal-like states in glioblastoma. Cancer Cell, 39(6), 779-792.e11. https://doi.org/10.1016/j.ccell.2021.05.002

Harper, J. W., Elledge, S. J., Keyomarsi, K., Dynlacht, B., Tsai, L. H., & Zhang, P. (n.d.). [Incomplete citation]

Heddleston, J. M., Li, Z., McLendon, R. E., Hjelmeland, A. B., & Rich, J. N. (2009). The hypoxic microenvironment maintains glioblastoma stem cells and promotes reprogramming towards a cancer stem cell phenotype. Cell Cycle, 8(20), 3274-3284. https://doi.org/10.4161/cc.8.20.9701

Heddleston, J. M., Li, Z., Lathia, J. D., Bao, S., Hjelmeland, A. B., & Rich, J. N. (2010). Hypoxia inducible factors in cancer stem cells. British Journal of Cancer, 102(5), 789-795. https://doi.org/10.1038/sj.bjc.6605551

Hegi, M. E., Diserens, A.-C., Gorlia, T., Hamou, M.-F., de Tribolet, N., Weller, M., ... & Stupp, R. (2005). MGMT gene silencing and benefit from temozolomide in glioblastoma. New England Journal of Medicine, 352(10), 997-1003. https://doi.org/10.1056/NEJMoa043331

He, Z. C., Liu, Q., Yang, K. D., Chen, C., Zhang, X. N., Wang, W. Y., Zeng, H., Wang, B., Liu, Y. Q., Luo, M., Li, L., Niu, Q., Lu, H. M., Luo, T., Yao, X. H., Guo, H. T., Ji, J. L., Cao, M. F., Shi, Y., Ping, Y. F., & Bian, X. W. (2022). HOXA5 is amplified in glioblastoma stem cells and promotes tumour progression by transcriptionally activating PTPRZ1. Cancer Letters, 533, 215605. https://doi.org/10.1016/j.canlet.2022.215605

Heimberger, A. B., Hlatky, R., Suki, D., Yang, D., Weinberg, J., Gilbert, M., Sawaya, R., & Aldape, K. (2005). Prognostic effect of epidermal growth factor receptor and EGFRvIII in glioblastoma multiforme patients. Clinical Cancer Research, 11(4), 1462-1466. https://doi.org/10.1158/1078-0432.CCR-04-1737

Heimberger, A. B., Suki, D., Yang, D., Shi, W., & Aldape, K. (2005). The natural history of EGFR and EGFRvIII in glioblastoma patients. Journal of Translational Medicine, 3(1), 38. https://doi.org/10.1186/1479-5876-3-38

Hermenean, A., Oatis, D., Herman, H., Ciceu, A., D'Amico, G., & Trotta, M. C. (2022). Galectin 1—A key player between tissue repair and fibrosis. International Journal of Molecular Sciences, 23(10), 5548. https://doi.org/10.3390/ijms23105548

Huang, H. J., Nagane, M., Klingbeil, C. K., Lin, H., Nishikawa, R., Ji, X., Huang, C. M., Gill, G. N., Cavenee, W. K., & Huang, H. J. (1997). The enhanced tumourigenic activity of a mutant epidermal growth factor receptor common in human cancers is mediated by threshold levels of constitutive tyrosine phosphorylation and unattenuated signalling. Journal of Biological Chemistry, 272(5), 2927-2935. https://doi.org/10.1074/jbc.272.5.2927

Huang, Y., Wang, H. C., Zhao, J., Wu, M. H., & Shih, T. C. (2021). Immunosuppressive roles of galectin-1 in the tumour microenvironment. Biomolecules, 11(10), 1398. https://doi.org/10.3390/biom11101398

Hwang, J. M., Kang, S., Kim, W., & Lim, S.-C. (2017). EGFRvIII/OSMR/STAT3 signalling axis in glioblastoma stemness and immune evasion. Oncogene, 36(2), 202-212.

Jahani-Asl, A., Yin, H., Soleimani, V. D., Haque, T., Luchman, H. A., Chang, N. C., Sincennes, M. C., Puram, S. V., Scott, A. M., Lorimer, I. A., Perkins, T. J., Ligon, K. L., Weiss, S., Rudnicki, M. A., & Bonni, A. (2016). Control of glioblastoma tumourigenesis by feed-forward cytokine signalling. Nature Neuroscience, 19(6), 798-806. https://doi.org/10.1038/nn.4295

Kanderi, T., Munakomi, S., & Gupta, V. (2025). Glioblastoma multiforme. In StatPearls. StatPearls Publishing. https://www.ncbi.nlm.nih.gov/books/NBK559183/

Kim, J. Y., Lee, J. H., Jung, E. J., Son, Y. S., Park, H. J., Kim, J. M., Park, T., Jeong, S. H., Lee, J., Kim, T. H., Lee, S. M., & Heo, J. D. (2025). Therapeutic targeting of the galectin-1/miR-22-3p axis regulates cell cycle and EMT depending on the molecular subtype of breast cancer. Cells, 14(4), 310. https://doi.org/10.3390/cells14040310

Koshiji, M., Kageyama, Y., Pete, E. A., Horikawa, I., Barrett, J. C., & Huang, L. E. (2004). HIF-1alpha induces cell cycle arrest by functionally counteracting Myc. EMBO Journal, 23(9), 1949-1956. https://doi.org/10.1038/sj.emboj.7600196

Kriegstein, A., & Alvarez-Buylla, A. (2009). The glial nature of embryonic and adult neural stem cells. Annual Review of Neuroscience, 32, 149-184. https://doi.org/10.1146/annurev.neuro.051508.135600

Krumlauf, R. (1994). Hox genes in vertebrate development. Cell, 78(2), 191-201. https://doi.org/10.1016/0092-8674(94)90290-9

Laderach, D. J., & Compagno, D. (2023). Inhibition of galectins in cancer: Biological challenges for their clinical application. Frontiers in Immunology, 13, 1104625. https://doi.org/10.3389/fimmu.2022.1104625

Laderach, D. J., Gentilini, L. D., Giribaldi, L., Delgado, V. C., Nugnes, L., Croci, D. O., Al Nakouzi, N., Sacca, P., Casas, G., Mazza, O., Shipp, M. A., Vazquez, E., Chauchereau, A., Kutok, J. L., Rodig, S. J., Elola, M. T., Compagno, D., & Rabinovich, G. A. (2013). A unique galectin signature in human prostate cancer progression suggests galectin-1 as a key target for treatment of advanced disease. Cancer Research, 73(1), 86-96. https://doi.org/10.1158/0008-5472.CAN-12-1260

Lan, X., Jörg, D. J., Cavalli, F. M. G., Richards, L. M., Nguyen, L. V., Vanner, R. J., Lee, L., Kushida, M., Pellacani, D., Park, N., Mungall, A. J., Smith, A., Cowdrey, C., Ramaswamy, V., Laks, E., Moksa, M., Moore, R. A., Ma, Y., Greaves, M., ... & Dirks, P. B. (2017). Fate mapping of human glioblastoma reveals an invariant stem cell hierarchy. Nature, 549(7671), 227-232. https://doi.org/10.1038/nature23666

Landry-Truchon, K., Gotti, F., & Jeannotte, L. (2016). [See above - entry same as Gotti et al.]

Lathia, J. D., Mack, S. C., Mulkearns-Hubert, E. E., Valentim, C. L. L., & Rich, J. N. (2015). Cancer stem cells in glioblastoma. Genes & Development, 29(12), 1203-1217. https://doi.org/10.1101/gad.261982.115

Le Mercier, M., Fortin, S., Mathieu, V., Kiss, R., & Lefranc, F. (2010). Galectins and gliomas. Brain Pathology, 20(1), 17-27. https://doi.org/10.1111/j.1750-3639.2009.00270.x

Lee, J., Kotliarova, S., Kotliarov, Y., Li, A., Su, Q., Donin, N. M., Pastorino, S., Purow, B., Christopher, N., Zhang, W., Park, J. K., & Fine, H. A. (2018). tumour stem cells derived from glioblastomas cultured in bFGF and EGF more closely mirror the phenotype and genotype of primary tumours than do serum-cultured cell lines including U87. Cancer Cell, 9(5), 391-403. https://doi.org/10.1016/j.ccr.2006.03.030

Li, C. H., Chang, Y. C., Chan, M. H., Yang, Y. F., Liang, S. M., & Hsiao, M. (2021). Galectins in cancer and the microenvironment: Functional roles, therapeutic developments, and perspectives. Biomedicines, 9(9), 1159. https://doi.org/10.3390/biomedicines9091159

Li, X.-P., Guo, Z.-Q., Wang, B.-F., & Zhao, M. (2023). EGFR alterations in glioblastoma play a role in antitumour immunity regulation. Frontiers in Oncology, 13, Article 1236246. https://doi.org/10.3389/fonc.2023.1236246

Lin, N., Yan, W., Gao, K., Wang, Y., Zhang, J., You, Y., ... & You, Y. (2014). Prevalence and clinicopathologic characteristics of the molecular subtypes in malignant glioma: A multi-institutional analysis of 941 cases. PLOS ONE, 9(4), e94871. https://doi.org/10.1371/journal.pone.0094871

Lin, Y. T., Chen, J. S., Wu, M. H., Hsieh, I. S., Liang, C. H., Hsu, C. L., Hong, T. M., & Chen, Y. L. (2015). Galectin-1 accelerates wound healing by regulating the neuropilin-1/Smad3/NOX4 pathway and ROS production in myofibroblasts. Journal of Investigative Dermatology, 135(1), 258-268. https://doi.org/10.1038/jid.2014.288

Liu, F. T., Patterson, R. J., & Wang, J. L. (2002). Intracellular functions of galectins. Biochimica et Biophysica Acta, 1572(2-3), 263-273. https://doi.org/10.1016/s0304-4165(02)00313-6

Makale, M., McDonald, C., Hattangadi-Gluth, J., & et al. (2017). Mechanisms of radiotherapy-associated cognitive disability in patients with brain tumours. Nature Reviews Neurology, 13, 52-64. https://doi.org/10.1038/nrneurol.2016.185

Mallo, M., Wellik, D. M., & Deschamps, J. (2010). Hox genes and regional patterning of the vertebrate body plan. Developmental Biology, 344(1), 7-15. https://doi.org/10.1016/j.ydbio.2010.04.024

Manley, N. R., & Capecchi, M. R. (1997). Hox group 3 paralogous genes act synergistically in the formation of somitic and neural crest-derived structures. Developmental Biology, 192(2), 274-288. https://doi.org/10.1006/dbio.1997.8765

Mamatjan, Y., Voisin, M. R., Nassiri, F., Moraes, F. Y., Bunda, S., So, J., Salih, M., Shirahata, M., Ono, T., Shimizu, H., Schrimpf, D., von Deimling, A., Aldape, K. D., & Zadeh, G. (2023). Integrated molecular analysis reveals hypermethylation and overexpression of HOX genes to be poor prognosticators in isocitrate dehydrogenase mutant glioma. Neuro-Oncology, 25(11), 2028-2041. https://doi.org/10.1093/neuonc/noad126

Martinez-Bosch, N., Barranco, L. E., Orozco, C. A., Moreno, M., Visa, L., Iglesias, M., Oldfield, L., Neoptolemos, J. P., Greenhalf, W., Earl, J., Carrato, A., Costello, E., & Navarro, P. (2018). Increased plasma levels of galectin-1 in pancreatic cancer: Potential use as biomarker. Oncotarget, 9(68), 32984-32996. https://doi.org/10.18632/oncotarget.26034

McGinnis, W., & Krumlauf, R. (1992). Homeobox genes and axial patterning. Cell, 68(2), 283-302. https://doi.org/10.1016/0092-8674(92)90471-n

Meunier, D., Aubin, J., & Jeannotte, L. (2003). Perturbed thyroid morphology and transient hypothyroidism symptoms in Hoxa5 mutant mice. Developmental Dynamics, 227(3), 367-378. https://doi.org/10.1002/dvdy.10325

Neftel, C., Laffy, J., Filbin, M. G., Hara, T., Shore, M. E., Rahme, G. J., Richman, A. R., Silverbush, D., Shaw, M. L., Hebert, C. M., ... & Suvà, M. L. (2019). An integrative model of cellular states, plasticity, and genetics for glioblastoma. Cell, 178(4), 835-849.e21. https://doi.org/10.1016/j.cell.2019.06.024

Novák, J., Takács, T., Tilajka, Á., László, L., Oravecz, O., Farkas, E., Than, N. G., Buday, L., Balogh, A., & Vas, V. (2025). The sweet and the bitter sides of galectin-1 in immunity: Its role in immune cell functions, apoptosis, and immunotherapies for cancer with a focus on T cells. Seminars in Immunopathology, 47(1), 24. https://doi.org/10.1007/s00281-025-01047-8

Orozco, C. A., Martinez-Bosch, N., Guerrero, P. E., Vinaixa, J., Dalotto-Moreno, T., Iglesias, M., Moreno, M., Djurec, M., Poirier, F., Gabius, H. J., Fernandez-Zapico, M. E., Hwang, R. F., Guerra, C., Rabinovich, G. A., & Navarro, P. (2018). Targeting galectin-1 inhibits pancreatic cancer progression by modulating tumour-stroma crosstalk. Proceedings of the National Academy of Sciences of the United States of America, 115(16), E3769-E3778. https://doi.org/10.1073/pnas.1722434115

Packer, A. I., Mailutha, K. G., Ambrozewicz, L. A., & Wolgemuth, D. J. (2000). Regulation of the Hoxa4 and Hoxa5 genes in the embryonic mouse lung by retinoic acid and TGFbeta1: Implications for lung development and patterning. Developmental Dynamics, 217(1), 62-74. https://doi.org/10.1002/(SICI)1097-0177(200001)217:1<62::AID-DVDY6>3.0.CO;2-U

Papadimitriou, E., & Kanellopoulou, V. K. (2023). Protein tyrosine phosphatase receptor zeta 1 as a potential target in cancer therapy and diagnosis. International Journal of Molecular Sciences, 24(9), 8093. https://doi.org/10.3390/ijms24098093

Patel, A. P., Tirosh, I., Trombetta, J. J., Shalek, A. K., Gillespie, S. M., Wakimoto, H., Cahill, D. P., Nahed, B. V., Curry, W. T., Martuza, R. L., Louis, D. N., Rozenblatt-Rosen, O., Suvà, M. L., Regev, A., & Bernstein, B. E. (2014). Single-cell RNA-seq highlights intratumoural

heterogeneity in primary glioblastoma. Science, 344(6190), 1396-1401. https://doi.org/10.1126/science.1254257

Pastorekova, S., & Gillies, R. J. (2019). The role of carbonic anhydrase IX in cancer development: Links to hypoxia, acidosis, and beyond. Cancer Metastasis Reviews, 38(1-2), 65-77. https://doi.org/10.1007/s10555-019-09799-0

Pearson, J. C., Lemons, D., & McGinnis, W. (2005). Modulating Hox gene functions during animal body patterning. Nature Reviews Genetics, 6(12), 893-904. https://doi.org/10.1038/nrg1726

Peng, X., Zha, L., Chen, A., & Wang, Z. (2018). HOXA5 is a tumour suppressor gene that is decreased in gastric cancer. Oncology Reports, 40(3), 1317-1329. https://doi.org/10.3892/or.2018.6537

Perillo, N. L., Pace, K. E., Seilhamer, J. J., & Baum, L. G. (1995). Apoptosis of T cells mediated by galectin-1. Nature, 378(6558), 736-739. https://doi.org/10.1038/378736a0
(Note: This reference appeared twice in your list; only one copy is shown here.)

Phillips, H. S., Kharbanda, S., Chen, R., Forrest, W. F., Soriano, R. H., Wu, T. D., ... & Modrusan, Z. (2006). Molecular subclasses of high-grade glioma predict prognosis, delineate a pattern of disease progression, and resemble stages in neurogenesis. Cancer Cell, 9(3), 157-173. https://doi.org/10.1016/j.ccr.2006.02.019

Poon, C. C., Sarkar, S., & Yong, V. W., Kelly, J. J. P. (2017). Glioblastoma-associated microglia and macrophages: Targets for therapies to improve prognosis. Brain, 140(6), 1548-1560. https://doi.org/10.1093/brain/aww355

Porciúncula-González, C., Cagnoni, A. J., Fontana, C., Mariño, K. V., Saenz-Méndez, P., Giacomini, C., & Irazoqui, G. (2021). Structural insights in galectin-1-glycan recognition: Relevance of the glycosidic linkage and the N-acetylation pattern of sugar moieties. Bioorganic & Medicinal Chemistry, 44, 116309. https://doi.org/10.1016/j.bmc.2021.116309

Quail, D. F., & Joyce, J. A. (2017). The microenvironmental landscape of brain tumours. Cancer Cell, 31(3), 326-341. https://doi.org/10.1016/j.ccell.2017.02.009

Rabinovich, G. A., Toscano, M. A., Jackson, S. S., & Vasta, G. R. (2007). Functions of cell surface galectin-glycoprotein lattices. Current Opinion in Structural Biology, 17(5), 513-520. https://doi.org/10.1016/j.sbi.2007.09.002

Raman, V., Martensen, S. A., Reisman, D., Evron, E., Odenwald, W. F., Jaffee, E., Marks, J., & Sukumar, S. (2000). Compromised HOXA5 function can limit p53 expression in human breast tumours. Nature, 405(6789), 974-978. https://doi.org/10.1038/35016125

Rehman, S. K., Haynes, J., Collignon, E., Brown, K. R., Wang, Y., Nixon, A. M. L., ... & O'Brien, C. A. (2021). Colorectal cancer cells enter a diapause-like DTP state to survive chemotherapy. Cell, 184(1), 226-242.e21. https://doi.org/10.1016/j.cell.2020.11.018

Ritesh, K. C., de Boer, R. L., Lin, M., Jeannotte, L., & Philippidou, P. (2024). Multimodal Hox5 activity generates motor neuron diversity. bioRxiv. https://doi.org/10.1101/2024.02.08.579338

Sabouri, M., Dogonchi, A. F., Shafiei, M., & et al. (2024). Survival rate of patient with glioblastoma: A population-based study. Egyptian Journal of Neurosurgery, 39, 42. https://doi.org/10.1186/s41984-024-00294-5

Shah, N., & Sukumar, S. (2010). The Hox genes and their roles in oncogenesis. Nature Reviews Cancer, 10(5), 361-371. https://doi.org/10.1038/nrc2826

Sharanek, A., Burban, A., Hernandez-Corchado, A., Madrigal, A., Fatakdawala, I., Najafabadi, H. S., Soleimani, V. D., & Jahani-Asl, A. (2021). Transcriptional control of brain tumour stem cells by a carbohydrate binding protein. Cell Reports, 36(9), 109647. https://doi.org/10.1016/j.celrep.2021.109647

Shi, Z. F., Li, G. Z., Zhai, Y., Pan, C. Q., Wang, D., Yu, M. C., Liu, C., Zhang, W., & Yu, X. G. (2023). EGFRvIII promotes the proneural-mesenchymal transition of glioblastoma multiforme and reduces its sensitivity to temozolomide by regulating the NF-κB/ALDH1A3 axis. Genes, 14(3), 651. https://doi.org/10.3390/genes14030651

Singh, A. K., Arya, R. K., Maheshwari, S., Singh, A., Meena, S., & Pandey, A. K. (2020). Dormancy and cancer stem cells: Potential for new therapies. Critical Reviews in Oncology/Hematology, 150, 102961. https://doi.org/10.1016/j.critrevonc.2020.102961

Sipos, D., Raposa, B. L., Freihat, O., Simon, M., Mekis, N., Cornacchione, P., & Kovács, Á. (2025). Glioblastoma: Clinical presentation, multidisciplinary management, and long-term outcomes. Cancers, 17(1), 146. https://doi.org/10.3390/cancers17010146

Starossom, S. C., Mascanfroni, I. D., Imitola, J., Cao, L., Raddassi, K., Hernandez, S. F., Bassil, R., Croci, D. O., Cerliani, J. P., Delacour, D., Wang, Y., Elyaman, W., Khoury, S. J., & Rabinovich, G. A. (2012). Galectin-1 deactivates classically activated microglia and protects from inflammation-induced neurodegeneration. Immunity, 37(2), 249-263. https://doi.org/10.1016/j.immuni.2012.05.023

Stasinopoulos, I. A., Mironchik, Y., Raman, A., Wildes, F., Winnard, P. Jr., & Raman, V. (2005). HOXA5-twist interaction alters p53 homeostasis in breast cancer cells. Journal of Biological Chemistry, 280(3), 2294-2299. https://doi.org/10.1074/jbc.M411018200

Steens, J., & Klein, D. (2022). HOX genes in stem cells: Maintaining cellular identity and regulation of differentiation. Frontiers in Cell and Developmental Biology, 10, 1002909. https://doi.org/10.3389/fcell.2022.1002909

Szatmári, T., Lumniczky, K., Désaknai, S., Trajcevski, S., Hidvégi, E., Hamada, H., & Sáfrány, G. (2006). Detailed characterization of the mouse glioma 261 tumour model for experimental glioblastoma therapy. Cancer Science, 97(6), 546-553. https://doi.org/10.1111/j.1349-7006.2006.00208.x

Taylor, T. E., Furnari, F. B., & Cavenee, W. K. (2012). Targeting EGFR for treatment of glioblastoma: Molecular basis to overcome resistance. Current Cancer Drug Targets, 12(3), 197-209. https://doi.org/10.2174/156800912799277557

Teo, W. W., Merino, V. F., Cho, S., Korangath, P., Liang, X., Wu, R. C., Neumann, N. M., Ewald, A. J., & Sukumar, S. (2016). HOXA5 determines cell fate transition and impedes tumour initiation and progression in breast cancer through regulation of E-cadherin and CD24. Oncogene, 35(42), 5539-5551. https://doi.org/10.1038/onc.2016.95

Thijssen, V. L., Postel, R., Brandwijk, R. J., Dings, R. P., Nesmelova, I., Satijn, S., Verhofstad, N., Nakabeppu, Y., Baum, L. G., Bakkers, J., Mayo, K. H., Poirier, F., & Griffioen, A. W. (2006). Galectin-1 is essential in tumour angiogenesis and is a target for antiangiogenesis therapy. Proceedings of the National Academy of Sciences of the United States of America, 103(43), 15975-15980. https://doi.org/10.1073/pnas.0603883103

Thompson, C. A., DeLaForest, A., & Battle, M. A. (2018). Patterning the gastrointestinal epithelium to confer regional-specific functions. Developmental Biology, 435(2), 97-108. https://doi.org/10.1016/j.ydbio.2018.01.006

Tang, K., Chen, B., Cheng, Z., Ye, X., & Luo, J. (2020). Single-cell sequencing analysis and weighted co-expression network analysis based on public databases identifies potential diagnostic biomarkers associated with glioblastoma. Frontiers in Genetics, 11, 568621. https://doi.org/10.3389/fgene.2020.568621

Tirosh, I., Venteicher, A. S., Hebert, C., Escalante, L. E., Patel, A. P., Yizhak, K., ... & Suvà, M. L. (2016). Single-cell RNA-seq supports a developmental hierarchy in human oligodendroglioma. Nature, 539(7628), 309-313. https://doi.org/10.1038/nature20123

Toscano, M. A., Bianco, G. A., Ilarregui, J. M., Croci, D. O., Correale, J., Hernandez, J. D., Zwirner, N. W., Poirier, F., Riley, E. M., Baum, L. G., & Rabinovich, G. A. (2007). Differential glycosylation of TH1, TH2 and TH-17 effector cells selectively regulates susceptibility to cell death. Nature Immunology, 8(8), 825-834. https://doi.org/10.1038/ni1482

Uchida, H., & Shitara, S. (2021). Treatment strategy for glioblastoma in elderly patients: Is it different? Neurologia Medico-Chirurgica, 61(5), 238-245. https://doi.org/10.2176/nmc.st.2020-0327

Van Meir, E. G., Hadjipanayis, C. G., Norden, A. D., Shu, H. K., Wen, P. Y., & Olson, J. J. (2010). Exciting new advances in neuro-oncology: The avenue to a cure for malignant glioma. CA: A Cancer Journal for Clinicians, 60(3), 166-193. https://doi.org/10.3322/caac.20069

Venteicher, A. S., Tirosh, I., Hebert, C., Yizhak, K., Neftel, C., Filbin, M. G., ... & Suvà, M. L. (2017). Decoupling genetics, lineages, and microenvironment in IDH-mutant gliomas by single-cell RNA-seq. Science, 355(6332), eaai8478. https://doi.org/10.1126/science.aai8478

Vecht, C. J., Kerkhof, M., & Duran-Pena, A. (2014). Seizure prognosis in brain tumours: New insights and evidence-based management. The Oncologist, 19(7), 751-759. https://doi.org/10.1634/theoncologist.2014-0060

Verhaak, R. G. W., Hoadley, K. A., Purdom, E., Wang, V., Qi, Y., Wilkerson, M. D., ... & Hayes, D. N. (2010). Integrated genomic analysis identifies clinically relevant subtypes of glioblastoma characterized by abnormalities in PDGFRA, IDH1, EGFR, and NF1. Cancer Cell, 17(1), 98-110. https://doi.org/10.1016/j.ccr.2009.12.020

Wang, Q., Hu, B., Hu, X., Kim, H., Squatrito, M., Scarpace, L., deCarvalho, A. C., Lyu, S., Li, P., Li, Y., Barthel, F. P., ... & Verhaak, R. G. (2017). tumour evolution of glioma intrinsic gene expression subtype associates with immunological changes in the microenvironment. Cancer Cell, 32(1), 42-56.e6. https://doi.org/10.1016/j.ccell.2017.06.003

Warot, X., Fromental-Ramain, C., Fraulob, V., Chambon, P., & Dollé, P. (1997). Gene dosage-dependent effects of the Hoxa-13 and Hoxd-13 mutations on morphogenesis of the terminal parts of the digestive and urogenital tracts. Development, 124(23), 4781-4791. PMID: 9428414

Weller, M., Cloughesy, T., Perry, J. R., & Wick, W. (2013). Standards of care for treatment of recurrent glioblastoma—Are we there yet? Neuro-Oncology, 15(1), 4-27. https://doi.org/10.1093/neuonc/nos273

Weller, M., van den Bent, M., Hopkins, K., Tonn, J. C., Stupp, R., Falini, A., ... & Reifenberger, G. (2014). EANO guidelines on the diagnosis and treatment of diffuse gliomas of adulthood. Nature Reviews Clinical Oncology, 15(3), 83-95. https://doi.org/10.1038/nrclinonc.2017.7

Weller, M., Wick, W., Aldape, K., Brada, M., Berger, M., Pfister, S. M., & van den Bent, M. J. (2015). Glioma. Nature Reviews Disease Primers, 1, 15017. https://doi.org/10.1038/nrdp.2015.17

Wen, P. Y., & Kesari, S. (2008). Malignant gliomas in adults. The New England Journal of Medicine, 359(5), 492-507. https://doi.org/10.1056/NEJMra0708126

Wick, W., Platten, M., & Weller, M. (2009). Glioma stem cells: A new target for cancer therapy? Nature Reviews Cancer, 9(10), 799-809. https://doi.org/10.1038/nrc2728

Xu, H., Wu, Q., & Bao, S. (2021). Cancer stem cells in glioma: Challenges and opportunities. Seminars in Cancer Biology, 72, 144-160. https://doi.org/10.1016/j.semcancer.2020.09.011

Yang, D., Zhang, X., Dong, Y., Liu, X., Wang, T., Wang, X., Geng, Y., Fang, S., Zheng, Y., Chen, X., Chen, J., Pan, G., & Wang, J. (2015). Enforced expression of Hoxa5 in haematopoietic stem cells leads to aberrant erythropoiesis in vivo. Cell Cycle, 14(4), 612-620. https://doi.org/10.4161/15384101.2014.992191

Yang, Y., Zhong, F., Huang, X., Zhang, N., Du, J., Long, Z., Zheng, B., Lin, W., Liu, W., & Ma, W. (2021). High expression of HOXA5 is associated with poor prognosis in acute myeloid leukemia. Current Problems in Cancer, 45(3), 100673. https://doi.org/10.1016/j.currproblcancer.2020.100673

Yabo, Y. A., Ndom, B. H., & Clement, V. (2022). Cancer cell heterogeneity and plasticity: A paradigm shift in glioblastoma. Neuro-Oncology, 24(5), 669-682. https://doi.org/10.1093/neuonc/noab269

Yuan, F., Wang, Y., Yuan, L., Zhang, R., Li, Y., & Zhao, H. (2025). EGFRvIII-positive glioblastoma contributes to immune escape and malignant progression via the c-Fos-MDK-LRP1 axis. Cell Death & Disease, 16, 453. https://doi.org/10.1038/s41419-025-07771-1

Zhang Z, Chen J, Huo X, Zong G, Huang K, Cheng M, Sun L, Yue X, Bian E, Zhao B. Identification of a mesenchymal-related signature associated with clinical prognosis in glioma. Aging (Albany NY). 2021 Apr 19;13(9):12431-12455. doi: 10.18632/aging.202886. Epub 2021 Apr 19. PMID: 33875619; PMCID: PMC8148476.

Zhou, B., Chen, L., Wu, X., Wang, J., Yin, Y., & Zhu, G. (2008). MH1 domain of SMAD4 binds N-terminal residues of the homeodomain of Hoxc9. Biochimica et Biophysica Acta (BBA) - Proteins and Proteomics, 1784(5), 747-752. https://doi.org/10.1016/j.bbapap.2008.01.021

Zhou, W., Chen, C., Shi, Y., Wu, Q., Gimple, R. C., Fang, X., ... & Bao, S. (2021). Interactions between cancer cells and immune cells drive transitions to mesenchymal-like states in glioblastoma. Cancer Cell, 39(6), 779-792.e11. https://doi.org/10.1016/j.ccell.2021.05.002